aer

ATMOSPHERIC AND ENVIRONMENTAL RESEARCH, INC.
CAMBRIDGE, MASSACHUSETTS

Reanalysis of Mariner 9 UV Spectrometer Data for Ozone, Cloud, and Dust Abundances, and their Interaction over Climate Timescales

Contract No. NASW-4614

Final Report

Submitted Feb. 7, 1994

by Bernhard Lee Lindner

Atmospheric and Environmental Research, Inc.
840 Memorial Drive
Cambridge, MA 02139-3794

TECHNICAL REPORT STANDARD TITLE PAGE

1. *Report No.*	2. *Government Accession No.*	3. *Recipient's Catalog No.*

4. *Title of Project* Reanalysis of Mariner 9 UV Spectrometer Data for Ozone, Cloud, and Dust Abundances, and their Interaction over Climate Timescales	5. *Report Date* Feb. 7, 1994 6. *Performing Organization Code*
7. *Author(s)* Bernhard Lee Lindner	8. *Performing Organization Report No.*
9. *Performing Organization Name and Address* Atmospheric and Environmental Research, Inc. 840 Memorial Drive Cambridge, MA 02139-3794	10. *Work Unit No.* 11. *Contract or Grant No.* NASW-4614
12. *Sponsoring Agency Name and Address* NASA Headquarters Headquarters Contract Divisions Washington, DC 20546	13. *Type of Report and Period Covered* Final Report 5/1/91-12/31/93 14. *Sponsoring Agency Code* EL
15. *Supplementary Notes*	

16. *Abstract*

In brief, the primary objectives for the work have been completed. Mariner 9 UV Spectrometer data have been reinverted for the ozone abundance. The spectra were fit by models which covered the full range in observed solar zenith angle, cloud, dust and ozone amount, ice albedo and look angles. Errors in ozone retrieval with this data are tabulated over a range in these conditions and are shown graphically. This work shows that significant underestimation of ozone occurred in earlier analysis of Mariner 9 data, and that much of the observed variability in Mars ozone is due to masking of ozone by clouds and dust. As these previously published abundances have been used as a benchmark for all theoretical photochemical models of Mars, some of this work will have to be reinvestigated. The efficacy of the reflectance spectroscopy technique at retrieving the ozone abundance on Mars is questioned. The technique is incapable of retrieving ozone at night and during dust storms, and has as much as a factor of 3 error at other times. An in-situ measurement by balloon is recommended as it is the only technique capable of accurately inferring the ozone abundance in all conditions. Recommendations for future research are also presented.

7 manuscripts have been published in refereed journals, and three are in review. Papers have been presented and published at 13 conferences. 4 of these conferences are MSATT Workshops. A review of these publications and presentations is in the report, and preprints and reprints of publications are enclosed in the report appendix.

I was also honored to be elected to the International Association of Meteorology and Atmospheric Physics Commission on Planetary Atmospheres and their Evolution and was honored to be nominated for the European Geophysical Society Young Scientists' Publication Award.

17. *Key Words (selected by Author(s))*	18. *Distribution Statement*
Mars, ozone, Mariner 9	

19. *Security Classif. (of this report)*	20. *Security Classif. (of this page)*	21. *No of Pages*	22. *Price*
Unclassified	Unclassified	136	

Table of Contents

I. Abstract for the project (reprinted from the proposal)

Mariner 9 UV spectrometer data would be reinverted for the ozone abundance, cloud abundance, dust abundance, and polar-cap albedo. The original reduction of the spectra ignored the presence of atmospheric dust and clouds, even though their abundance is substantial and can mask appreciable amounts of ozone if not accounted for (Lindner, 1988). The Mariner 9 ozone data has been used as a benchmark in all theoretical models of atmospheric composition, escape, and photochemistry. A second objective is to examine the data for the interrelationship of the ozone cycle, dust cycle, and cloud cycle, on an annual, inter-annual, and climatic basis, testing predictions by Lindner (1988). This also has implications for many terrestrial ozone studies, such as the ozone hole, acid rain, and ozone-smog. A third objective is to evaluate the efficacy of the reflectance spectroscopy technique at retrieving the ozone abundance on Mars. This would be useful for planning ozone observations on future Mars missions or the terrestrial troposphere.

II. Summary of Research to Date

II.1 Model development.

The photochemical-radiative transfer model of Lindner (1985; 1988) has been updated. The code has been modified to run on AER's computer system, has been updated to use new cloud and dust scattering parameters as determined by Clancy and Lee (1991), and has been updated with new improvements to the Discrete Ordinate Method by Stamnes et al. (1988). Briefly, the code runs in 3 parts. First a code has been written which sets up the base atmosphere, including photochemistry, and then computes the wavelength-dependent atmospheric opacity, single-scattering albedo and phase function. Figure 1 shows the atmospheric opacity as a function of wavelength for one atmosphere scenario. This opacity includes Rayleigh scattering (strongest at 1500 Angstroms, and decreasing rapidly with wavelength), CO_2 absorption (the prominent component of the opacity shortward of 2000 Angstroms), and ozone absorption (the "bump" in opacity between 2000 and 3000 Angstroms). In addition, there is a virtually wavelength-independent opacity of cloud and dust. It is this "bump" that leaves a characteristic signature of the ozone abundance in the measured UV spectra. The radiative transfer model then computes intensities as a function of wavelength based on this atmospheric opacity and scattering. Finally, a code has been written which converts these intensities into a ratio of UV spectra which can be compared to the data.

II.2 Acquire Mariner 9 UV Spectrometer data.

While at the MSATT workshop held in Boulder, Colorado Sept. 23-25, 1991, the principal investigator discussed the procedure for obtaining the Mariner 9 UV Spectrometer data with Steve Lee, the director for the node of the Planetary Database System (PDS) at the University of Colorado. This and subsequent discussions have indicated that the data are not on the PDS system as promised years ago, and are not expected to be on the PDS for several years, due mostly to budget cuts. Steve has offered to help us retrieve the original data, however, we have been denied access to this data by Charles Barth of the University of Colorado, despite our requests to him to release this 20 year old data. Nonetheless, there have been several good spectra published in Lane et al. (1973) and Wehrbein (1977), which are quite adequate for us to complete all of our objectives for this project. A sample data spectra is

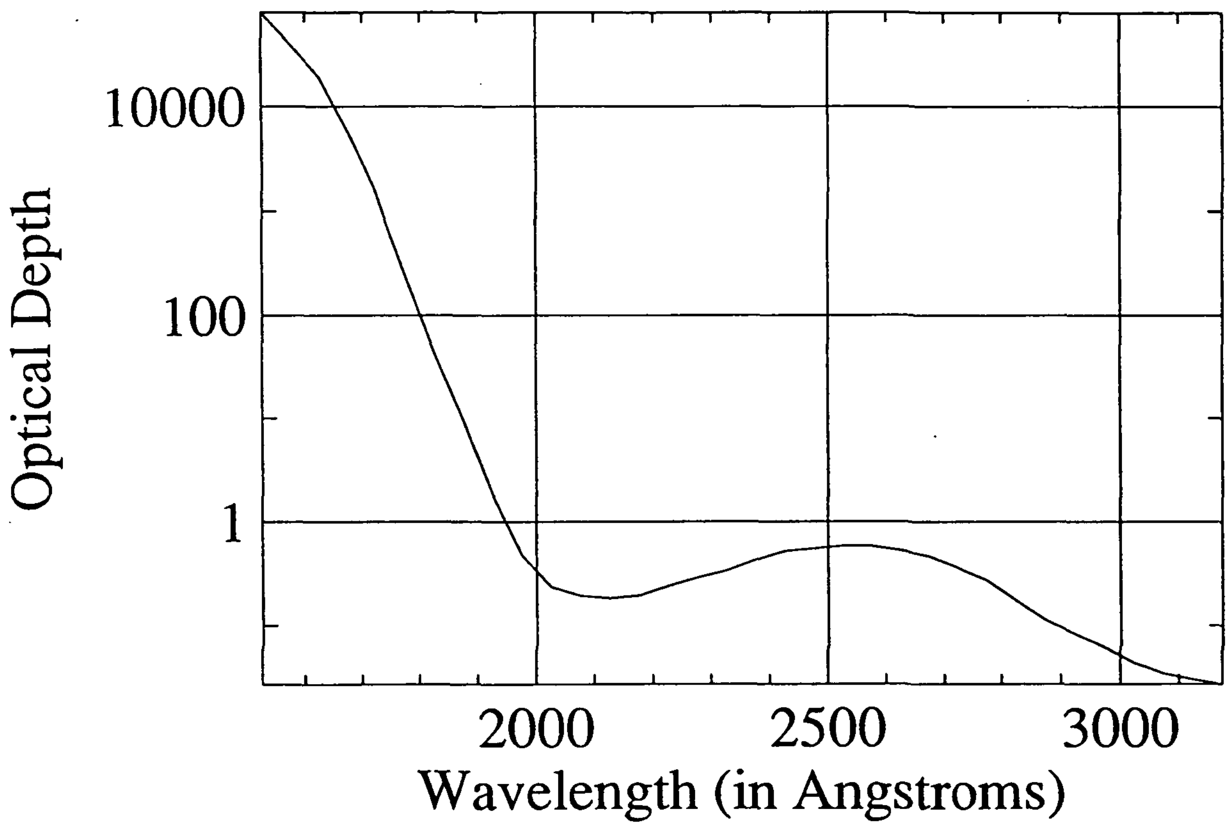

Figure 1. Vertical opacity of the atmosphere for 30 μm-atm of ozone, no dust and no cloud. A winter polar temperature profile is adopted (see Lindner, 1988).

shown in Figure 2.

II.3. Simulate UV Spectra.

The theoretical model was run with a variety of inputs to generate synthetic UV spectra. Parameters within the base atmosphere were varied as shown in Table 1 and synthetic spectra were calculated for each case. This is done to examine how changes in atmosphere affect ozone retrieval efficacy, affect errors in retrieved ozone abundance, and affect scatter in data. For ease of comparison to data (see Fig. 2), we have computed ratio of spectra to that at 20N latitude, where little ozone is present. Computed spectra for 20N latitude show little wavelength dependence. Figure 3 shows how spectra can vary for a single base atmosphere depending upon the viewing geometry of the spacecraft. Hence, comparison of synthetic spectra to observed spectra must properly account for the correct geometry. Synthetic spectra for various scenario for base atmospheres are shown in Figures 4 through 7.

TABLE 1

Synthetic spectra calculated for the following ranges in parameters

Ozone	0 to 100 μm-atm.
Ozone distribution	well-mixed, and concentrated down low
Solar Zenith Angle	50 to 85 degrees
Dust opacity	0 to 1
Cloud opacity	0 to 1
Ice albedo	0.3 to 0.8
Look Angle	0 to 90 degrees
Azimuth of Look Angle	0 to 90 degrees

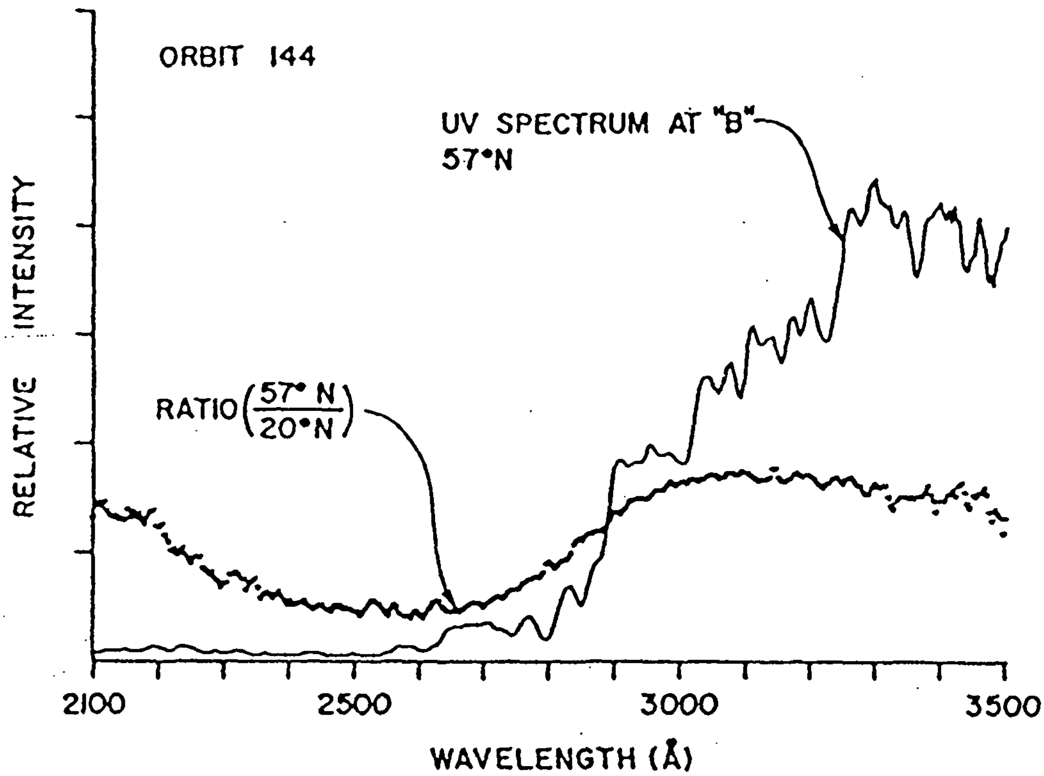

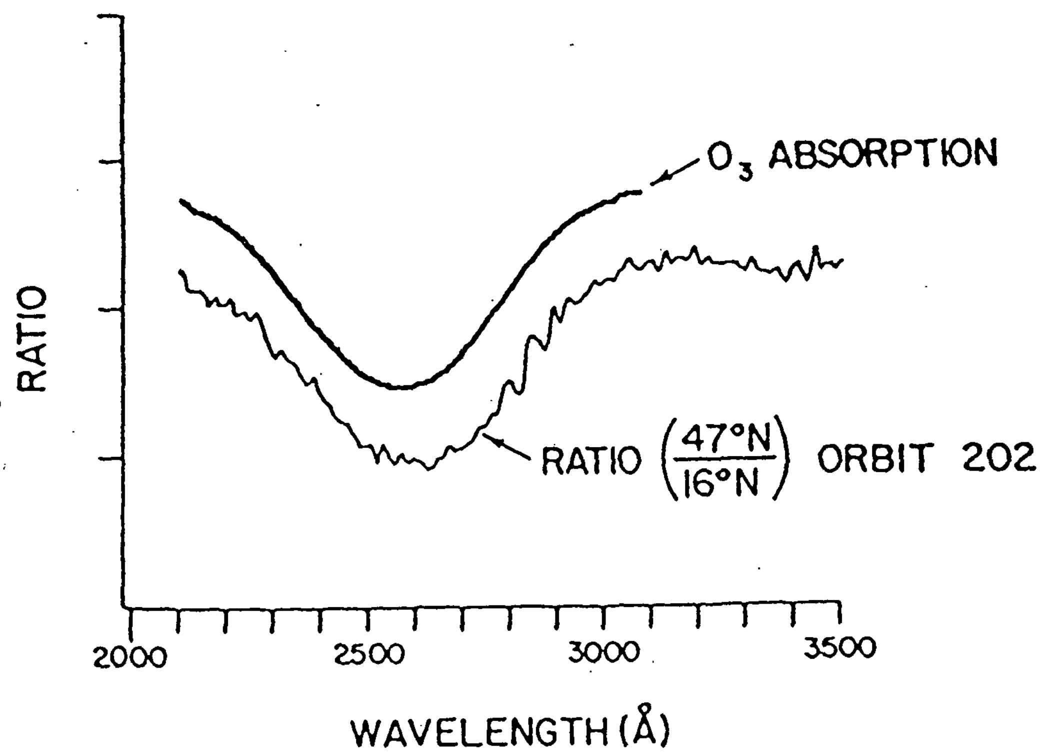

Figure 2 Ultraviolet spectrum measured by Mariner 9 at 57°N latitude on orbit 144 (upper plot). To enhance the ozone absorption feature, this spectrum was divided by one obtained at 20°N latitude on orbit 144, where ozone abundances are minimal. The ozone absorption feature for orbit 202 is compared to laboratory data in the lower plot (laboratory data is offset to facilitate comparison). Both figures are taken from Lane et al. (1973).

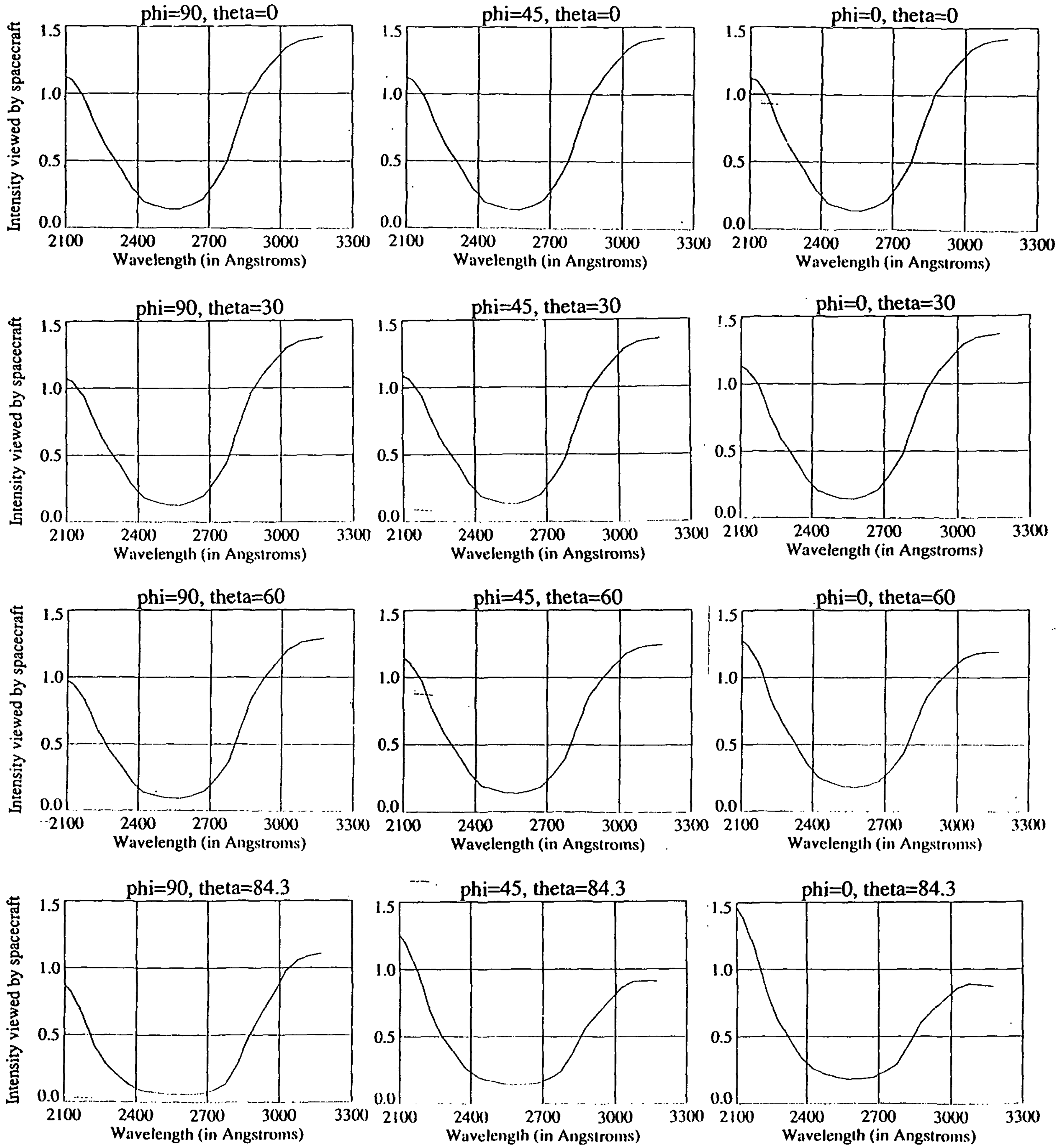

Figure 3. Synthetic ultraviolet spectra, ratioed to synthetic spectra for 20N latitude, shown for various viewing geometries (viewing angle theta relative to the zenith and azimuthal angle phi relative to the sun). As with Lane et al. (1973; see Fig. 2), intensity is unitless and relative. 30 μm-atm ozone, no dust or cloud, a solar zenith angle of 75 degrees, ice albedo 0.5, and uniform mixing ratio of ozone are assumed.

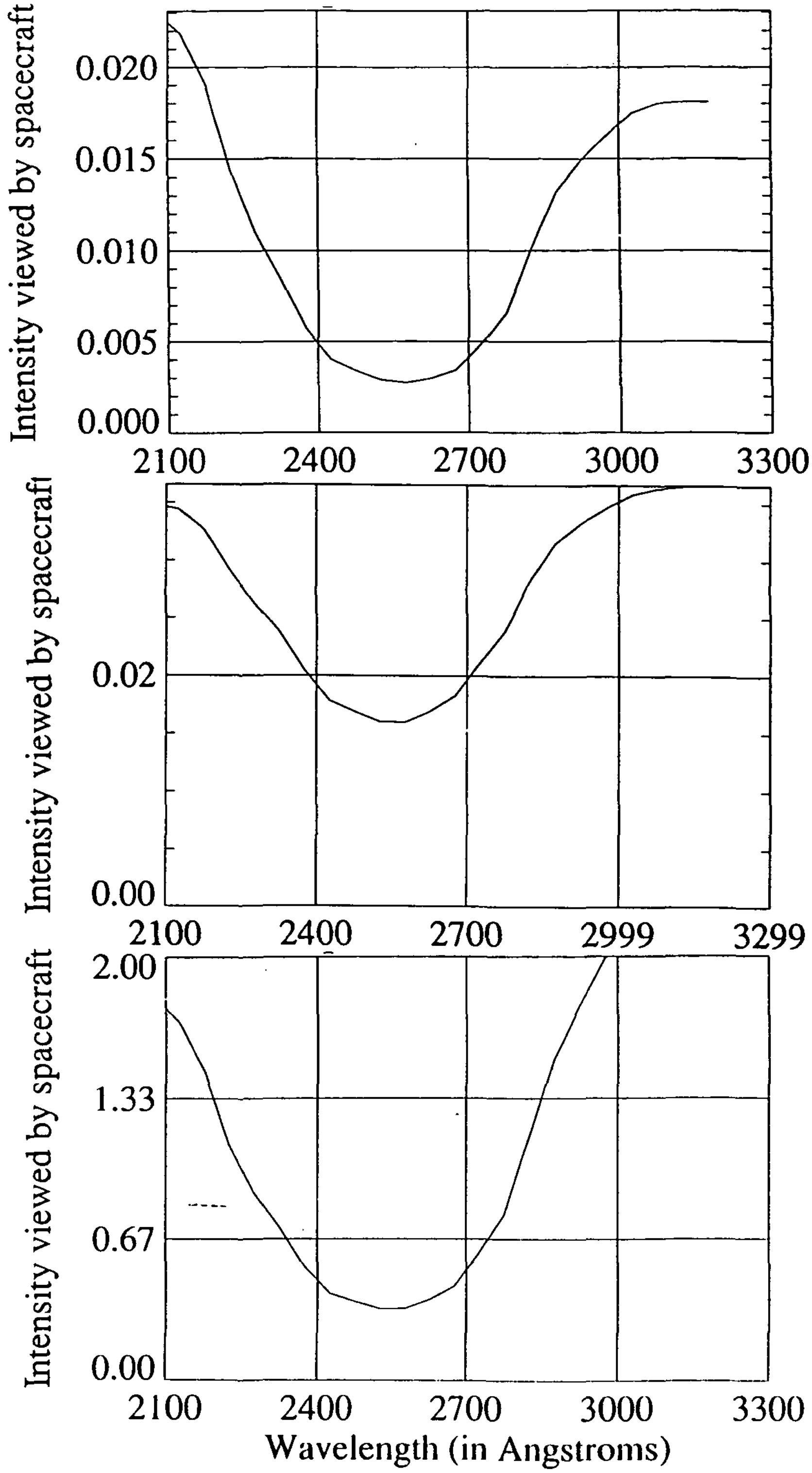

Figure 4. Synthetic ultraviolet spectra, ratioed to synthetic spectra for 20N latitude. Viewing geometry in all cases is viewing angle of 60 degrees, and azimuthal angle of 0 degrees. Atmospheric and surface parameters for the plots are as follows (showing ozone abundance, solar zenith angle (SZA), ice albedo, and cloud and dust opacity):

4(a) Ozone 30 μm-atm, SZA 75 degrees, Albedo 0.5, No dust, No cloud

4(b) Ozone 30 μm-atm, SZA 75 degrees, Albedo 0.5, dust 0.3, cloud 1.0

4(c) Ozone 100 μm-atm, SZA 75 degrees, Albedo 0.5, dust 0.3, cloud 1.0

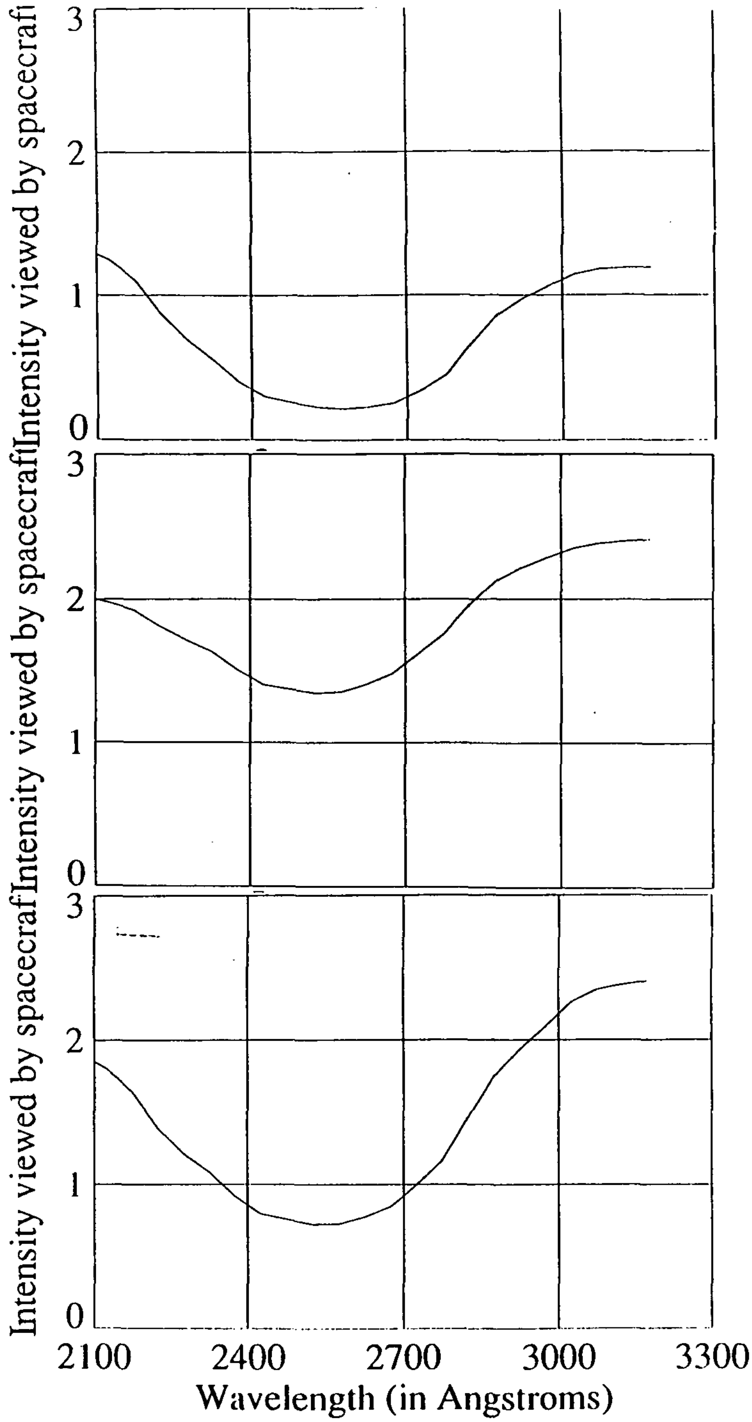

Figure 5. Synthetic ultraviolet spectra, ratioed to synthetic spectra for 20N latitude. Viewing geometry in all cases is viewing angle of 60 degrees, and azimuthal angle of 0 degrees. Atmospheric and surface parameters for the plots are as follows (showing ozone abundance, solar zenith angle (SZA), ice albedo, and cloud and dust opacity):

5(a) Ozone 30 µm-atm concentrated low in the atmosphere, SZA 75 degrees, Albedo 0.5, No dust, No cloud

5(b) Ozone 30 µm-atm concentrated low in the atmosphere, SZA 75 degrees, Albedo 0.5, dust 0.3, cloud 1.0

5(c) Ozone 100 µm-atm concentrated low in the atmosphere, SZA 75 degrees, Albedo 0.5, dust 0.3, cloud 1.0

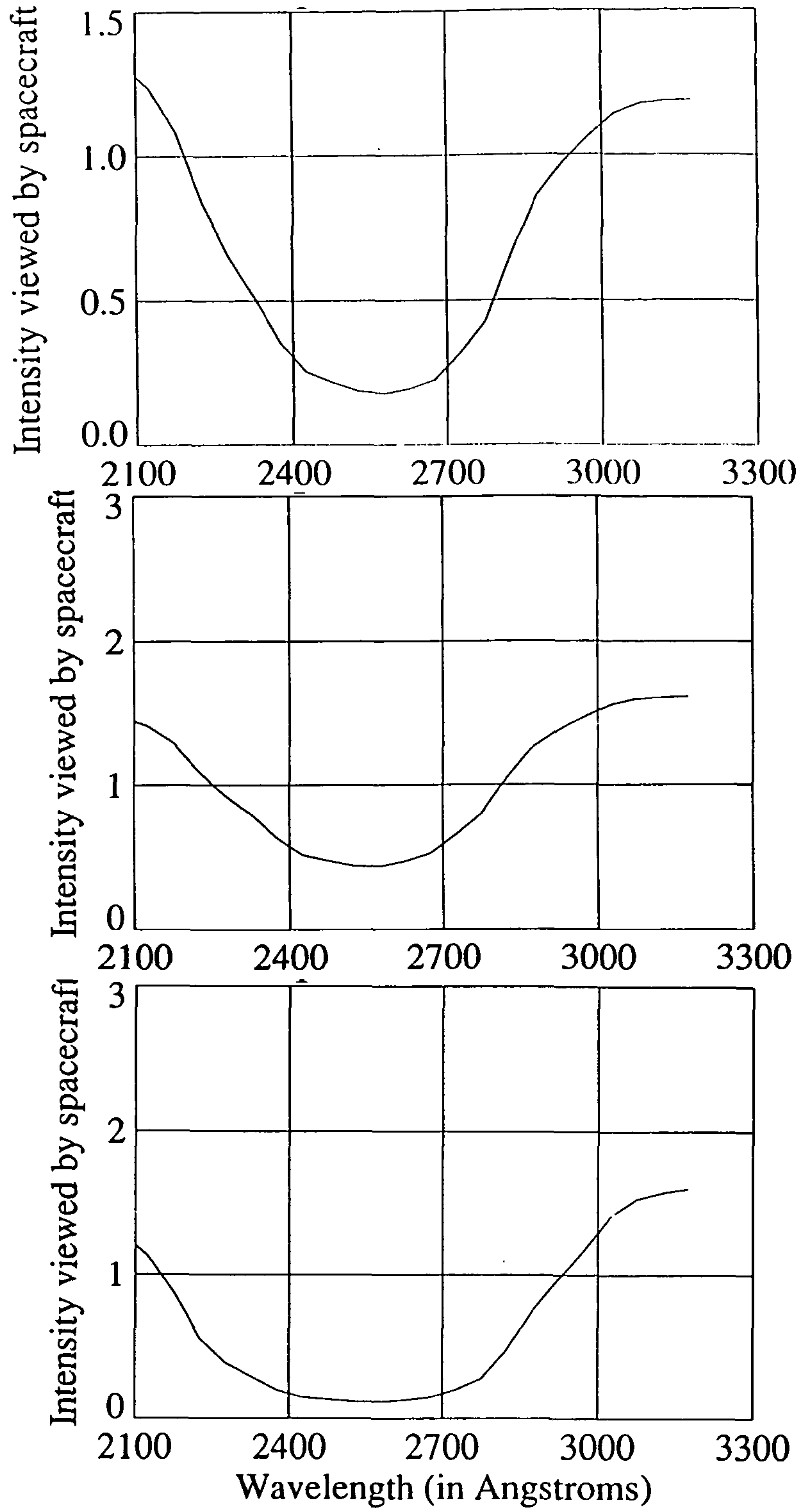

Figure 6. Synthetic ultraviolet spectra, ratioed to synthetic spectra for 20N latitude. Viewing geometry in all cases is viewing angle of 60 degrees, and azimuthal angle of 0 degrees. Atmospheric and surface parameters for the plots are as follows (showing ozone abundance, solar zenith angle (SZA), ice albedo, and cloud and dust opacity):

6(a) Ozone 30 μm-atm, SZA 75 degrees, Albedo 0.5, No dust, No cloud

6(b) Ozone 30 μm-atm, SZA 75 degrees, Albedo 0.5, dust 0.3, No cloud

6(c) Ozone 100 μm-atm, SZA 75 degrees, Albedo 0.5, dust 0.3, No cloud

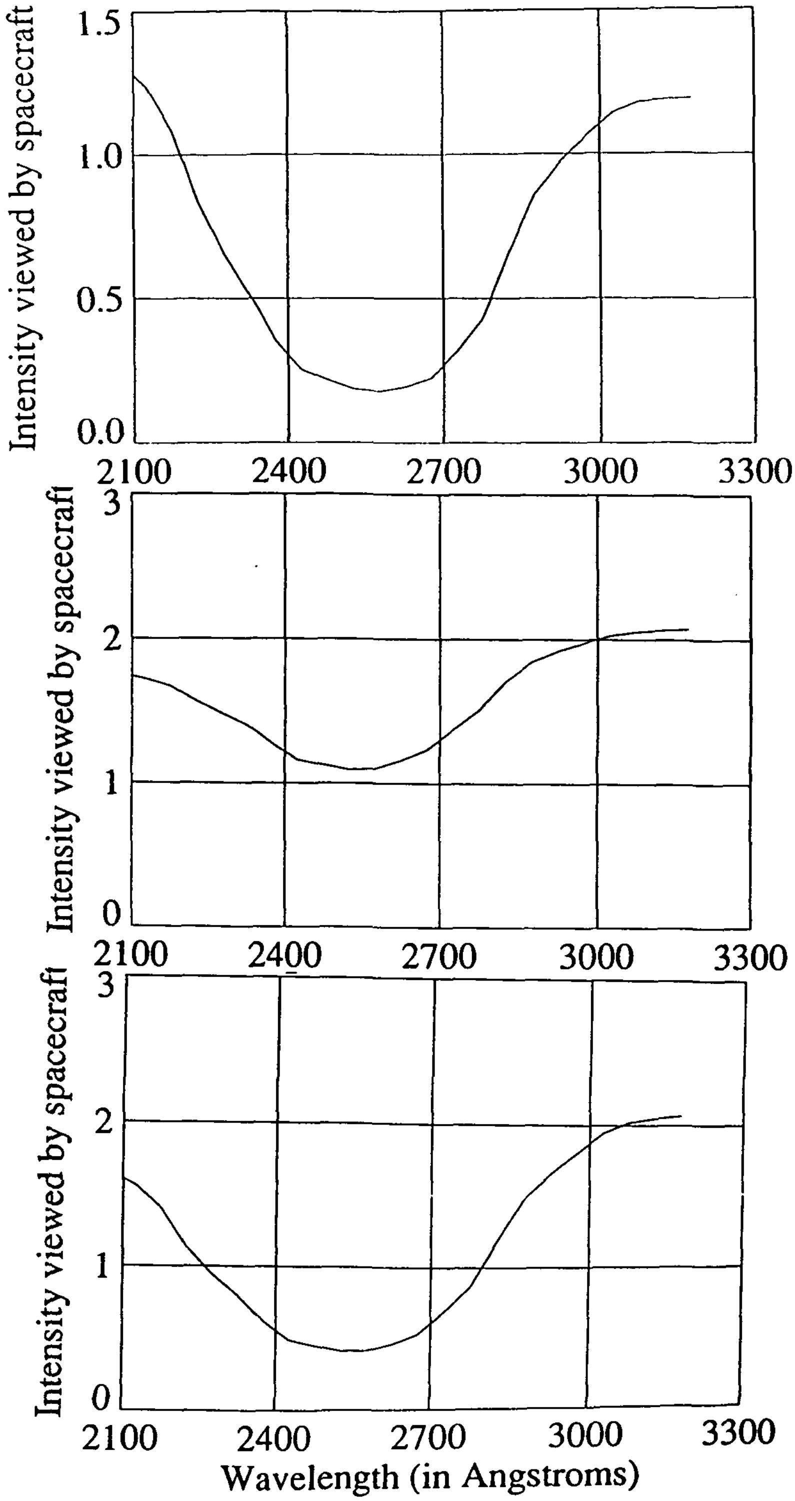

Figure 7. Synthetic ultraviolet spectra, ratioed to synthetic spectra for 20N latitude. Viewing geometry in all cases is viewing angle of 60 degrees, and azimuthal angle of 0 degrees. Atmospheric and surface parameters for the plots are as follows (showing ozone abundance, solar zenith angle (SZA), ice albedo, and cloud and dust opacity):

7(a) Ozone 30 μm-atm, SZA 75 degrees, Albedo 0.5, No dust, No cloud

7(b) Ozone 30 μm-atm, SZA 75 degrees, Albedo 0.5, dust 1.0, cloud 1.0

7(c) Ozone 100 μm-atm, SZA 75 degrees, Albedo 0.5, dust 1.0, cloud 1.0

II.4. Compare synthetic and observed spectra.

The synthetic and observed spectra compare quite favorably. In fact, the inclusion of dust and cloud absorption and scattering improve the synthetic fit to the slope in the data from 2100 to 2300 Angstroms. Comparison of Figures 4 and 5 shows how difficult it is to try to infer the ozone distribution from UV spectra. Two radically different ozone profiles were used, and yet the spectra exhibit similar behavior. Wehrbein (1977) examined the data in depth to retrieve the ozone distribution, and concluded that ozone is fairly well mixed in the atmosphere. Lindner (1988) also showed that ozone should be fairly well mixed based on theoretical simulations of atmospheric chemistry.

II.5. Error in inferring O_3 without considering dust/cloud.

Ozone has been classically inferred from the spectra by fitting the depth of the absorption at 2500 Angstroms. We have summarized the depth of absorption in Table 2 for many cases we have tried. What can be most clearly seen is that for all the cases we have tried, the amount of ozone inferred from the UV spectra is underestimated by about a factor of 3 when the inversion uses simply ozone absorption (i.e. ignoring cloud and dust). This is seen in Table 2 in that approximately 3 times as much O_3 is needed to produce the same depth in absorption for scenario in which we fully include the masking effects of cloud and dust to the case for which cloud and dust are ignored. This is particularly noteworthy in that even if the effect of cloud and dust is included in the retrieval, the uncertainty in cloud and dust opacity and scattering properties will still leave an uncertainty in retrieved ozone abundance of a factor of 2! Considering that the published ozone abundances retrieved from the

TABLE 2

2550/3200 ANGSTROM RATIO

O3	SZA	DUST	CLOUD	ALBEDO	O3 DIST.	RATIO
30	75	0	0	0.5	mixed	0.15
30	75	0.3	1	0.5	mixed	0.43
50	75	0.3	1	0.5	mixed	0.30
100	75	0.3	1	0.5	mixed	0.14
30	75	0.3	0	0.5	mixed	0.27
100	75	0.3	0	0.5	mixed	0.07
30	75	1	1	0.5	mixed	0.52
100	75	1	1	0.5	mixed	0.20
30	75	0	0	0.5	low	0.18
30	75	0.3	1	0.5	low	0.56
100	75	0.3	1	0.5	low	0.30
30	75	0	0	0.8	mixed	0.12
30	75	0.3	1	0.8	mixed	0.41
100	75	0.3	1	0.8	mixed	0.13
30	75	0	0	0.3	mixed	0.21
30	75	0.3	1	0.3	mixed	0.45
100	75	0.3	1	0.3	mixed	0.14
30	85	0	0	0.5	mixed	0.14
30	85	0.3	1	0.5	mixed	0.40
100	85	0.3	1	0.5	mixed	0.10
30	50	0	0	0.5	mixed	0.17
30	50	0.3	1	0.5	mixed	0.35
100	50	0.3	1	0.5	mixed	0.10

Mariner 9 data are used as a benchmark by all photochemical models of the Mars atmosphere, this has important implications for much of the modeling work done over the last 20 years.

Figure 6 shows that even simply ignoring a minimal dust opacity of 0.3 in a cloud-free atmosphere will underestimate the ozone abundance by a factor of 2. This is noteworthy in that dust was completely ignored in the earlier inferences of ozone from the spectra by Lane et al. (1973) and others. Dust abundances are always of this order or higher (Pollack et al., 1979).

Figure 7 shows that for high dust/cloud loading the inferred ozone abundance is a factor of 4 or 5 below what is truly there. Pollack et al. (1979) note that perhaps 20% of the martian year during the Viking observation period had this extent of dust loading or greater.

Table 2 does show that errors in retrieval are the same for all solar zenith angles we looked at, and for all ice albedo below 0.5. For high ice albedo, ozone becomes even more severely underestimated.

II.6. Reflectance Spectroscopy efficacy.

Figures 3 through 7 and Table 2 show that to properly retrieve the ozone abundance from the Mariner 9 UV spectra with the reflectance spectroscopy technique, the effects of cloud and dust must be considered. Therefore, the efficacy of the reflectance spectroscopy technique is only as good as the accuracy with which we know the opacity and scattering properties of the dust and cloud itself. Clancy and Lee (1991) have done the definitive study to date of retrieving these cloud and dust parameters. However, even with their study, there remain large uncertainties in the spatial and temporal variability in opacity and scattering properties, and also in the wavelength dependence of these properties.

The amount of other spacecraft sensors and observations needed to obtain these properties to the degree needed to obtain ozone abundance to within a 10 to 20 % uncertainty is enormous. This raises serious doubts about the efficacy of this technique for retrieving ozone. Also, the reflectance spectroscopy technique does not convey any information about night-time ozone, and since most of the winter polar region where ozone is abundant is in night, most of the region where ozone is abundant is unexplored. I seriously recommend that other techniques be examined before designing future Mars Aeronomy sensors; perhaps detecting ozone at other wavelengths such as in the infrared, or by detecting ozone in-situ, as I have proposed to NASA.

II.7. Presentations made at conferences.

Several conferences were attended which were partly or fully funded by this contract. Reprints of papers and abstracts published at these meetings are included in the Appendix.

IUGG Assembly. I attended the International Union of Geodesy and Geophysics Assembly in Vienna, Austria, in August 11-24 1991, and presented a paper entitled "Mars seasonal CO_2-ice lifetimes and the angular dependence of albedo" in the special Mars climate session. The abstract appeared in the conference proceedings (see Appendix). Half of expenses were paid by NASW-4614 and half were paid by another contract.

PCI Symposium. I attended the International Symposium on the chemistry and physics of ice, held in Sapporo, Japan Sept. 1-7, 1991, and presented a paper entitled "Why is the north polar cap on Mars different than the south polar cap?" in the extraterrestrial ice session. The abstract appeared in the conference proceedings (see Appendix). Contract NASW-4614 paid for registration and publication costs only.

MSATT Workshop. I attended the Mars Surface and Atmosphere Through Time Workshop, held in Boulder, Colorado Sept. 23-25, 1991, and presented a paper entitled "Simulations of the seasonal polar caps on Mars". The abstract appeared in the workshop proceedings put out by the Lunar and Planetary Institute in Houston (see Appendix). NASW-4614 paid for expenses, but these were limited mostly to airfare and registration due to gratis accommodations, food, and car (paid by LPI).

MSATT Workshop. I attended the Mars Surface and Atmosphere Through Time Workshop on innovative instrumentation for the in situ study of atmosphere-surface interactions on Mars held in Mainz, Germany October 8-9, 1992. Results presented in this report were presented in a paper entitled "Does UV instrumentation effectively measure ozone abundance?" (see Appendix). Grant NASW-4614 paid partial support (45%) (with remaining support coming from another contract).

Lab. Research Planetary Atmospheres Conference. I attended the Fourth International Conference on Laboratory Research for Planetary Atmospheres held in Munich, Germany October 10-11, 1992. A paper entitled "How well is martian ozone inferred with reflectance spectroscopy?" presented results from this contract (see Appendix). Grant NASW-4614 provided for partial support (note that this conference was concurrent with the MSATT Workshop, limiting costs).

Planetary Science Conference. I attended the American Astronomical Society Division of Planetary Science Conference held in Munich, Germany October 12-16, 1992. A paper entitled "Martian polar cap seasonal regression simulations" was presented (see Appendix). Grant NASW-4614 provided for partial support (note that this conference was concurrent with the MSATT Workshop, limiting costs).

MSATT Workshop. I attended the Mars Surface and Atmosphere Through Time Workshop on The Polar Regions of Mars: Geology, Glaciology, and Climate History held in Houston, Texas November 13-15, 1992. A paper entitled "Is carbon dioxide ice permanent?" was presented and published by LPI (see appendix). Grant NASW-4614 provided support.

AMS Annual Meeting Chemistry Session. I attended the American Meteorological Society Annual Meeting Session on Atmospheric Chemistry held in Anaheim, California January 1993. A paper entitled "Atmospheric chemistry on Mars" presented results from this contract (see Appendix). The bulk of support came from another contract, but grant NASW-4614 paid for registration and publication costs for this session.

AAAS Annual Meeting. I attended the American Association for the Advancement of Science annual meeting held in Boston, Mass., Feb. 1993. A paper presenting results from this contract entitled "The abundance of ozone on Mars" was presented and published by the AAAS (see appendix). Grant NASW-4614 provided support (limited to registration since I live in Boston).

Optical Remote Sensing of the Atmosphere. I attended the Optical Remote Sensing of the Atmosphere conference held by the Optical Society of America in Salt Lake City, Utah, March, 1993 and presented a paper entitled "Probing the martian atmosphere in the ultraviolet" which presented results from this contract (see Appendix). Grant NASW-4614 provided partial support, with the bulk of support supplied by another contract.

MSATT Workshop. I attended the Final Mars Surface and Atmosphere Through Time Workshop on Mars: Past, Present, and Future -

Results from the MSATT Program held in Houston, Texas November, 1993 and presented two papers entitled "The effect of polar caps on obliquity" and "How well was total ozone abundance inferred with Mariner 9?", which presented results from this contract. Both papers were published by the Lunar and Planetary Institute (see appendix). Grant NASW-4614 provided support.

Low-Cost Planetary Missions Conference. An abstract entitled "In-Situ Mars Ozone Detector" has been accepted for presentation at the International Academy of Astronautics International Conference on Low-Cost Planetary Missions to be held in Baltimore, Maryland in April 1994. The abstract (copy enclosed in the appendix) will be published in a book of abstracts.

II.8. Publications

An invited contribution for the Questions and Answers section was published in The Planetary Report, Volume 14, p.21, 1994. This is an overview of ozone on Mars for the general public. A reprint is included in the Appendix.

A paper entitled "Mars Ozone: Mariner 9 Revisited" has been submitted to Geophysical Research Letters. This paper summarizes the principal findings within this project. A preprint is included in the Appendix.

A paper entitled "In-Situ Mars Ozone Detector" will soon be submitted to Acta Astronautica. This paper will describe a possible new ozone measurement technique which would avoid most of the error and uncertainty involved with the reflectance spectroscopy technique. Dr. Elliot Weinstock of the Harvard University Applied Physics Lab. has been part of a team which has measured ozone in the Earth's stratosphere via balloon, and we have been involved in examining the feasibility of sending this instrument to Mars. An abstract by the same name is in the appendix describing more details. A proposal by Dr. Weinstock and myself to undertake these studies is currently under consideration at the NASA PIDDP Program and the NASA Advanced Studies Program.

A paper entitled "Ozone heating in the martian atmosphere" was published in Icarus, Volume 93, pp. 354-361, 1991. This paper describes the contribution of ozone to the energy budget of the martian atmosphere. This work was completed earlier, but would not have been published had I not received assistance under this contract. A reprint is included in the Appendix.

A paper entitled "Sunlight penetration through the martian polar caps: Effects on the thermal and frost budgets" was published in Geophysical Research Letters, Vol. 19, pp. 1675-1678, 1992. This paper describes modeling studies of the polar cap frost and thermal budgets and the effect of including the penetration of sunlight into the caps, which was previously always assumed to be absorbed only at the surface. This work was completed earlier, but would not have been published had I not received assistance under this contract. A reprint is included in the Appendix.

A manuscript entitled "The hemispherical asymmetry in the martian polar caps" was published in J. Geophys. Res. , Vol. 98, pp.3339-3344, 1993, in their special MSATT issue commemorating papers presented at the Workshop on the Martian Surface and Atmosphere Through Time. This paper describes how the radiative effects of clouds and dust result in a hemispherical asymmetry in the residual polar caps, as has been observed. This work was completed earlier, but would not have been published had I not received assistance under this contract. A reprint is included in the Appendix.

A chapter in the book Physics and Chemistry of Ice entitled "CO_2-ice on Mars: Theoretical Simulations" has been published by Hokkaido University Press, Sapporo, N. Maeno and T. Hondoh, ed.s, 1992. This chapter describes how CO2 ice stability can be modeled and what has been learned. This work was completed earlier, but would not have been published had I not received assistance under this contract. A reprint is included in the Appendix.

A manuscript entitled "Cooling the martian atmosphere: The spectral overlap of the CO_2 15 μm band and dust" has been accepted for publication in Planet. Space Sci. and is in Press. This paper describes the proper procedure for calculating the infrared radiative transfer in the martian atmosphere. This work was completed earlier, but would not have been published had I not received assistance under this contract. A preprint is included in the Appendix.

A manuscript entitled "Martian atmospheric radiation budget" has been submitted to Publ. Astron. Soc. Japan. This paper describes the contribution of CO2 and dust to the solar and IR energy budgets of the martian atmosphere. This work was completed earlier, but would not have been published had I not received assistance under this contract. A preprint is included in the Appendix.

A paper entitled 'Comment on "Mars secular obliquity change due to the seasonal polar caps" by David Parry Rubincam' has been submitted to J. Geophys. Res.. This paper describes the interaction between the orbital parameters of Mars and the polar caps of Mars. This work was completed under this contract, but is really nothing more than a comment and hence does not merit any discussion here other than a reference to the preprint which is included in the Appendix.

II.9. Honors Awarded. During the course of this research, Dr. Lindner received 2 honors for his Mars research. Dr. Lindner was elected as a new member of the International Association of Meteorology and Atmospheric Physics Commission on Planetary Atmospherics and their Evolution (a part of the International Union of Geodesy and Geophysics).

Dr. Lindner was also recently nominated for the European Geophysical Society Young Scientists' Publication Award for his Planetary and Space Science Manuscript entitled "Cooling the martian atmosphere: The spectral overlap of the CO_2 15 μm band and dust". The winner of this award will be announced soon.

III. Recommendations and Conclusions

The primary objectives for the work have been completed. Mariner 9 UV Spectrometer data have been reinverted for the ozone abundance. The spectra were fit by models which covered the full range in observed solar zenith angle, cloud, dust and ozone amount, ice albedo and look angles. This work has shown that significant underestimation of ozone occurred in earlier analysis of Mariner 9 data, and that much of the observed variability in Mars ozone is due to masking of ozone by clouds and dust. As these previously published abundances have been used as a benchmark for all theoretical photochemical models of Mars, some of this work will have to be reinvestigated. The efficacy of the reflectance spectroscopy technique at retrieving the ozone abundance on Mars is questioned. The technique is incapable of retrieving ozone at night and during dust storms, and has as much as a factor of 3 error at other times. An in-situ measurement by balloon is recommended as it is the only technique capable of accurately inferring the ozone abundance in all conditions. Studies of the effectiveness of such a mission are recommended.

Publications wholely or partly under this contract

(reprints are in the appendix)

1. Refereed Papers

Lindner, B. L., Ozone heating in the martian atmosphere, Icarus, 93, 354-361, 1991a.

Lindner, B. L., Sunlight penetration through the martian polar caps: Effects on the thermal and frost budgets, Geophys. Res. Lett., 19, 1675-1678, 1992a.

Lindner, B. L., CO_2-ice on Mars: Theoretical simulations, in Physics and Chemistry of Ice, N. Maeno and T. Hondoh, ed.s, pp. 225-228, Hokkaido University Press, Sapporo, 1992c.

Lindner, B. L., The hemispherical asymmetry in the martian polar caps, J. Geophys. Res., 98, 3339-3344, 1993a.

Lindner, B. L., Questions and Answers, in The Planetary Report, 14, 21,1994a.

Lindner, B. L., Cooling the martian atmosphere: The spectral overlap of the CO_2 15 μm band and dust, Planet. Space Sci., in Press,1994b.

Lindner, B. L., Martian atmospheric radiation budget, submitted to Publ. Astron. Soc. Japan, 1994c.

Lindner, B. L., Mars Ozone: Mariner 9 Revisited, submitted to Geophys. Res. Lett., 1994d.

Lindner, B. L., Comment on "Mars secular obliquity change due to the seasonal polar caps" by David Parry Rubincam, submitted to J. Geophys. Res., 1994e.

2. Conference Proceedings Publications

Lindner, B. L., Why is the north polar cap on Mars different than the south polar cap?, Summaries, International Symposium on the Physics and Chemistry of Ice, p. 120-121, held in Sapporo Japan, Sept. 1-6, 1991b.

Lindner, B. L., Mars seasonal CO_2-ice lifetimes and the angular dependence of albedo (abstract), in International Union of Geodesy and Geophys. General Assembly XX, IAMAP Program and Abstracts, p. 309, published by RM-Druck- and Verlagsgesellschaft, Graz, Austria, 1991c.

Lindner, B. L., Simulations of the seasonal polar caps on Mars, in Workshop on the martian surface and atmosphere through time, p. 76-77, published by Lunar and Planetary Institute, Houston, Texas, 1991d.

Lindner, B. L., Does UV instrumentation effectively measure ozone abundance?, in Workshop on innovative instrumentation for the in situ study of atmosphere-surface interactions on Mars, B. Fegley, Jr. and H. Waenke, ed.s, pp. 10-11, LPI Tech. Rep. #92-07, Part 1, Lunar and Planetary Institute, Houston, Texas, 1992b.

Lindner, B. L., Martian polar cap seasonal regression simulations (abstract), Bull. Amer. Astron. Soc., 24, 1013-1014, 1992d.

Lindner, B. L., How well is martian ozone inferred with reflectance spectroscopy? (abstract), in Program of invited papers and contributed posters, for the Fourth International Conference on Laboratory Research for Planetary Atmospheres, pp. 46, held in Munich, Germany, Oct. 10-11, 1992e.

Lindner, B. L., Is carbon dioxide ice permanent?, in Workshop on the polar regions of Mars: Geology, glaciology and climate history, Clifford, S.M., Howard, A.D., and Paterson, W.S.B., eds., pp. 16-17, LPI Tech. Rpt. 92-08, Part 1, Lunar and Planetary Institute, Houston, Texas, 1992f.

Lindner, B. L., The abundance of ozone on Mars (abstract), in American Association for the Advancement of Science 1993 annual meeting program, pp.236-237, AAAS Publication 93-03S, American Assoc. Advance. Sci., Washington, D.C., 1993b.

Lindner, B. L., Atmospheric chemistry on Mars, in Conference on Atmospheric Chemistry, pp. 11-14, American Meteorological Society, Boston, Mass.,1993c.

Lindner, B. L., Probing the martian atmosphere in the ultraviolet, in Optical Remote Sensing of the Atmosphere, 1993 Technical Digest Series Volume 5, pp.153-156, Optical Society of America, Washington, D.C., 1993d.

Lindner, B. L., The effect of polar caps on obliquity, in Mars: Past, Present, and Future - Results from the MSATT Program, Haberle, R., eds., LPI Tech. Rpt. No. 93-06,Pt. 1, pp. 26-27, Lunar and Planetary Institute, Houston, Texas, 1993i.

Lindner, B. L., How well was total ozone abundance inferred with Mariner 9?, in Mars: Past, Present, and Future - Results from the MSATT Program, Haberle, R., eds., LPI Tech. Rpt. No. 93-06,Pt. 1, pp. 25-26, Lunar and Planetary Institute, Houston, Texas, 1993j.

Lindner, B.L., In-Situ Mars Ozone Detector, in Proceedings, International Conference on Low-Cost Planetary Missions, International Academy of Astronautics, Paris, France, 1994f.

Bibliography

Clancy, R.T. and S. W. Lee, A new look at dust and clouds in the Mars atmosphere: Analysis of emission-phase-function sequences from global Viking IRTM observations, Icarus, 93, 135-158, 1991.

Lane, A. L., C. A. Barth, C. W. Hord and A. I. Stewart, Mariner 9 ultraviolet spectrometer experiment: Observations of ozone on Mars, Icarus, 18, 102-108, 1973.

Lindner, B. L., The aeronomy and radiative transfer of the Martian atmosphere, Ph.D. Dissertation, 470 pp., University of Colorado, Boulder, 1985.

Lindner, B. L., Ozone on Mars: The effects of clouds and airborne dust, Planet. Space Sci., 36, 125-144, 1988.

Pollack, J. B., D. S. Colburn, F. M. Flasar, R. Kahn, C. E. Carlston, and D. Pidek, Properties and effects of dust particles suspended in the martian atmosphere, J. Geophys. Res., 84, 2929-2945, 1979.

Stamnes, K., S.C. Tsay, W. Wiscombe, and K. Jayaweera, Numerically stable algorithm for discrete-ordinate-method radiative transfer in multiple scattering and emitting layered media, App. Optics, 27, 2502-2509, 1988.

Wehrbein, W. M., Description of the vertical distribution of ozone in the martian atmosphere from Mariner 9 ultraviolet spectrometer data, Ph. D. Dissertation, 174 pp., University of Colorado, Boulder, 1977.

Appendix

Reprints and preprints of publications made under this contract

(in the order listed earlier)

ICARUS 93, 354–361 (1991)

Ozone Heating in the Martian Atmosphere

BERNHARD LEE LINDNER

AER, Inc., 840 Memorial Drive, Cambridge, Massachusetts 02139

Received November 19, 1990; revised May 28, 1991

Ozone is shown to be a minor, although nonnegligible, heat source in the martian atmosphere, in contradiction to earlier reports which had suggested a larger contribution to the atmospheric heat budget by ozone. It is further shown that the observed hemispherical asymmetry in ozone abundance is unlikely to be a significant factor in the observed hemispherical asymmetry in the permanent polar caps. Ozone heating may still be an important consideration in the formation and decay of clouds and snowfall, although not as important as previously suggested. © 1991 Academic Press, Inc.

INTRODUCTION

Prabhakara and Hogan (1965) constructed the first and only photochemical-radiative transfer model of the Martian atmosphere. Their model indicated that ozone had a significant influence on the temperature structure. However, they ignored the odd hydrogen catalytic cycle and, thus, overestimated the ozone abundance by several orders of magnitude. Also, since the abundance and composition of the atmosphere were poorly known prior to spacecraft exploration of Mars, many inaccurate assumptions regarding the atmospheric properties were made.

Ozone was first measured on Mars by the Mariner 7 UV spectrometer (Barth and Hord 1971) and was mapped across the planet for half a Mars year by Mariner 9 (Barth *et al.* 1973). Based on these measurements, ozone was suggested to be an important contributor to the atmospheric temperature in the polar regions by Kuhn *et al.*(1979). Radiative equilibrium temperatures computed by Kuhn *et al.* were up to 10 K higher when ozone heating was included. Kuhn *et al.* also suggested that ozone may be important as a heat source in determining precipitation and cloud formation, as temperatures at polar winter latitudes are very near the condensation temperature of CO_2 and H_2O. They further speculated that the observed hemispherical asymmetry in O_3 (Barth *et al.* 1973) may explain the observed hemispherical asymmetry in the composition of the residual polar caps (Kieffer *et al.* 1976, Kieffer 1979).

This study examines the absorption of solar radiation by ozone in the Martian atmosphere more closely. Both earlier studies neglected dust heating rates, which are included here. Furthermore, the possibility that ozone may have an effect on polar-cap ice abundance is examined.

MODELING APPROACH

The radiative intensity as a function of altitude from the surface to 40 km is calculated for 57 solar wavelength intervals. The discrete ordinate method of Stamnes and Conklin (1984) is used to compute the scattering and absorption of solar radiation by O_3, CO_2, O_2, H_2O, H_2, HO_2, H_2O_2, and dust. The mixing ratios of CO_2, O_2, and H_2 are taken as 95.4, 0.13, and 0.002%, respectively (Anderson 1974, Liu and Donahue 1976, Owen *et al.* 1977, Krasnopolsky and Parshev 1979). Significant reduction in the mixing ratio of CO_2 over the winter polar region because of the condensation of CO_2 is unlikely, based on meterological constraints (Hess 1979). The mixing ratio of O_2 is based on observations (Trauger and Lunine 1983), but is also reproduced through photochemical modeling (e.g., Lindner and Jakosky 1985). The winter polar atmosphere appears to be saturated in H_2O at all altitudes, although evidence is sparse (Davies, 1979, Jakosky, 1985). Thus the vapor pressure there of H_2O as a function of temperature is given by the Clausius–Clapeyron equation for saturation pressure. HO_2 and H_2O_2 abundances are taken from Lindner (1988). The existence of H_2O_2 has not been confirmed by direct measurement, and thus remains speculative. However, it has been predicted by atmospheric modeling (e.g., Kong and McElroy 1977b). The altitude profiles of CO_2, O_2, H_2, and the pressure are determined from the hydrostatic equation. The surface pressure for 57°N latitude in late winter is taken to be 8 mbar, based on Viking lander observations (Hess *et al.* 1980) corrected for elevation (Lindal *et al.* 1979, Jakosky and Farmer 1982).

Late winter (L_s = 343°) conditions for a latitude of 57°N were chosen for this study, as these were the conditions

0019-1035/91 $3.00

when Mariner 9 observed the maximum O_3 column abundance of 57 μm-atm (Barth *et al.* 1973). (The aerocentric longitude of the Sun, L_s, is the seasonal index; $L_s = 0°$, 90°, 180°, and 270° correspond to northern spring equinox, summer solstice, autumnal equinox, and winter solstice, respectively). The O_3 mixing ratio used here is virtually constant between 10 and 30 km altitude. The surface loss of ozone (Kong and McElroy 1977b) causes a reduction in the mixing ratio at the surface of 30% (Lindner 1988). Ozone surface loss is not as active in the winter polar regions because of the cold temperatures and frost-covered surface. Ozone decreases above 30 km because the primary production mechanism is a three-body reaction which becomes ineffective at high altitudes. The altitude dependence of O_3 abundance has not been measured in the polar regions, but is predicted by photochemical models (Lindner 1988), and is therefore subject to the usual uncertainties of these models.

The properties of dust are extrapolated from observations at mid-latitudes, given the lack of observations at winter polar latitudes. Background (i.e., non-dust-storm) dust opacities over the Viking landers varied seasonally from 0.2 to 1.0 (Pollack *et al.* 1979), although year-to-year differences seem likely. The altitude profile of the background dust mixing ratio is approximated here with a Gaussian profile of the form $\exp(-z^2/650)$, where z is altitude in kilometers. This results in background dust opacity confined mostly below 20 km altitude. The wavelength dependence of the dust opacity is taken from Toon *et al.*(1977). The single-scattering albedo of airborne dust as a function of wavelength is taken from Zurek (1978, 1982), using a solar average of 0.86 (Pollack *et al.* 1979). The Haze–L phase function (Diermendjian 1969) is used to describe the scattering of radiation by martian dust. The Haze–L phase function provided the best fit to Mariner 9 IR spectra (Toon *et al.* 1977).

Small temperature inversions are common for winter polar latitudes. The temperature profile at 57°N latitude that is used in this study rises linearly with altitude from 150 K at the surface to 170 K at 6 km altitude and then falls linearly with increasing altitude to 130 K at 40 km. The temperature profile at 70°N latitude is the same as that used at 57°N latitude except that it has a peak temperature of 155 K at 6 km. These temperature profiles are extrapolated from radio occultation observations made near winter polar latitudes during background dust conditions (Lindal *et al.* 1979) and agree with temperatures obtained by the Viking IRTM experiment (Kieffer 1979). Temperatures are markedly higher at the time of the global dust storms, but global dust storms are not considered here. The surface at 57°N and 70°N latitude in late winter is covered with old ice (Iwasaki *et al.* 1982), with a typical albedo of 0.5 (Kieffer *et al.* 1976). The surface is assumed to reflect according to Lambert's law.

TABLE I
Absorption Cross-Section References

CO_2	Shemansky 1972, Lewis and Carver 1983
O_3	Daumont *et al.* 1983, Freeman *et al.* 1984, Paur and Bass 1985; Griggs 1968
O_2	Ogawa 1971
H_2O	Thompson *et al.* 1963, Hudson 1971
H_2O_2	Lin *et al.* 1978, Molina and Molina 1981, Demore *et al.* 1985
HO_2	Hochandel *et al.* 1972, Demore *et al.* 1985
H_2	Hudson 1971

Absorption cross-sections (σ) for CO_2, O_3, O_2, H_2O, H_2O_2, HO_2, and H_2 are taken from the references shown in Table I, taking into account the temperature dependencies of $\sigma(CO_2)$ and $\sigma(O_3)$. The temperature dependence causes $\sigma(CO_2)$ to change as much as a factor of 3 at some wavelengths. The importance of the temperature dependence of $\sigma(CO_2)$ was stressed in a study of martian photodissociation and heating rates by Parisot and Zucconi (1984). The UV heating rate of CO_2 and other constituents differs by as much as a factor of 2 or more depending on whether or not the temperature correction is included (Parisot and Zucconi 1984). However, Parisot and Zucconi (1984) did not use the improved measurements of the temperature dependence of $\sigma(CO_2)$ by Lewis and Carver (1983). Using the Lewis and Carver measurements, I find an even greater change in UV heating rates due to the temperature dependence. Furthermore, the temperature dependence of $\sigma(CO_2)$ is even more important to consider in the winter polar region where temperatures are the lowest on the planet (Parisot and Zucconi studied equatorial latitudes).

The only appreciable (>10%) temperature-dependent changes in O_3 cross-sections are longward of 2700 Å. Total O_3 heating rates are lowered by up to 30% when the temperature dependence is included. Temperature dependencies for the cross-sections of O_2, H_2O, HO_2, and H_2O_2 are not available, although this is expected to be a small effect (Frederick and Hudson 1980). All absorption of solar radiation is assumed to go completely into instantaneous and local heating.

The cross-sections and solar intensities were treated as constant over 50-Å intervals. These intervals were then summed from 1500 to 3200 Å, with an added term for the Chappuis bands of ozone from 4000 to 7000 Å, in 100-Å intervals. At wavelengths less than 1500 Å, cross-sections were not needed since CO_2 is optically thick and no contribution to the heating rate is made, even at 40 km altitude. Wavelength intervals of 1 μm are used out to 5 μm to compute dust heating rates. The solar intensity is taken from Rottman (1981), corrected for the orbital eccentricity and orbital radius of Mars.

Atmospheric properties are zonally averaged and assumed azimuthally independent. To account for vertical inhomogeneity, the atmosphere is divided into twenty layers, each of which is characterized by one pressure and one temperature. Rodgers and Walshaw (1966) have shown that an altitude spacing of 0.2 scale height results in errors in heating and cooling rates of less than 0.03 degrees per day, and so a grid spacing of 2 km was chosen.

Heating rates are diurnally averaged as in Cogley and Borucki (1976), except that their derivation is repeated using the Chapman function instead of the secant function, integrating over time numerically. Because diurnal variations are characteristically double-valued (one value for daytime, switching quickly to another nighttime value), a two-level parameterization is adopted here. The day/night ratio in the number of densities of O_3, HO_2, and H_2O_2 is taken from Shimazaki (1981), which shows agreement with day/night ratios from Krasitskii (1978) despite the large difference in latitude (equatorial versus polar).

The value of the specific heat was taken to be 840 J kg^{-1} K^{-1}. Values ranging from 750 to 900 have been used over the years by the various researchers studying the Mars atmosphere (see Lindner 1985). Further experimental research as to the value of the specific heat of the martian atmosphere is recommended in view of its importance in atmospheric heating rates. An exponentially averaged density over each layer was used in the calculation of heating rates to prevent an artificially sloping profile of the heating rate with altitude. Aerosols were not included in the density as the column abundance of airborne aerosols for normal dust loadings is 5×10^{-4} g cm^{-2} (Pollack *et al.* 1979), five orders of magnitude below the column abundance of gas. It is also important to remember that the atmosphere is only 95% CO_2 and that the flux calculations based on absorption by CO_2 use 95% of the atmospheric number density, while the heating rate applies to the density of all species combined. Ignoring this effect can change heating rates by 5%, and resultant temperatures by 6 K (Kondrat'ev *et al.* 1973).

RESULTS

Figure 1 compares the vertical optical depths of dust, Rayleigh scattering, CO_2, and O_3 as functions of wavelength. Wavelengths shortward of 1700 Å are optically thick even at 40 km altitude, due to absorption by CO_2 in the upper atmosphere. Appreciable contribution to atmospheric heating rates does not occur until 1800 Å, at which point the opacities of Rayleigh scattering and dust are both appreciable. Gaseous absorption shortward of 1900 Å is due primarily to CO_2, with some contribution by O_2. Between 1950 and 2150 Å, Rayleigh scattering and dust each have optical depths greater than that of CO_2 and O_3. Ozone absorption is appreciable between 2000 and 3000 Å, having vertical optical depths of almost 2 at 2500 Å. Because solar zenith angles are very large in the winter polar region, the optical depth the solar radiation actually traverses is many times the vertical optical depth shown in Fig. 1. This means that very little ultraviolet radiation shortward of 3000 Å actually reaches the surface. At visible wavelengths, the optical depth is dominated by dust absorption and scattering. The only gaseous absorption is that of the ozone Chappuis bands. As these bands are far weaker than the ultraviolet bands, the optical depth is much smaller.

Rayleigh scattering is an important consideration in the computation of UV heating rates. Including Rayleigh scattering causes an increase in CO_2 UV heating rates above 20 km altitude, and a decrease in CO_2 UV heating rates below 20 km altitude. A 30% increase in CO_2 UV heating rates occurs at 40 km altitude, and a 50% decrease occurs at the surface (Lindner 1988). The Rayleigh scattering optical depth as a function of wavelength is given by Hansen and Travis (1974). The refractive indices of CO_2, Ar, N_2, CO, and O_2 (the major gases in the martian atmosphere) are 1.000450, 1.000281, 1.000300, 1.000300, and 1.000272, respectively (Handbook of Chemistry and Physics 1983). Upon evaluation, it is found that CO_2 provides well over 99% of the Rayleigh scattering optical depth, due not only to comprising 95% of the atmosphere, but more to the larger index of refraction for CO_2. Rayleigh scattering is significant in the ultraviolet; at 2000 Å, τ_R (Rayleigh scattering opacity) = 0.224; at 2500 Å, τ_R = 0.084; at 3000 Å, τ_R = 0.038. Note that the Rayleigh scattering optical depth at 3000 Å reported by Kuhn and Atreya (1979) of less than 0.01 is in error, most likely a typographical error since their value of 0.07 at 2500 Å is good.

Ozone heating. Figure 2 shows the total atmospheric heating due to ozone at 57°N latitude in late winter (L_s = 343°), when the maximum ozone abundance of 57 μm-atm was observed by Mariner 9 (Barth *et al.* 1973). Note that this heating rate is directly related to the assumed altitude dependence of the O_3 mixing ratio, and is therefore dependent on the accuracy of the photochemical model. Also shown in Fig. 2 is the contribution to the overall heating by a few select wavelength bins, which provides an idea of the wavelength dependence. Extreme ultraviolet heating (EUV) at wavelengths less than 1700 Å is unimportant in the lower atmosphere of Mars due to absorption in the upper atmosphere. Ozone heating at wavelengths less than 1900 Å is only important at altitudes above the surface. Large optical depths of CO_2 prevents solar radiation from reaching lower altitudes, and explain the strong altitude variation in the heating rate at these wavelengths. At 2000 Å, the atmospheric optical depth has a minimum (see Fig. 1). Solar flux at 2000 Å is only weakly attenuated at the surface and the heating rate is virtually constant in altitude.

Beyond 2000 Å, absorption cross-sections of ozone in-

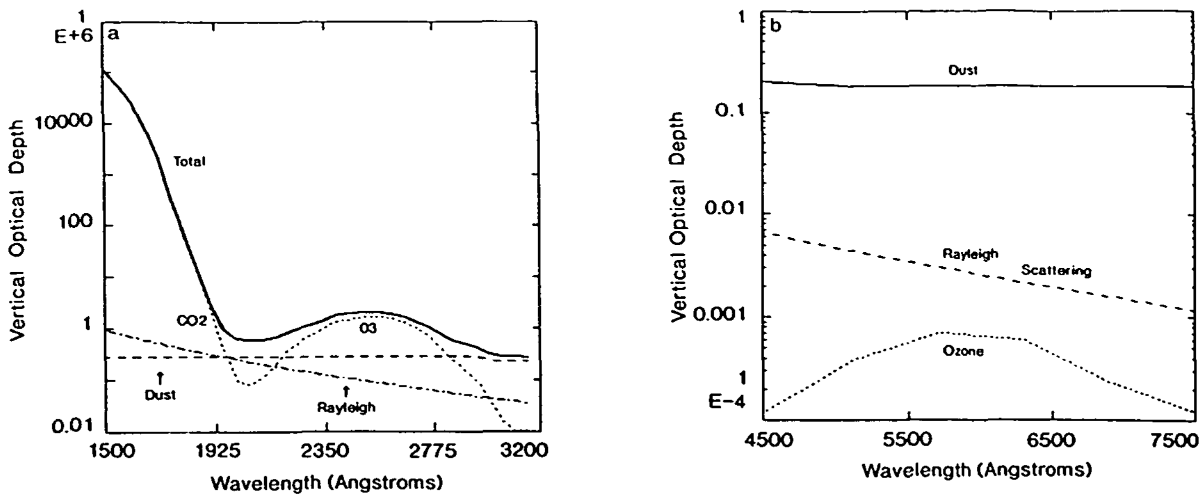

FIG. 1. Contribution of O_3, CO_2, dust, and Rayleigh scattering to the vertical optical depth of the atmosphere at the surface at 57°N latitude and L_s of 343° at UV wavelengths (a) and visible wavelengths (b).

crease with wavelength to a maximum at 2500 Å (see Fig. 1). Increasing cross-sections and increasing solar fluxes result in larger heating rates, as shown in Fig. 2. Large optical depths attenuate the solar flux at lower altitudes, which results in a strong altitude dependence in the ozone heating rate at 2500 Å. While heating increases with wavelength from 2000 to 2500 Å at altitudes greater than 10 km above the surface, heating at the surface actually decreases with increasing wavelength due to the attenuation of solar flux. From 2500 to 2700 Å the absorption cross-sections of ozone decrease with increasing wavelength. However, the solar flux increases strongly with increasing wavelength from 2500 to 2700 Å, resulting in a maximum ozone heating above 10 km at 2700 Å. Beyond 2700 Å, O_3 cross-sections drop dramatically, which results in decreasing heating rates, but also allows more solar flux to reach the surface. As a result, the maximum ozone heating at the surface occurs at 2900 Å.

Ozone cross-sections reach a secondary maximum at visible wavelengths in the Chappuis bands. While not the major source of ozone heating, the Chappuis bands provide over 10% of the total ozone heating near the surface. As the atmosphere is optically thin at visible wavelengths (see Fig. 1), the heating is virtually constant

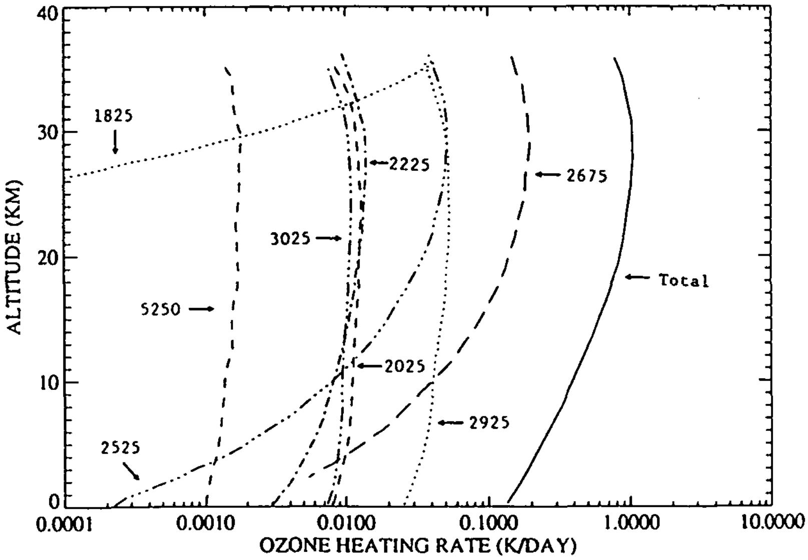

FIG. 2. Total atmospheric heating rate due to O_3 at 57°N latitude and the contribution by a few 50-Å wavelength intervals in the UV and by a 500-Å wavelength interval in the visible, centered at the wavelengths shown (in Å).

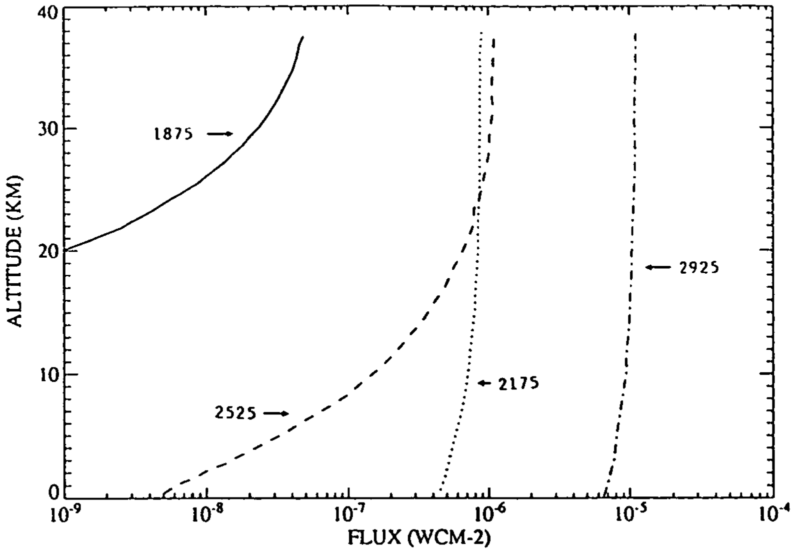

FIG. 3. Downward solar flux integrated over a few 50-Å wavelength intervals centered at the wavelengths shown.

with atltitude. The maximum ozone heating in the Chappuis bands occurs at 5200 Å.

The downward solar flux as a function of wavelength and altitude is shown in Fig. 3. Flux shortward of 2000 Å is absorbed by CO_2. Note the strong decrease in the solar flux striking the polar cap between 2200 and 2800 Å due to ozone absorption. In the center of the Hartley bands at 2500 Å, the solar flux impinging on the polar cap is reduced by two orders of magnitude due to ozone absorption. Above 20 km altitude, the solar flux is not significantly attenuated due to the low ozone abundances at these altitudes (Lindner 1988).

Significantly lower ozone abundances exist at 70°N latitude (Barth *et al.* 1973) and result in lower ozone heating rates. To emphasize latitudinal variations, the ratio of the O_3 heating rate at 70°N latitude to O_3 heating rates at 57°N latitude is shown in Fig. 4, along with a few select wavelength intervals. While ozone abundances are lower at 70°N latitude, the slant path is larger. Larger slant paths result in greater solar flux reductions near the surface, particularly where large CO_2 absorption (e.g., 1825 Å) or large O_3 absorption (e.g., 2525 Å) exists. This causes larger reductions in heating rates near the surface at those wavelengths. As Rayleigh scattering optical depths are greater than CO_2 and O_3 absorption optical depths at 2000 Å (see Fig. 1), the reduction in the heating rate is less at 70°N latitude at 2000 Å. At 3000 and 5000 Å the altitude behavior is the same at both latitudes because the vertical optical depth of the atmosphere is small.

Ozone heating relative to dust heating. Figure 5 compares ozone and dust heating rates for two latitudes, all summed over the solar spectrum. Dust heating is larger than O_3 heating at all altitudes, particularly above 20 km. O_3 heating is at least a factor of 3 less than dust heating. Figure 5 also shows that O_3 heating is less important relative to dust at 70°N latitude than it is at 57°N latitude, due to the lower O_3 abundances at 70°N latitude. Therefore, while dust heating is less at higher latitudes due to the decreased solar flux, the importance of dust heating relative to O_3 heating has increased. The relative importance of dust heating continues to increase right up to the edge of the polar night. O_3 heating will also not be important relative to dust at equatorial and mid-latitudes because negligible ozone abundances exist there (Barth *et al.*1973).

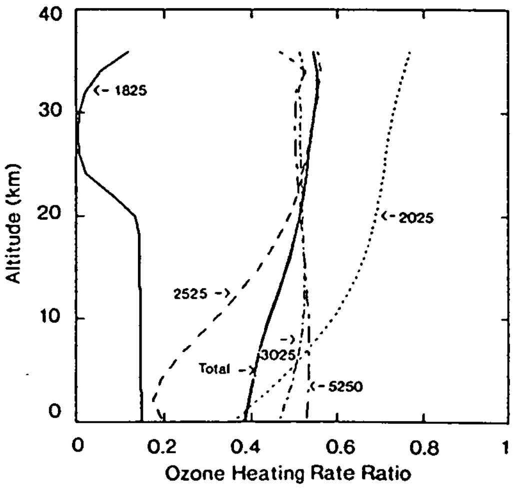

FIG. 4. Ratio of the total O_3 heating rate at 70°N latitude to that at 57°N latitude. Also shown are the ratios of the O_3 heating rate in a few 50-Å wavelength intervals.

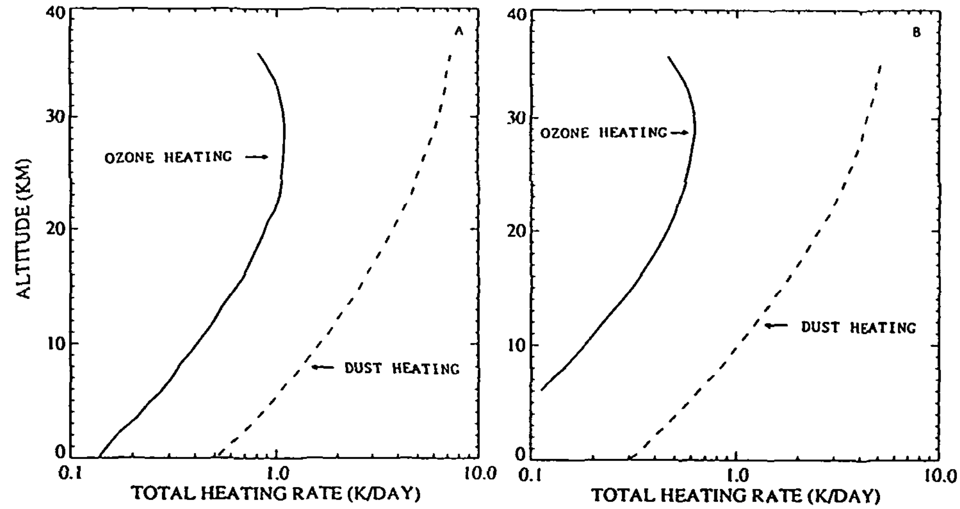

FIG. 5. Total atmospheric heating due to O_3 and dust (τ_v = 0.2) at 57°N latitude (A) and 70°N latitude (B).

Ultraviolet CO_2, O_2, H_2O, HO_2, and H_2O_2 heating. CO_2, O_2, H_2O, HO_2, and H_2O_2 also absorb in the UV. Integrating the heating from 1500 to 3200 Å gives the total heating rates for each molecule, shown in Fig. 6 as the ratio of the heating to the total O_3 heating. H_2O, HO_2, and H_2O_2 number densities are too low for any appreciable UV heating. However, H_2O UV heating rates are much higher at polar summer, equatorial, or mid-latitudes where H_2O abundances are appreciable. CO_2 and O_2 UV heating rates are appreciable in the upper atmosphere, being in fact the dominant source of atmospheric heating above 40 km altitude, but are ineffective at low altitudes due to optically thick absorption bands. However, CO_2 and O_2 UV heating rates are also higher at polar summer, equatorial, or mid-latitudes, due to lower solar zenith angles which result in less optically thick absorption paths.

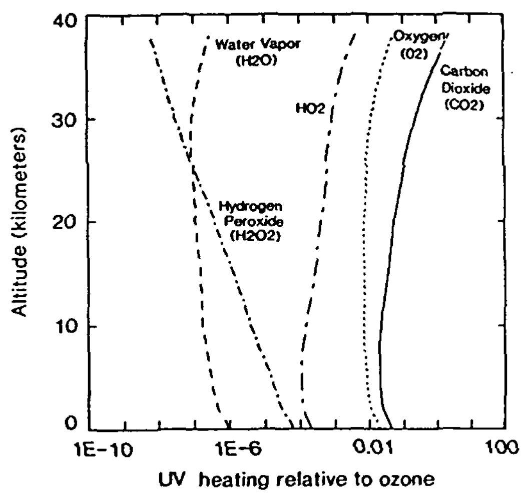

FIG. 6. Ratio of the UV heating rates of CO_2, O_2, H_2O, HO_2, and H_2O_2 to those of O_3 at 57°N latitude.

DISCUSSION

Prabhakara and Hogan (1965) and Kuhn *et al.*(1979) have shown that O_3 UV heating rates are comparable to CO_2 near-IR heating rates. However, neither work considered dust heating, which is at least a factor of 3 larger than O_3 heating rates at all altitudes and latitudes. O_3 abundances are usually much smaller than the maximum observed, which will further reduce the importance of O_3 heating to the atmospheric thermal budget. Moreover, the UV measurements of Martian O_3 cannot distinguish vapor-phase O_3 from O_3 adsorbed in the polar cap (Lane *et al.* 1973), and therefore the atmospheric burden may be less than the assumed O_3 abundance. Furthermore, 0.2 vertical optical depths of dust as used in Fig. 5 represent the minimum amount of dust observed (Pollack *et al.* 1979). Larger dust loading will provide proportionally greater dust heating (Lindner 1985). Therefore, O_3 is a minor, although nonnegligible, heat source in the Martian atmosphere. UV heating from CO_2, O_2, H_2O, HO_2, and H_2O_2 is also a minor heat source in the lower winter polar atmosphere.

Mariner 7 and 9 observations indicate almost twice as much O_3 over the northern polar cap as over the southern polar cap (Barth *et al.*1973, Lane *et al.* 1973), due primarily to the hemispherical differences in airmass (Kong and McElroy 1977a, Lindner 1988). Kuhn *et al.* (1979) suggested that the observed hemispherical asymmetry in the composition of the permanent polar caps (Kieffer *et al.* 1976, Kieffer 1979) could be related to this hemispherical asymmetry in O_3. O_3 affects surface frost formation by changing the atmospheric temperature, thus changing the heat received by the surface from atmospheric thermal radiation and from atmospheric heat transport. However, ozone has been shown here to be a minor solar heating source, compared to dust, and has been also shown to be a minor thermal radiator on Mars by Crisp (1990). Hence, the hemispherical asymmetry in O_3 should not cause any significant hemispherical asymmetry in atmospheric temperature. O_3 also affects surface frost formation through absorption of solar radiation which would otherwise strike the polar cap. However, dust absorbs or scatters to space most UV light before it strikes the polar cap (Lindner 1990). Furthermore, while O_3 strongly absorbs at UV wavelengths as shown in Fig. 3, O_3 absorbs less than 1% of the total solar flux which strikes the polar cap. Hence, the hemispherical asymmetry in O_3 should not cause any significant hemispherical asymmetry in the total solar flux absorbed by surface frost. Since atmospheric temperatures are near the condensation temperature of CO_2 and H_2O at winter polar latitudes, O_3 may still be important in the formation of clouds and snow, as Kuhn *et al.* (1979) suggested. The importance of O_3 in cloud and snow formation is less than Kuhn *et al.* predict since they ignored meridional transport (Pollack *et al.* 1990) and dust heating, but an O_3 heating rate of 1 K/day will still significantly reduce atmospheric condensation. However, while the ratio of CO_2 frost to CO_2 snow in the polar cap is difficult to determine, Pollack *et al.* (1990) have predicted that surface frost formation dominates over snowfall. Therefore, the hemispherical asymmetry in O_3 is unlikely to play an important role in explaining the hemispherical asymmetry in the permanent polar caps.

ACKNOWLEDGMENTS

I am grateful to Gary Thomas and the reviewers for helpful comments and discussions, and to Knut Stamnes for providing computer code. Support for this research was provided by NSF Grant ATM 8305841, NASA Grants NAGW-389 and NAGW-552, and NASA Contracts NASW-~~4444~~ and NASW-4614.

REFERENCES

ANDERSON, D. E., JR. 1974. Mariner 6, 7, and 9 ultraviolet spectrometer experiment: Analysis of hydrogen lyman alpha data. *J. Geophys. Res.* 79, 1513–1518.

BARTH, C. A., AND C. W. HORD 1971. Mariner ultraviolet spectrometer: Topography and polar cap. *Science*, 173, 197–201.

BARTH, C. A., C. W. HORD, A. I. STEWART, A. L. LANE, M. L. DICK, AND G. P. ANDERSON. 1973. Mariner 9 ultraviolet experiment: Seasonal variation of ozone on Mars. *Science* 179, 795–796.

COGLEY, A. C. AND W. J. BORUCKI 1976. Exponential approximations for daily average solar heating or photolysis. *J. Atmos. Sci.* 33, 1347–1356.

CRISP, D. 1990. Infrared radiative transfer in the dust-free martian atmosphere. *J. Geophys. Res.* 95, 14,577–14,588.

DAUMONT, D., J. BRION, AND J. MALICET 1983. Measurement of total atmospheric ozone: Consequences entailed by new values of ozone absorption cross-sections at 223 K in the 310–350 nm spectral range. *Planet. Space Sci.* 31, 1229–1234.

DAVIES, D. W. 1979. The relative humidity of Mars' atmosphere. *J. Geophys. Res.* 84, 8335–8340.

DEIRMENDJIAN, D. 1969. *Electromagnetic Scattering on Spherical Polydispersions*. New York, American Elsevier.

DEMORE, W. B., J. J. MARGITAN, M. J. MOLINA, R. T. WATSON, D. M. GOLDEN, R. F., HAMPSON, M. J., KURYLO, C. J., HOWARD, AND A. R. RAVISHANKARA 1985. Chemical kinetics and photochemical data for use in stratospheric modeling, evaluation no. 7, JPL Publication 85-67, Jet Propulsion Laboratory, Pasadena, CA.

FREDERICK, J. E., AND R. D. HUDSON 1980. Atmospheric opacity in the Schumann-Runge bands and the aeronomic dissociation of water vapor. *J. Atmos. Sci.* 37, 1088–1098.

FREEMAN, D. E., K. YOSHINO, J. R. ESMOND, AND W. H. PARKINSON 1984. High resolution absorption cross-section measurements of ozone at 195 K in the wavelength region 240–350 nm. *Planet. Space Sci.* 32, 239–248.

GRIGGS, M. 1968. Absorption coefficients of ozone in the ultraviolet and visible regions. *J. Chem. Phys.* 49, 857–859.

HABERLE, R. M., C. B. LEOVY, AND J. B. POLLACK 1979. A numerical model of the Martian polar cap winds. *Icarus* 39, 151–183.

Handbook of Chemistry and Physics, 64th ed., 1983. Chemical Rubber Publishing Co., Cleveland, OH.

HANSEN, J. E., AND L. D. TRAVIS 1974. Light scattering in planetary atmospheres. *Space Sci. Rev.* 16, 527–610.

HESS, S. L. 1979. Static stability and thermal wind in an atmosphere of variable composition: Applications to Mars. *J. Geophys. Res.* 84, 2969–2973.

HESS, S. L., J. A. RYAN, J. E. TILLMAN, R. M. HENRY, AND C. B. LEOVY 1980. The annual cycle of pressure on Mars measured by Viking Landers 1 and 2. *Geophys. Res. Lett.* 7, 197–200.

HOCHANADEL, C. J., J. A. GHORMLEY, AND P. J. OGREN 1972. Absorption spectrum and reaction kinetics of the HO2 radical in the gas phase. *J. Chem. Phys.* 56, 4426–4432.

HUDSON, R. D. 1971. Critical review of ultraviolet photoabsorption cross sections for molecules of astrophysical and aeronomic interest. *Rev. Geophys. Space Phys.* 9, 305–406.

IWASAKI, K., Y. SAITO, AND T. AKABANE 1982. Martian north polar cap 1979–1980. *J. Geophys. Res.* 87, 10,265–10,269.

JAKOSKY, B. M. 1985. The seasonal cycle of water on Mars. *Space Sci. Rev.* 41, 131–200.

JAKOSKY, B. M., AND C. B. FARMER 1982. The seasonal and global behavior of water vapor in the Mars atmosphere: Complete global results of the Viking atmospheric water detector experiment. *J. Geophys. Res.* 87, 2999–3019.

KIEFFER, H. H. 1979. Mars south polar spring and summer temperatures: A residual CO_2 frost. *J. Geophys. Res.* 84, 8263–8288.

KIEFFER, H. H., S. C. CHASE, JR., T. Z. MARTIN, E. D. MINER, AND F. D. PALLUCONI 1976. Martian north pole summer temperatures: Dirty water ice. *Science* 194, 1341–1343.

KONDRAT'EV, K. YA., YU. M. TIMOFEEV, O. M. POKROVSKII, AND T. A. DVOROVIK 1973. Determination of vertical temperature profile in the atmosphere of Mars from Mariner 9 infrared thermal radiation measurements, *Dokl. Akad. Nauk SSSR*, 211, 801–803. [English trans. 1974. *Sov. Phys. Dokl.* 18, 509–510.]

KONG, T. Y., AND M. B. MCELROY 1977a. The global distribution of O_3 on Mars. *Planet. Space Sci.* 25, 839–857.

KONG, T. Y., AND M. B. MCELROY 1977b. Photochemistry of the Martian atmosphere. *Icarus* **32**, 168–189.

KRASITSKII, O. P. 1978. A model for the diurnal variation of the composition of the Martian atmosphere. *Kosm. Issled.* **16**, 434–442. [English trans. 1978, *Cosmic Res.* **16**, 350–356.]

KRASNOPOLSKY, V. A., AND V. A. PARSHEV 1979. Ozone and photochemistry of the Martian lower atmosphere. *Planet. Space Sci.* **27**, 113–120.

KUHN, W. R., AND S. K. ATREYA 1979. Solar radiation incident on the Martian surface. *J. Mol. Evol.* **14**, 57–64.

KUHN, W. R., S. K. ATREYA, AND S. E. POSTAWKO 1979. The influence of ozone on Martian atmospheric temperature. *J. Geophys. Res.* **84**, 8341–8342.

LANE, A. L., C. A. BARTH, C. W. HORD, AND A. I. STEWART 1973. Mariner 9 ultraviolet spectrometer experiment: Observations of ozone on Mars. *Icarus* **18**, 102–108.

LEWIS, B. R., AND J. H. CARVER 1983. Temperature dependence of the carbon dioxide photoabsorption cross section between 1200 and 1970 Angstroms. *J. Quant. Spectrosc. Radiat. Transfer* **30**, 297–309.

LIN, C. L., N. K. ROHATGI, AND W. B. DEMORE. 1978. Ultraviolet absorption cross sections of hydrogen peroxide. *Geophys. Res. Lett.* **5**, 113–115.

LINDAL, G. F., H. B. HOTZ, D. N. SWEETNAM, Z. SHIPPONY, J. P. BRENKLE, G. V. HARTSELL, R. T. SPEAR, AND W. H. MICHAEL, JR. 1979. Vikine radio occultation measurements of the atmosphere and topography of Mars: Data acquired during 1 Martian year of tracking. *J. Geophys. Res.* **84**, 8443–8456.

LINDNER, B. L. 1985. The aeronomy and radiative transfer of the Martian atmosphere, Ph.D. dissertation, 470 pp., Univ. of Colorado, Boulder.

LINDNER, B. L. 1988. Ozone on Mars: The effect of clouds and airborne dust. *Planet. Space Sci.* **36**, 125–144.

LINDNER, B. L. 1990. The martian polar cap: Radiative effects of ozone, clouds and airborne dust. *J. Geophys. Res.* **95**, 1367–1379.

LINDNER, B. L., AND B. M. JAKOSKY 1985. Martian atmospheric photochemistry and composition during periods of low obliquity. *J. Geophys. Res.* **90**, 3435–3440.

LIU, S. C., AND T. M. DONAHUE 1976. The regulation of hydrogen and oxygen escape from Mars. *Icarus* **28**, 231–246.

MOLINA, L. T., AND M. J. MOLINA 1981. UV absorption cross-section of HO_2 NO_2 vapors. *J. Photochem.* **15**, 97–108.

OGAWA, M. 1971. Absorption cross sections of O_2 and CO_2 continua in the Schumann and far-uv regions. *J. Chem. Phys.* **54**, 2550–2556.

OWEN, T., K. BIEMANN, D. R. RUSHNECK, J. E. BILLER, D. W. HOWARTH, AND A. L. LAFLEUR 1977. The composition of the atmosphere at the surface of Mars. *J. Geophys. Res.* **82**, 4635–4639.

PARISOT, J. P., AND J. M. ZUCCONI 1984. Temperature effect on the photodissociation rates in the atmospheres of Mars and Venus. *Icarus* **60**, 327–331.

PAUR, R. J., AND A. M. BASS 1985. The ultraviolet cross-sections of ozone: II. Results and temperature dependence. In *Atmospheric Ozone* (C. E. Zerefos and A. Ghazi, Eds.), Reidel, Dordrecht, Holland.

POLLACK, J. B., D. S. COLBURN, F. M. FLASAR, R. KAHN, C. E. CARLSTON, AND D. PIDEK 1979. Properties and effects of dust particles suspended in the Martian atmosphere. *J. Geophys. Res.* **84**, 2929–2945.

POLLACK, J. B., R. M. HABERLE, J. SCHAEFFER, AND H. LEE 1990. Simulations of the general circulation of the Martian atmosphere I. Polar processes. *J. Geophys. Res.* **95**, 1447–1473.

PRABHAKARA, C., AND J. S. HOGAN, JR. 1965. Ozone and carbon dioxide heating in the martian atmosphere. *J. Atmos. Sci.* **22**, 97–109.

RODGERS, C. D., AND C. D. WALSHAW 1966. The computation of infrared cooling rate in planetary atmospheres. *Q. J. R. Meteorol. Soc.* **92**, 67–92.

ROTTMAN, G. J. 1981. Rocket measurements of the solar spectral irradiance during solar minimum, 1972-1977. *J. Geophys. Res.* **86**, 6697–6705.

SHEMANSKY, D. E. 1972. Carbon dioxide extinction coefficient 1700–3000 Angstroms. *J. Chem. Phys.* **56**, 1582–1587.

SHIMAZAKI, T. 1981. A model of temporal variations of ozone density in the martian atmosphere. *Planet. Space Sci.* **29**, 21–33.

STAMNES, K., AND P. CONKLIN 1984. A new multi-layer discrete ordinate approach to radiative transfer in vertically inhomogeneous atmospheres. *J. Quant. Spectrosc. Radiat. Transfer* **31**, 273–282.

THOMPSON, B. A., P. HARTECK, AND R. R. REEVES, JR. 1963. Ultraviolet absorption coefficients of CO_2, CO, O_2, H_2O, N_2O, NH_3, NO, SO_2, and CH_4 between 1850 and 4000 Angstroms. *J. Geophys. Res.* **68**, 6431–6436.

TOON, O. B., J. B. POLLACK, AND C. SAGAN 1977. Physical properties of the particles composing the Martian dust storm of 1971–1972. *Icarus* **30**, 663–696.

TRAUGER, J. T., AND J. I. LUNINE 1983. Spectroscopy of molecular oxygen in the atmospheres of Venus and Mars. *Icarus* **55**, 272–281.

ZUREK, R. W. 1978. Solar heating of the Martian dusty atmosphere. *Icarus* **35**, 196–208.

ZUREK, R. W. 1982. Martian great dust storms: An update. *Icarus* **50**, 288–310.

GEOPHYSICAL RESEARCH LETTERS, VOL. 19, NO. 16, PAGES 1675-1678, AUGUST 21, 1992

SUNLIGHT PENETRATION THROUGH THE MARTIAN POLAR CAPS: EFFECTS ON THE THERMAL AND FROST BUDGETS

Bernhard Lee Lindner

Atmospheric and Environmental Research, Inc.

Abstract. An energy balance model of the seasonal polar caps on Mars is modified to include penetration of solar radiation into and through the ice. Penetration of solar radiation has no effect on subsurface temperature or total frost sublimation if seasonal ice overlies a dust surface. An effect is noted for seasonal ice which overlies the residual polar caps. For the case of an exposed water-ice residual polar cap, the temperature at depth is calculated to be up to several degrees warmer and the calculated lifetime of seasonal CO_2 frost is slightly lower when penetration of sunlight is properly treated in the model. For the case of a residual polar cap which is perennially covered by CO_2 frost, the calculated lifetime of seasonal CO_2 frost is very slightly increased as a result of sunlight penetration through the ice. Hence, penetration of sunlight into the ice helps to stabilize the observed dichotomy in the residual polar caps on Mars, although it is a small effect.

Introduction

Computer simulation of the condensation and sublimation of CO_2 frost in the martian polar caps has been fairly successful in reproducing the annual cycle in atmospheric pressure observed by the Viking Landers [Leighton and Murray, 1966; Cross, 1971; Briggs, 1974; Davies et al., 1977; James and North, 1982; Lindner, 1985, 1986]. However, these studies have not been able to uniquely explain why CO_2 frost survives summer in the southern hemisphere and not summer in the northern hemisphere. Several theories have been advanced to explain this discrepancy, including hemispherical asymmetries in albedo [Paige, 1985; Paige and Ingersoll, 1985; Lindner, 1985; 1986], in snowfall [Pollack et al., 1990], in the radiative effects of clouds and airborne dust [Briggs, 1974; James and North, 1982; Lindner, 1990; 1992], in subsurface heat conduction [Jakosky and Haberle, 1990], and in ozone [Kuhn et al., 1979; Lindner, 1988; 1990; 1991]. It is also possible that a permanent reservoir of CO_2 frost from an earlier epoch is being uncovered in the southern hemisphere, although this seems unlikely [e.g., Jakosky and Barker, 1984].

Prior models have used the assumption that all non-reflected sunlight is absorbed at the surface, when in reality sunlight penetrates into the surface, sometimes to several meters depth [Clow, 1987]. This paper describes studies of how this phenomenon affects the thermal and frost budgets of the polar caps and the subsurface.

Paper number 92GL01505
0094-8534/92/92GL-01505$03.00

Modeling Approach

To perform this study, the energy-balance model of Jakosky and Haberle [1990] is combined with the ice microphysics model of Clow [1987]. The energy budget at the surface of the geographic poles involves balance between absorbed sunlight, absorbed and emitted thermal-IR radiation (from the surface to space and from the atmosphere to the surface), conduction to or from the subsurface (the subsurface is taken to begin at the base of the seasonal ice), and condensation or sublimation of CO_2. The instantaneous energy balance at the surface can be written as

$$\frac{S_o}{R^2}(1-A)P(t)\cos(\iota) - \varepsilon\sigma T^4(z,t) - K\left.\frac{\delta T(z,t)}{\delta z}\right|_{z=0} + L\frac{dm(t)}{dt} = 0 \quad (1)$$

where S_o is the solar constant at 1 AU corrected for atmospheric absorption and scattering [Lindner, 1985; 1990; Lindner et al., 1990]; R is the distance of Mars from the Sun in AU; A is the bolometric Bond albedo of the surface material at the pole; P(t) is the fraction of non-reflected sunlight which is absorbed by the seasonal polar cap at time t (the remainder being absorbed by the surface underneath the seasonal ice); ι is the solar incidence angle; ε is the effective emissivity of the surface; σ is the Stefan-Boltzmann radiation constant; T(z,t) is the temperature at depth z (surface temperature is set to the condensation temperature of CO_2 if CO_2 frost is present); K is the thermal conductivity of the surface and subsurface materials; L is the latent heat of sublimation of CO_2 frost; dm(t)/dt is the time derivative of the CO_2 surface frost abundance (set to zero when no frost is present); and the temperature gradient $\delta T/\delta z$ is evaluated at the surface (z=0).

Sunlight penetration and heat conduction into the subsurface are accounted for by

$$\frac{\delta T(z,t)}{\delta t} = \frac{1}{\rho C}\left\{K\frac{\delta^2 T(z,t)}{\delta z^2} + \frac{S_o}{R^2}(1-A)\,(1-P(t))\cos(\iota)\frac{\delta F(z,t)}{\delta z}\right\} \quad (2)$$

where ρ is the bulk density of the subsurface material, C is its specific heat, and $\delta F(z,t)$ is the fraction of the sunlight which passes through the seasonal cap and is absorbed within depth δz of the subsurface. The derivatives in (2) apply locally. The values used for ρ and C of the subsurface dust are 0.93 gcm^{-3} and 0.15 cal $g^{-1}K^{-1}$, respectively, and K is allowed to vary depending on the thermal inertia. The albedo and thermal inertia for dust material is assumed to be comparable to the typical regolith values (0.25 and 0.006 cal $cm^{-2}s^{-1/2}K^{-1}$, respectively). The albedo and thermal inertia for a residual polar cap are taken to be like those of the north residual polar cap (0.45 and 0.03 cal $cm^{-2}s^{-1/2}K^{-1}$, respectively [see Kieffer et al., 1976; Paige, 1985]. When the model uses an albedo of 0.65

for seasonal CO_2 ice, all seasonal ice sublimes during the summer and the underlying surface becomes exposed. Hence, an albedo of 0.65 is used to simulate the case of an exposed residual polar cap. An albedo of 0.74 is needed in this model to retain seasonal CO_2 ice through the summer. While energy is deposited at depth by solar radiation, it is not effectively transported by IR radiation relative to conduction. Optical absorption coefficients are large in the IR, and temperatures are low, both of which inhibit transport by radiation. Hence, IR radiation is not included in (2). Terms in (1) and (2) other than P and F are evaluated as in Jakosky and Haberle [1990].

Clow [1987] calculated the multiple scattering of sunlight by the matrix of water-ice grains and dust particles on Mars by inserting the average single-scattering parameters for these particles into the δ-Eddington method of solving the radiative-transfer equation. Figure 1 shows the integral of net shortwave flux with respect to depth, which Clow calculated for pure snow and dirty snow (1000 ppmw dust) and for fine-grained snow (ice-grain radii of 50 μm, bulk density of 50 kg m^{-3}) and coarse-grained snow (ice-grain radii of 1000 μm, bulk density of 400 kg m^{-3}). Values for P, the fraction of non-reflected solar radiation absorbed by the seasonal polar cap, are extracted from Figure 1 using the thickness of the seasonal polar cap as predicted by the energy balance model. Values for F(z), the fraction of non-reflected solar radiation absorbed by the surface under the seasonal ice, are then computed by taking the remainder (1-P) of the non-reflected solar radiation and apportioning it with depth as shown in Figure 1.

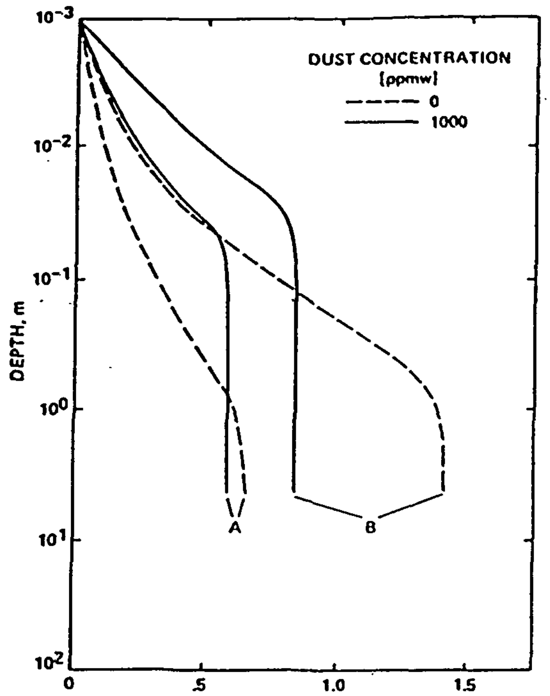

Fig. 1. The integral of net shortwave flux with respect to depth for clean and dusty water snow on Mars, using the mean-annual incident solar flux at latitude -38°. Curves (A) correspond to a snow with ice grain radii of 50 μm and bulk density 50 kg m^{-3} while curves (B) are for a snow with 1000-μm ice grains and a density of 400 kg m^{-3}. (Reproduced by permission from Clow [1987]).

Kieffer [1990] and Mooré [1988] have both deduced that ice-grain radii in the residual polar cap are over 100 μm and that dust concentrations are less than 1/1000. This means that ice in the residual polar cap is believed to be between fine-grained and coarse-grained and between pure and dirty, as I have defined them. There is no evidence for the grain size and dust content of seasonal ice, although it is likely to be less dirty and more fine grained than ice in the residual polar cap. I have assumed that the residual polar cap is at least several meters thick, which is believed to be the case [Toon et al, 1980].

The Clow [1987] calculations presented in Figure 1 assume water ice, perfectly valid for the residual polar cap composed of water ice. Recent calculations by Warren et al. [1990] suggest that CO_2 ice on Mars is more absorbing than water ice on Mars. Greater absorption of sunlight by ice would decrease the penetration depth of sunlight shown in Figure 1 (G. Clow, personal communication, 1992). Hence, the penetration of sunlight calculated here for seasonal ice may be an upper limit case, which enhances the conclusions as shown below.

To apply the model, (2) is numerically integrated at the geographic pole through a martian orbit around the Sun, subject to the boundary condition of (1). The model is iterated for six Mars years, by which time convergence is achieved. The subsurface is divided up into discrete layers, each of which is described by a center temperature. A 5 cm surface layer thickness is used. This is required since the layering needs to be on a finer scale than the sunlight penetration depth (see Figure 1) and the thermal skin depth. The thermal skin depth varies from 1 m to 10 m at the pole, depending on the choice of subsurface material. Succeeding layers are thicker by a factor of 1.2 each; this reaches to a depth of 37 m (over 4 annual skin depths). This subsurface thermal model produced excellent agreement to the depth profiles of temperature computed by

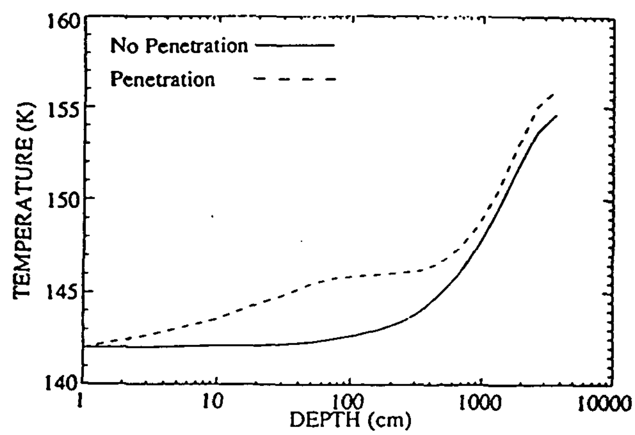

Fig. 2. Temperature versus depth in a water-ice residual polar cap for the case where seasonal ice sublimes completely in the summer. The surface is still covered by CO_2 ice at this time (late summer, $L_s = 260°$). The dashed curve is simulated by the model including the effect of penetration of solar radiation, and the solid curve is simulated by the model with no penetration of solar radiation. Surface values are shown at 1 cm depth. Seasonal ice albedo and thermal inertia is 0.65 and 0.03 cal cm^{-2} $s^{-1/2}$ K^{-1}, respectively. The flux profile for clean, fine-grained ice in Figure 1 is used for seasonal ice and that for clean, coarse ice is used for the residual polar cap.

Kieffer [1990] for the same case he presented in his Figure 3.

Results

In the case where seasonal ice overlies a dust surface, our model calculates no changes in either the frost budget of the polar cap or the thermal structure of the subsurface due to sunlight penetration. The top grains of dust under the ice absorb the solar radiation which passes through the ice, and it is much easier for these top grains to conduct or radiate heat back to the overlying ice than deep into the subsurface. Effectively, all non-reflected sunlight is absorbed by the seasonal frost, as was assumed in previous polar-cap models.

The behavior for seasonal CO_2 ice overlying a residual polar cap is different. Solar radiation which passes through the seasonal ice may penetrate quite deeply into the residual polar cap (see Figure 1). For a water-ice residual polar cap, the sunlight which penetrates the seasonal polar cap heats the residual polar cap by up to 3°K, primarily in late summer when the seasonal ice is thinnest, with the greatest heating occurring at 1 m depth in the residual polar cap (see Figure 2). Most of the penetrating radiation actually gets absorbed near the surface of the residual polar cap, but that easily conducts or radiates away to the seasonal CO_2 ice, accounting for the low heating rate at the surface of the residual polar cap. Dirty ice exhibits the same behavior seen in Figure 2, but with only half the magnitude of subsurface heating. The results are essentially the same no matter whether fine-grained or coarse-grained ice is used. However, the heating may be less than shown in Figure 2 since the seasonal ice may be more absorbing in the visible than assumed here. Different values for thermal inertia also change the degree of subsurface heating, with lower thermal inertia producing greater heating. For a residual polar cap which contains CO_2 ice, any subsurface heating goes into subliming local CO_2 ice, and does not change the local temperature until all local CO_2 ice has sublimed.

For the case of an exposed water-ice residual polar cap, the maximum surface temperature at the pole occurs just after the last of the seasonal ice sublimes. This is also when the maximum change due to sunlight penetration occurs in the calculated temperature at depth, as shown in Figure 3. I find that surface temperatures are cooler in early summer (L_s = 270° to L_s = 310°) for the model with light penetration than for the model which has no penetration. Solar radiation which penetrates into the subsurface must conduct to the surface to heat the surface, which is not as effective at heating the surface as direct absorption of all the solar radiation by the surface. In late summer (L_s = 310° to 360°), the surface is actually warmer for the model with light penetration, due to the increased heat conduction by the warmer subsurface. After L_s = 360°, the surface becomes covered with seasonal CO_2 frost. Again, the maximum subsurface heating occurs at 1 m depth in a water-ice residual polar cap.

The model which includes penetration of sunlight predicts less seasonal ice all year for the exposed water-ice residual cap case, as shown in Figure 4. By allowing solar radiation to be absorbed at depth, the surface does not become as warm in early summer when surface temperatures are their warmest. This decreases the annual-total energy lost as infrared radiation emitted by the surface and increases the amount of energy stored in the subsurface, which in turn decreases the amount of frost condensation needed in the early winter to maintain balance (see equation 1). Thus, there is an increasing difference in predicted frost abundances between the models from L_s = 0° to 180°. After L_s = 180°, the difference in the CO_2 frost amount between the models decreases because some sunlight penetrates the seasonal ice to heat the residual polar cap instead of subliming seasonal ice. However, this effect is not enough to compensate for the increased conduction of heat during early winter, and the net result is that the seasonal ice sublimes away earlier in the year for the model which includes penetration of sunlight. Furthermore, seasonal ice may be more absorbing than assumed here, which will decrease heating of the residual polar cap while seasonal ice is present, resulting in a slightly larger difference between models in Figure 4. The effect of light penetration on the frost budget for dirty ice shows the same behavior as in Figure 4, but only half the magnitude.

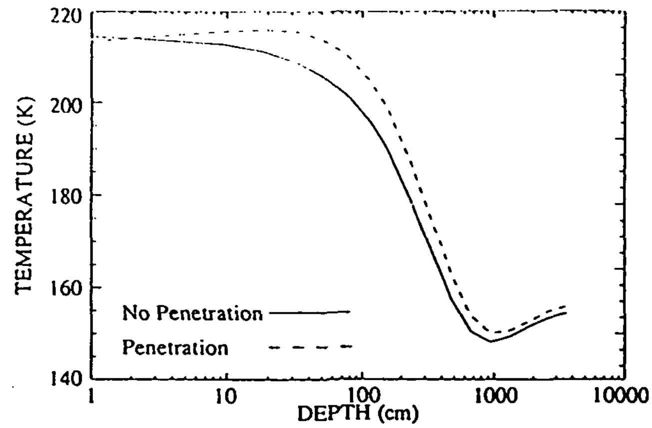

Fig. 3. As in Figure 2, except after all seasonal ice has sublimed in the model (L_s = 280°, 37 Mars days after Figure 2).

Discussion

The inclusion of light penetration in an energy balance model slightly decreases the albedo needed in the model to

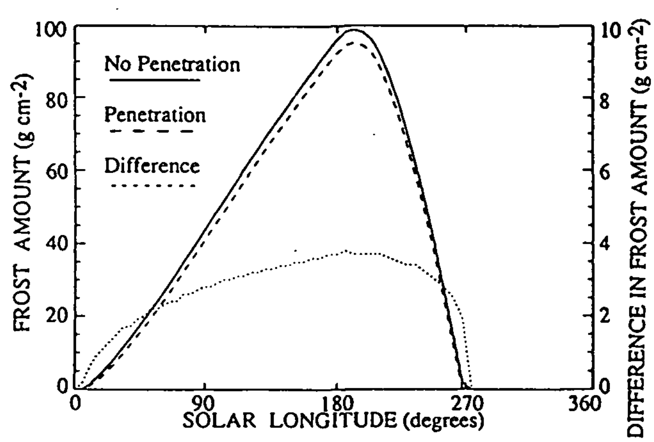

Fig. 4. Annual variation in seasonal CO_2 frost amount at the south pole for the case where seasonal ice sublimes completely in the summer. The difference between the two models is also plotted, using the scale on the right side. The same ice properties as described for Figure 2 are used.

keep seasonal CO_2 ice on a residual polar cap through the summer. Furthermore, the number of days that an energy-balance model calculates for which an exposed water-ice residual polar cap is free of seasonal CO_2 ice is increased by approximately 5 days when light penetration is included in the model. Thus, since the effect of light penetration slightly decreases CO_2 ice lifetimes when the ice does not exist year-round and slightly increases CO_2 ice survivability when ice does exist year-round, it also enhances the Jakosky and Haberle [1990] conclusion that there are two stable states for the residual polar caps; perennially covered by CO_2 ice or exposed every summer. These results also enhance the conclusion of Jakosky and Haberle that conduction of heat to and from the subsurface plays an important role in the energy balance of the polar cap.

Currently CO_2 ice does not survive summer on the northern residual polar cap while CO_2 ice does survive summer on the southern residual polar cap. The CO_2 ice at the south pole could have originated from an earlier epoch, but that would make the large abundances of water vapor observed in southern summer in 1969 harder to explain [Jakosky and Barker, 1984]. The inclusion of light penetration in an energy balance model makes it slightly easier for energy balance models to maintain seasonal CO_2 ice on an existing CO_2 residual polar cap, as now exists in the south, and to totally sublimate seasonal CO_2 ice on an exposed water ice residual polar cap, as now exists in the north. Hence, the effect of sunlight penetration makes it easier for energy balance models to explain the dichotomy in the residual polar caps.

While of some importance directly at the poles, the penetration of light into the polar cap has only a small effect on the globally-integrated energy budget of the polar cap, specifically the globally-integrated CO_2 sublimation and condensation as inferred by the Viking Lander measurements of atmospheric pressure and as predicted by theoretical models of the general atmospheric circulation. Given the uncertainties currently present in albedo and other parameters, the effect of light penetration is second order, and can be currently neglected in models of the globally-integrated energy budget of the polar caps. Further work remains to be done on other processes involved in the frost budget of the polar caps, as discussed in the introduction. These processes would not affect the major results of our work, but may have a significant impact on the globally-integrated frost budgets.

Acknowledgements. This work would not have been possible without the assistance of B. Jakosky. I also appreciate discussions with G. Clow and comments from anonymous reviewers. This research was supported under NASA contracts NASW-4444 and NASW-4614.

References

Clow, G.D., Generation of liquid water on Mars through the melting of a dusty snowpack, Icarus, 72, 95-127, 1987.

Jakosky, B.M. and E.S. Barker, Comparison of ground-based and Viking orbiter measurements of martian water vapor: Variability of the seasonal cycle, Icarus, 57, 322-334, 1984.

Jakosky, B.M. and R.M. Haberle, Year-to-year instability of the Mars south polar cap, J. Geophys. Res., 95, 1359-1365, 1990.

James, P.B. and G.R. North, The seasonal CO_2 cycle on Mars: An application of an energy-balance climate model, J. Geophys. Res., 87, 10271-10283, 1982.

Kieffer, H.H., Water grain size and the amount of dust in Mars' residual north polar cap, J. Geophys. Res., 95, 1481-1493, 1990.

Kieffer, H.H., S.C. Chase, Jr., T.Z. Martin, E.D. Miner, and F.D. Palluconi, Martian north pole summer temperatures: Dirty water ice, Science, 194, 1341-1344, 1976.

Kuhn, W.R., S.K. Atreya, and S.E. Postawko, The influence of ozone on martian atmospheric temperature, J. Geophys. Res., 84, 8341-8342, 1979.

Lindner, B.L., The aeronomy and radiative transfer of the Martian atmosphere, Ph.D. Dissertation, 470 pp., University of Colorado, Boulder, June 1985.

Lindner, B.L., Albedo of the polarcaps on Mars (abstract), EOS Trans. AGU, 67, 1078, 1986.

Lindner, B.L., Ozone on Mars: The effects of clouds and airborne dust, Planet. Space Sci., 36, 125-144, 1988.

Lindner, B.L., The martian polar cap: Radiative effects of ozone, clouds, and airborne dust, J. Geophys. Res., 95, 1367-1379, 1990.

Lindner, B.L., Ozone heating in the Martian Atmosphere, Icarus, 93, 354-361, 1991.

Lindner, B.L., CO_2 ice on Mars: Theoretical Simulations, in Physics and Chemistry of Ice, edited by N. Maeno and T. Hondoh, pp. 225-228, Hokkaido University Press, Sapporo, Japan, 1992.

Lindner, B.L., T.P. Ackerman, and J.B. Pollack, An efficient and accurate technique to compute the absorption, emission, and transmission of radiation by the martian atmosphere, in Scientific results of the NASA-sponsored study project on Mars: Evolution of volcanism, tectonics, and volatiles, edited by S.C. Soloman, V.L. Sharpton, and J.R. Zimbelman, pp. 198-200, LPI Tech. Rpt. 90-06, 322 pp., Lunar and Planetary Institute, Houston, 1990.

Moore, J.M., Experimental studies of sublimation in ice-particulate mixtures: Applications to Mars (abstract), Bull. Amer. Astron. Soc., 20, 847, 1988.

Paige, D.A., The annual heat balance of the martian polar caps from Viking observations, Ph.D. Dissertation, 207 pp., Calif. Inst. of Technol., Pasadena, Feb. 1985.

Paige, D.A. and A.P. Ingersoll, Annual heat balance of the martian polar caps: Viking observations, Science, 228, 1160-1168, 1985.

Pollack, J.B., R.M. Haberle, J. Schaeffer, and H. Lee, Simulations of the general circulation of the martian atmosphere. 1. Polar Processes, J. Geophys. Res., 95, 1447-1474, 1990.

Toon, O.B., J.B. Pollack, W. Ward, J.A. Burns, and K. Bilski, The astronomical theory of climate change on Mars, Icarus, 44, 552-607, 1980.

Warren, S.G., W.J. Wiscombe, and J.F. Firestone, Spectral albedo and emissivity of CO_2 in martian polar caps: Model results, J. Geophys. Res., 95, 14714-14741, 1990.

B.L. Lindner, Atmospheric and Environmental Research, Inc., 840 Memorial Drive, Cambridge, MA 02139.

(Received February 14, 1992;
revised June 15, 1992;
accepted June 29, 1992.)

CO_2 ice on Mars: Theoretical simulations

Bernhard Lee Lindner
Atmospheric and Environmental Research, Inc., 840 Memorial Drive, Cambridge, Mass. 02139-3794, USA

ABSTRACT: A theoretical model of the energy budget of the polar caps of Mars has been created which is used to study the hemispherical asymmetry in CO_2 ice. The observations which show survival of seasonal CO_2 ice in the southern hemisphere in summer and not in the northern hemisphere in summer have been reproduced.

1. INTRODUCTION

One of the most puzzling mysteries about the planet Mars is the hemispherical asymmetry in the polar caps. Every spring the seasonal polar cap of CO_2 recedes until the end of summer, when only a small part, the residual polar cap, remains. During the year that Viking observed Mars, the residual polar cap was composed of water ice in the northern hemisphere (1) but was primarily carbon dioxide ice in the southern hemisphere (2). Scientists have sought to explain this asymmetry by modeling observations of the latitudinal recession of the polar cap and seasonal variations in atmospheric pressure (since the seasonal polar caps are primarily frozen atmosphere, they are directly related to changes in atmospheric mass). These models reproduce most aspects of the observed annual variation in atmospheric pressure fairly accurately. Furthermore, the predicted latitudinal recession of the northern polar cap in the spring agrees well with observations, including the fact that the CO_2 ice is predicted to completely sublime away. However, these models all predict that the carbon dioxide ice will also sublime away during the summer in the southern hemisphere, unlike what is observed, as is shown in Figure 1. This paper will show how the radiative effects of ozone, clouds, and airborne dust, light penetration into and through the polar cap, and the dependence of albedo on solar zenith angle affect CO_2 ice formation and sublimation, and how they help explain the hemispherical asymmetry in the residual polar caps. These effects have not been studied with prior polar cap models.

2. MODEL DESCRIPTION

The energy budget of the surface of Mars has been studied with a model which includes all of the processes shown schematically in Figure 2. The sources and sinks of energy for a square centimeter of surface include solar insolation which strikes the surface, modified for the absorption due to clouds and aerosols; infrared emission by the clear atmosphere and by clouds and aerosols to the surface; infrared emission by the surface to space; penetration of solar radiation into the surface; atmospheric heat transport as represented by a thermal wind; heat conduction in the subsurface; and latent heat of condensation of CO_2. The net gain or loss of energy integrated over one martian day is used to compute either a change in the surface temperature or a change in the amount of CO_2 frost present. Details on the model are presented elsewhere (9,10,11).

Since O_3 is more prevalent in the northern hemisphere than in the southern hemisphere, O_3 was suggested as a cause for the hemispherical asymmetry in the residual polar caps (12). However, O_3 has since been shown to have a minor effect on the atmospheric temperature (13), and hence on the infrared radiation which strikes the polar cap, and it has been shown that O_3 absorbs less than 1% of the total solar radiation absorbed by the polar cap (9). Thus, O_3 is not an important consideration in the polar cap energy budget.

The solar and thermal flux striking the polar cap of Mars has been computed for various dust and cloud abundances and for three solar zenith angles (9). These calculations have been inserted in earlier versions of polar-cap models (10,11). Vertical optical

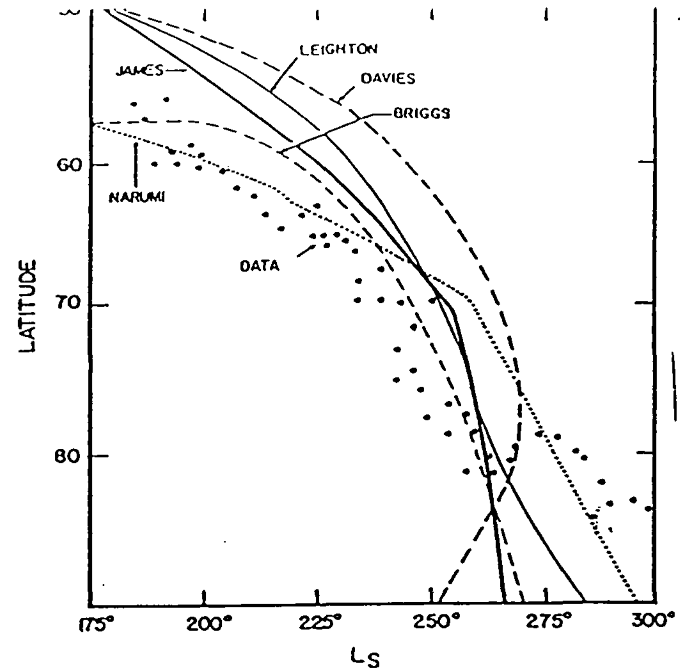

Fig. 1. The seasonal recession of the south polar cap as observed over the last 20 years (3) and as predicted by (4,5,6,7,8). (The aerocentric longitude of the sun, L_s, is the seasonal index; L_s = 0°, 90°, 180° and 270° correspond to northern spring equinox, summer solstice, autumnal equinox and winter solstice, respectively.)

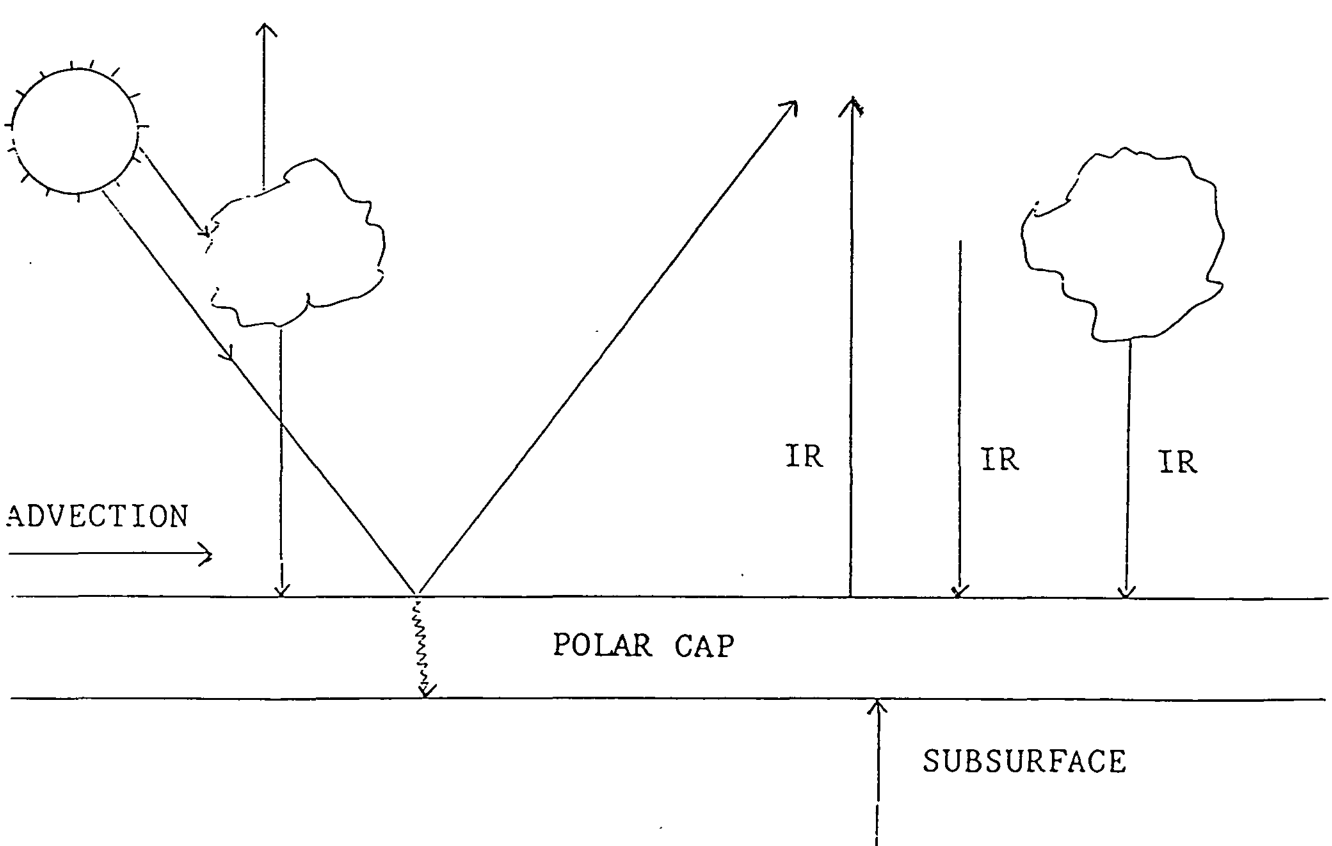

Fig. 2. Schematic of the model for the energy budget of the polar cap, showing the physical processes included.

depths of dust and cloud ranging from zero to 1 increase the absorbed flux significantly in polar night, where the pole spends half of the year, as shown in Table 1 (9). Observed hemispherical asymmetries in dust abundance, cloud cover, and surface pressure combine to cause a significant hemispherical asymmetry in the total flux absorbed by the residual polar caps (9), which helps to explain the dichotomy in the residual polar caps on Mars.

Penetration of solar radiation into the cap itself is included, based on theoretical work (14). The inclusion of light penetration slightly decreases the albedo needed in the model to keep CO_2-ice year-round at the south pole by on the order of 1%. The required albedo is decreased because some solar radiation is used to heat the subsurface, and not all of this heat is transported back to the surface. Overall, penetration of light into the polar cap has only a small effect on the polarcap energy budget.

Calculations of the dependence of the albedo of the martian polar caps on solar zenith angle (15) have also been included in the model. Since the albedo of ice increases and becomes more forward scattering at higher solar zenith angles, and since the solar zenith angle becomes higher as one approaches the pole, the albedo is greatest at the pole. This decreases absorption of sunlight, hence increasing survivability of CO_2 ice. In fact, this increases the survivability of ice enough to offset the decrease in survivability of ice due to the radiative effects of clouds and dust.

TABLE 1. Flux Striking the Surface of the Polar Cap in Polar Night (90°N Latitude, L_s = 343°)

Wavelength Interval, μm	Dust Opacity 0.0	0.2	0.5
5.4-10.0	0.0	0.7	1.3
10.0-21.0	14.7	29.4	43.4
21.0-99.9	0.0	13.5	29.9
Absorbed flux	14.7	43.6	74.7

The vertical optical depth of dust is given. Flux values are given in units of J cm^{-2} sol^{-1}.

3. DISCUSSION

The combination of the effects of solar zenith angle on albedo and the radiative effects of clouds and dust act to extend the lifetime of CO_2 ice on the south pole relatively more than on the north pole, explaining the hemispherical asymmetry in the residual polar caps without the need of a hemispherical asymmetry in polar cap albedo. Another positive aspect of this solution is that neither the inclusion of solar zenith angle effects on ice albedo nor the radiative effects of clouds and dust should appreciably change model predictions of the annual cycle of pressure or polar cap recession equatorward of 75° latitude, since approximately 90% of the seasonal CO_2 frost is equatorward of 80° latitude. Hence, the good model agreement noted by prior researchers to the seasonal cycle in atmospheric pressure and to the recession of the polar cap equatorward of 80° latitude is retained.

REFERENCES

1.H.Kieffer et. al., Science, 194, 1341 (1976).
2.H.Kieffer, J. Geophys. Res., 84, 8263, (1979).
3.P.James and K.Lumme, Icarus, 50, 368, (1982).
4.R.Leighton and B. Murray, Science, 153, 136, (1966).
5.D.Davies et al., J. Geophys. Res., 82, 3815, (1977).
6.G.Briggs, Icarus, 23, 167, (1974).
7.P.James and G.North, J. Geophys. Res., *J. Geophys. Res.* 87, *10271*, (1982).

8. Y. Narumi, Proc. 13th Lunar and Planet. Symp., (Inst. Space Aero. Sci., U. of Tokyo, 1980), p31.
9. B.L. Lindner, J. Geophys. Res., 95, 1367, (1990).
10. B.L. Lindner, "The Aeronomy and Radiative Transfer of the Martian Atmosphere", (University of Colorado Ph.D. Dissertation, 1985).
11. B. Jakosky and R. Haberle, J. Geophys. Res., 95, 1359, (1990).
12. W. Kuhn et al., J. Geophys. Res., 84, 8341, (1979).
13. B.L. Lindner, Icarus, 93, (1991).
14. G. Clow, Icarus, 72, 95, (1987).
15. S. Warren et al., J. Geophys. Res., 95, 14717, (1990).

JOURNAL OF GEOPHYSICAL RESEARCH, VOL. 98, NO. E2, PAGES 3339–3344, FEBRUARY 25, 1993

The Hemispherical Asymmetry in the Martian Polar Caps

BERNHARD LEE LINDNER

AER, Inc., Cambridge, Massachusetts

An energy balance model is used to study the behavior of CO_2 ice on Mars. The effect of the solar zenith angle dependence of albedo is to lengthen CO_2 ice lifetimes at the poles. Hemispherical asymmetries in cloud and dust abundance could result in the survival of seasonal CO_2 ice through summer in the south and not in the north, in agreement with observations. CO_2 ice observed in the summertime polar cap in the south could be of recent origin, although a permanent CO_2 polar cap cannot be ruled out.

INTRODUCTION

During the year that Viking observed Mars, the summertime polar cap consisted of water ice in the northern hemisphere [*Kieffer et al.*, 1976], but was primarily carbon dioxide ice in the southern hemisphere [*Kieffer*, 1979]. CO_2 ice was also inferred to be present in the summertime south polar cap during the Mariner 9 encounter [*Paige et al.*, 1990]. Open questions remain as to why a hemispherical asymmetry exists, and whether the summertime CO_2 ice in the southern hemisphere is primarily seasonal in origin, or whether a reservoir of CO_2 from an earlier epoch is being uncovered. A permanent exposed CO_2 ice cap would be one source of CO_2 for possible past climates on Mars with dense CO_2 atmospheres [e.g., *Sagan et al.*, 1973; *Toon et al.*, 1980; *Hoffert et al.*, 1981; *Fanale et al.*, 1982; *Francois et al.*, 1990]. However, Earth-based measurements made in 1969 of water vapor in the martian atmosphere suggest that all CO_2 ice sublimed from the southern polar cap and exposed underlying water ice [*Jakosky and Barker*, 1984], which would be inconsistent with the existence of a permanent CO_2 ice reservoir.

Theoretical models of the energy budget of the surface have been created which simulate the formation and dissipation of carbon dioxide ice and which have been compared to observations of polar cap regression and the annual cycle in atmospheric pressure [*Leighton and Murray*, 1966; *Cross*, 1971; *Briggs*, 1974; *Davies et al.*, 1977; *Narumi*, 1980; *James and North*, 1982; *Lindner*, 1985; *Moreau et al.*, 1991; *Wood and Paige*, 1992]. As shown in Figure 1, these models have been unable to preserve seasonal CO_2 ice at the south pole and still obtain agreement with observations of the polar cap regression and the annual cycle in atmospheric pressure. No combination of best-fit frost albedos and emissivities was consistent with the stability of permanent CO2 deposits at either pole [*Wood and Paige*, 1992]. This implies that either these models improperly treated the energy budget or that CO_2 ice from an earlier time is exposed.

Clouds have been observed to be more prevalent over the edge of the northern seasonal polar cap than over the edge of the southern seasonal polar cap, although observations of clouds are far from complete [*James*, 1983; *Christensen and Zurek*, 1983; *James et al.*, 1987]. Atmospheric dust experiences an annual cycle, with order of magnitude variations in dust opacity [*Pollack et al.*, 1979]. Surface pressure is lower during southern winter over the south pole than during northern winter over the north pole, due to differences in elevation [*Woiceshyn*, 1974; *Lindal et al.*, 1979] and due to the annual cycle in atmospheric pressure [*Hess et al.*, 1980]. The combination of these phenomena appear to result in a hemispherical asymmetry in the annual-total amount of solar and infrared radiation which strikes the residual polar caps, favoring the survival of CO_2 ice at the south pole [*Lindner*, 1990].

MODELING PROCEDURE

Figure 2 shows schematically all of the processes included in the model. The model is similar to those previously developed except as specified below. The sources and sinks of energy per unit area of surface include solar radiation, modified for the absorption and scattering due to cloud and dust; infrared emission by cloud, dust, and gas in the atmosphere; infrared emission by the surface to space; atmospheric heat transport; heat conduction into/from the subsurface; and latent heat of condensation of CO_2. The energy balance at the surface is represented by

$$F(x,t)A(x,t) - \varepsilon\sigma T^4(0,x,t) + L\frac{\delta M(x,t)}{\delta t} - K\frac{\delta T(z,x,t)}{\delta t} + H(x,t) = 0 \quad (1)$$

where $F(x,t)$ is the solar and infrared radiation which strikes the surface at latitude x and time t; $A(x,t)$ is the co-albedo (1-albedo); ε is the effective emissivity of the surface; σ is the Stefan-Boltzman radiation constant; $T(z,x,t)$ is the temperature and $\delta T/\delta z$ is the gradient in temperature with depth z, evaluated at the surface; L is the latent heat of condensation of CO_2; $\delta M(x,t)$ is the change in mass of CO_2 frost; δt is the time interval (taken to be 1/50 of a sol); K is the thermal conductivity of the surface and the subsurface; and $H(x,t)$ is the transport of heat by the atmosphere. The net gain or loss of energy over the time interval is used to compute either a change in surface temperature or a change in the mass of CO_2 frost. The solar and infrared radiation which strikes the surface as a function of latitude, time, and cloud and dust amount is taken from *Lindner* [1990]. The radiative effects of O_3 were suggested to be important for the energy budget [*Kuhn et al.*, 1979], but have been shown to be negligible [*Lindner*, 1991]. Penetration of radiation into and through the ice has been shown to have a minor effect on the energy budget [*Lindner*, 1992]. The solar zenith angle dependence of ice albedo is taken from *Warren et al.* [1990], using a solar zenith angle which is reduced by 10° as a rough correction for the effect of surface roughness. The albedo of ice in the infrared is taken to be zero. Heat transport

Paper number 92JE02975.
0148-0227/93/92JE-02975$05.00

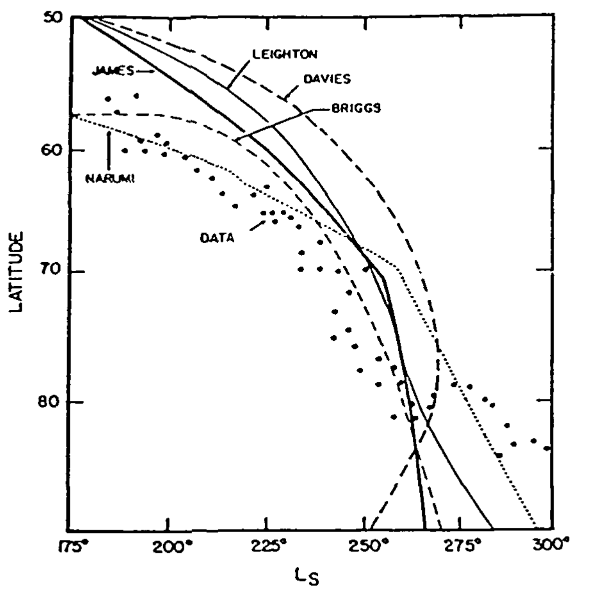

Fig. 1. The seasonal recession of the south polar cap as observed over the last 20 years [*James and Lumme*, 1982] and as predicted by *Leighton and Murray* [1966], *Briggs* [1974], *Davies et al.* [1977], *Narumi* [1980], and *James and North* [1982]. (The aerocentric longitude of the Sun, L_s, is the seasonal index; $L_s = 0°, 90°, 180°$, and 270° correspond to northern spring equinox, summer solstice, autumnal equinox, and winter solstice, respectively.)

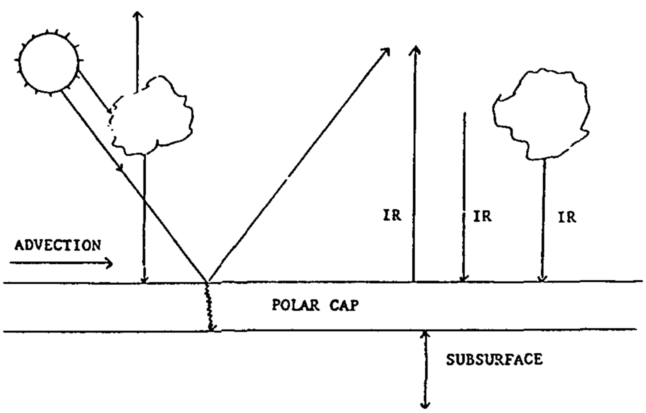

Fig. 2. Schematic of the model for the energy budget of the polar cap, showing the physical processes included. The sum of all sources and sinks of energy is balanced by either a change in temperature or a change in ice mass.

by the atmosphere is parameterized as by *James and North* [1982], that is, it simply depends on the latitudinal gradient of surface temperature multiplied by a constant [see also *North et al.*, 1981; *Hoffert et al.*, 1981]. Hence the heat transport term is most important near the edge of the polar cap in spring and summer when the surface temperature gradient is very large. This is obviously an oversimplification of the transport process, but is easily tractable and has produced satisfactory results in the past. Conduction of heat into the subsurface is represented by the heat conduction equation

$$\delta T(z,x,t)/\delta t = (K/\rho C)(\delta^2 T(z,x,t)/\delta z^2) \qquad (2)$$

where ρ is the bulk density of the subsurface material and C is its specific heat. Equations (1) and (2) are applied and evaluated as by *Jakosky and Haberle* [1990], every 2° in latitude.

Clouds are assumed to exist only where CO_2 frost exists. The existence and opacity of cloud are highly variable and uncertain, although observers have noted a "polar hood", a layer of clouds which cloaks the polar cap [e.g., *Leovy et al.*, 1972; *James et al.*, 1987]. Several values for cloud opacity are studied here. Atmospheric dust opacity is taken from *Pollack et al.* [1979], although the global dust storms are ignored because of the strong increase in atmospheric heat transport. However, global dust storms do not appear to have significantly affected polar cap recession [*Briggs*, 1974; *Davies*, 1979; *James et al.*, 1979; *Kieffer*, 1979; *Martin and Kieffer*, 1979; *James and North*, 1982; *Paige*, 1985]. Furthermore, the annual cycle in atmospheric pressure has repeated remarkably well from year to year, even though dust storms do not, which also implies that any linkage between dust storms and the CO_2 cycle is not strong.

COMPARISON OF THE MODEL RESULTS TO OBSERVATIONS

Figures 3-6 show the regression of the polar caps as predicted by the model and as observed. Agreement is good, particularly in the northern hemisphere. An exact comparison is difficult, considering that the edge of the polar cap is usually patchy and ill-defined [*Leovy et al.*, 1972; *Christensen and Zurek*, 1983], in large part due to terrain. The edge of the polar cap is also diurnally variable since ice frequently forms at night and sublimes during the day. There is also some year-to-year variability in polar cap regression [*Iwasaki et al.*, 1990; *James et al.*, 1990]. Observations hint that cloud opacity is of the order of 0.2 in the southern hemisphere and 0.5 in the northern hemisphere [e.g., *Briggs and Leovy*, 1974; *James et al.*, 1987], perhaps due in part to airmass differences. Such an asymmetry in cloud is used in Figures 3-6. An asymmetry in cloud opacity of 0.5 and 1.0 in the southern and northern hemisphere, respectively, will result in similar recession curves, although a higher ice albedo is required to counteract the increased polar night heating which results from increased cloud opacity. If no asymmetry in cloud opacity is assumed, then the model predicts seasonal CO_2 ice is more likely to be retained at the north pole than the south pole, as noted in earlier models.

These results are obtained with an albedo for old ice of 0.72. This value is consistent with those obtained by earlier models [e.g., *James and North*, 1982; *Jakosky and Haberle*, 1990] and, given model simplifications and uncertainties in albedo measurements, would appear to be consistent with observations [*Jakosky and Haberle*, 1990]. Fresh ice is assumed to have an albedo of 0.95. Based on terrestrial analogs, ice albedo is assumed to shift linearly from new to old over a period of 20 sols after net sublimation has started. This assumption did not result in significantly different results than just assuming an instantaneous shift from new to old ice. The inferred albedos are not unique, as there are many combinations and permutations of free parameters that will yield similarly good fits (e.g., changes in emissivity, cloud cover, heat transport, etc.). In fact, this lack of uniqueness did not allow for any determination of a latitudinal or seasonal dependence of ice albedo, and therefore given the lack of data on the albedo, no latitudinal or seasonal dependence in ice albedo was assumed.

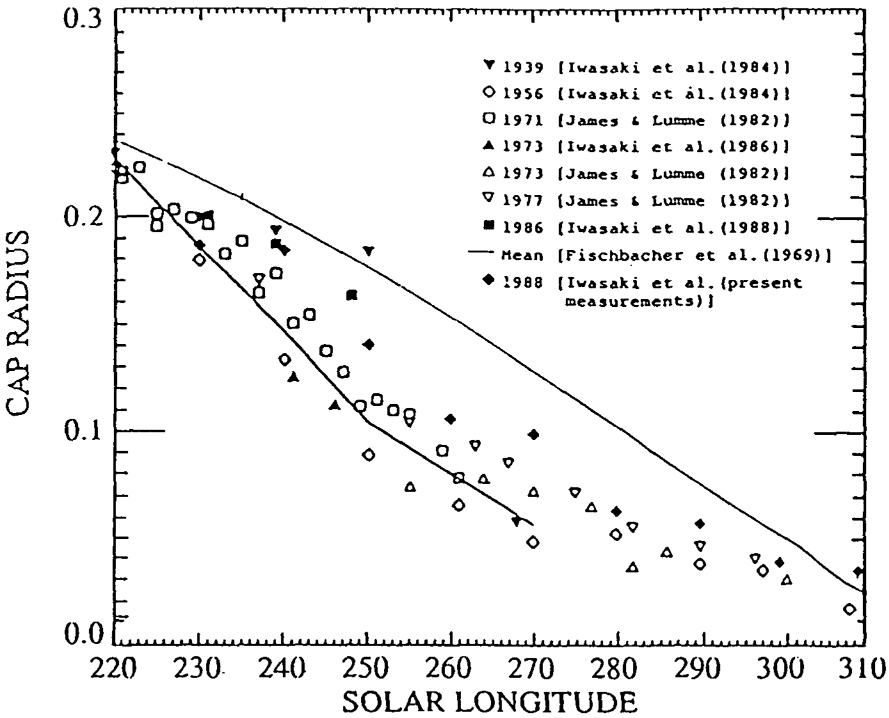

Fig. 3. The regression of the south polar cap, as observed for various years (taken from *Iwasaki et al.* [1990]) and as simulated by my model (thin line), as a function of the aerocentric longitude of the Sun (L_S). The cap radius is that which would be measured on a polar stereographic projection of the south polar region; the units of the radius are fractions of the planetary radius of Mars.

However, a hemispherical asymmetry in some parameter, such as in the albedo or in the opacity of cloud and dust, is needed to allow the models to retain some seasonal CO_2 ice year-round at the south pole and not at the north pole.

Atmospheric temperatures used in this model ranged from 130 K to 180 K [*Lindner*, 1990], some of the coldest inferred in the polar regions by the Viking orbiter [*Lindal et al.*, 1979]. Higher atmospheric temperatures than those used here would actually increase the thermal emission by dust and cloud even more, making their radiative effects yet more important to the overall energy budget. However, the temperatures used are not as important as one might expect, because most atmospheric dust and cloud lie near the surface (about 60% is within 8 km of the surface; one atmospheric scale height at 160 K), and atmospheric temperatures near the surface remain very close to the CO_2 frost point temperature during winter, except during global dust storms [*Lindal et al.*, 1979].

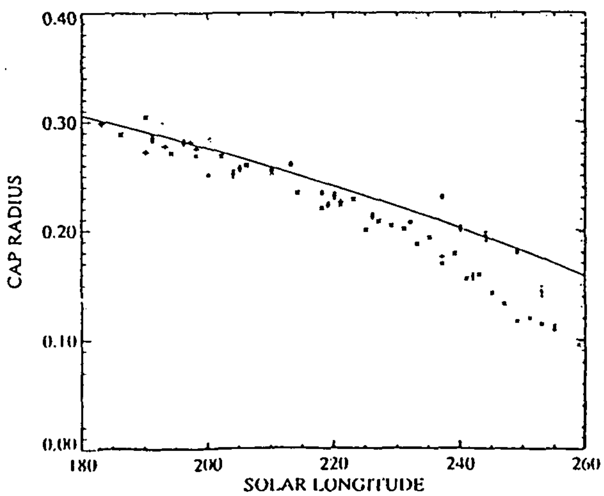

Fig. 4. The regression of the south polar cap, as observed in 1986 (solid circles), 1971 (crosses), and 1977 (pluses) (taken from *James et al.* [1990]) and as simulated by my model (thin line), as a function of the aerocentric longitude of the Sun (L_S). Two-sigma error bars are indicated for the 1986 data; the errors are smaller for the denser 1971 data and for the 1977 Viking data.

Discussion

If a hemispherical asymmetry in polar clouds is included in an energy balance model together with the solar zenith angle dependence of ice albedo, then the observations of polar cap regression can be reproduced while retaining seasonal CO_2 ice at the south pole and not at the north pole. The addition to the model of the radiative effects of cloud and background dust and of the solar zenith angle dependence of ice albedo causes little change in the total flux absorbed by the polar cap near its edge but becomes more important farther poleward from the polar cap edge [*Lindner*, 1990]. This would explain why earlier models were successful at reproducing the regression of the polar caps equatorward of 80° latitude but not at the pole (see Figure 1). Moreover, the integral of seasonal CO_2 ice over the 80° to 90° latitude band is an order of magnitude less than the integral of seasonal CO_2 ice over the planet. Thus any effect which is most important only for ice at the pole will not have a major effect on the atmospheric pressure, explaining the good fit to the atmospheric pressure data also obtained by earlier models.

James et al. [1979] and *Paige and Ingersoll* [1985] present evidence for the existence of a hemispherical asymmetry in polar cap albedo, with the south pole being 25% brighter,

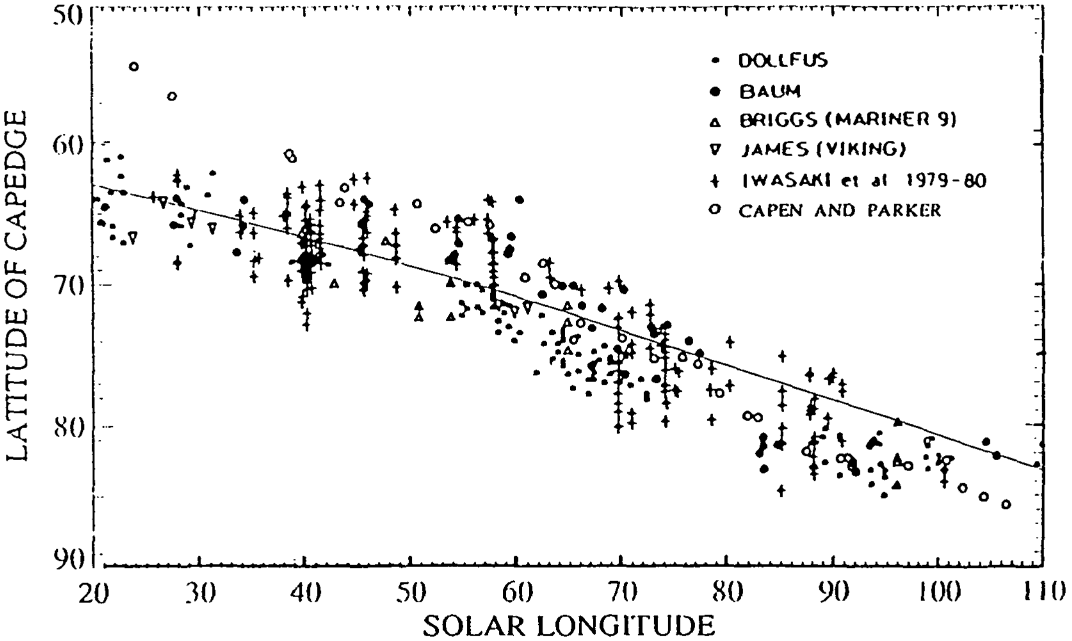

Fig. 5. The regression of the north polar cap, as observed for various years (taken from *Iwasaki et al.* [1982]; symbols refer to *Dollfus* [1973], *Baum* [1974], *Briggs* [1974], *James* [1979], *Capen and Parker* [1981], and *Iwasaki et al.* [1982]) and as simulated by my model (thin line), as a function of the aerocentric longitude of the Sun (L_s).

although the specifics of how a hemispherical asymmetry in ice albedo maintains itself remain to be completely worked out. If a hemispherical asymmetry in albedo plays an important role in the asymmetry in the polar caps, then the asymmetry in albedo would have to be as extreme as that suggested by *Paige and Ingersoll* [1985]. A substantial part of the energy budget of the polar caps comes from IR emission by cloud and dust, atmospheric heat transport, and heat conduction from the subsurface; sources which are unaffected by albedo variations at solar wavelengths. Furthermore, polar cap albedo does not have a linear effect on the energy budget, as cloud and dust will reflect some of the solar flux reflected from the polar cap back onto the polar cap. For these two reasons, the presence of cloud and dust lessens the ability for albedo changes to affect CO_2 ice lifetimes.

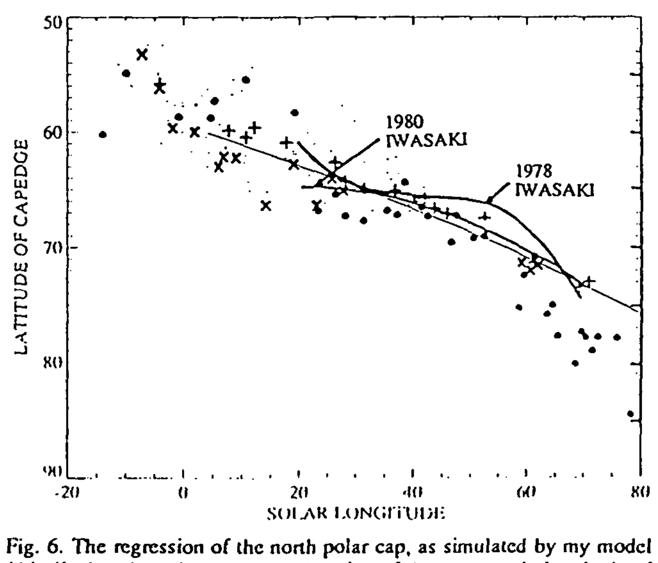

Fig. 6. The regression of the north polar cap, as simulated by my model (thin line) and as observed, as a function of the aerocentric longitude of the Sun (L_s). Data are taken from *James et al.* [1987]; also showing data of *Iwasaki et al.* [1979; 1982]. The symbols stand for 1977-1978 and 1980 Viking data (crosses and pluses, respectively) and ground-based 1975-1980 data (circles).

Many processes have yet to be examined as to their effect on the energy budget of the polar caps. The emissivity of CO_2 ice could be much lower, based on the theoretical simulations of *Warren et al.* [1990]. Ice is strongly forward scattering at high solar zenith angles [*Taylor and Stowe*, 1984], which has implications for multiple reflections between polar cap and polar hood. Surface roughness, particularly if present in the form of penitentes [*Svitek and Murray*, 1988], would change the effective solar zenith angle and IR surface cooling. Ice microphysics also requires further study with regard to the ice energy budget and may offer some hemispherical asymmetry [J. Eluszkiewicz, personal communication, 1992]. Snowfall also needs to be accounted for, particularly during periods of high dust opacity [*Pollack et al.*, 1990]. An insulating residue on the ice [*Saunders et al.*, 1986] and wind shifting of ice [*Briggs*, 1974; *James et al.*, 1979; *Kieffer*, 1979] may also be significant for the ice energy budget. Improved modeling of atmospheric heat transport is also needed. Possible hemispheric asymmetries in weather systems may contribute to the asymmetry in the polar caps [*Barnes*, 1991]. Moreover, more observations of the polar hood are needed to show the magnitude of a hemispherical asymmetry in cloud opacity, particularly in polar night, and to answer questions with regard to interannual variability.

Despite the work that remains, it appears possible to construct an energy balance model which maintains seasonal CO_2 ice at the south pole year-round and not at the north pole year-round and still reasonably simulates the overall polar cap regression data. Hence earlier model difficulties in retaining seasonal ice at the south pole have been removed. CO_2 ice observed in the summertime south polar cap could be seasonal in origin. Seasonal CO_2 ice at the south pole is also suggested by the water vapor observations of *Jakosky and Barker* [1984]. However, further research remains before it is certain whether the CO_2 ice observed in the summertime south pole is seasonal or is part of a permanent reservoir.

Acknowledgments. I am extremely grateful to Bruce Jakosky for many valuable discussions and assistance with computer codes. I thank P. James and S. Wood for thoughtful reviews. This work was supported by NASA contracts NASW-4444 and NASW-4614.

REFERENCES

Barnes, J. R., Midlatitude weather systems on Mars: Is there a hemispheric asymmetry?, in *Workshop on the Martian Surface and Atmosphere Through Time*, pp. 7-8, Lunar and Planetary Institute, Houston, Tex., 1991.

Baum, W. A., Results of current Mars studies at the IAU Planetary Research Center, in *Exploration of the Planetary System*, edited by A. Woszczyk and C. Iwaniszewska, pp. 241-151, D. Reidel, Norwell, Mass., 1974.

Briggs, G. A., The nature of the residual Martian polar caps, *Icarus, 23*, 167-191, 1974.

Briggs, G. A., and C. B. Leovy, Mariner 9 observations of the Mars north polar hood, *Bull. Am. Meteorol. Soc., 55*, 278-296, 1974.

Capen, C. G., and D. C. Parker, What is new on Mars---Martian 1979-1980 apparition report II, *J. Assoc. Lunar Planet Obs.*, 1981.

Christensen, P. R., and R. W. Zurek, Martian water-ice clouds: Location and seasonal variation (abstract), *Bull. Am. Astron. Soc., 15*, 847, 1983.

Cross, C. A., The heat balance of the Martian polar caps, *Icarus, 15*, 110-114, 1971.

Davies, D. W., Effects of dust on the heating of Mars' surface and atmosphere, *J. Geophys. Res., 84*, 8289-8293, 1979.

Davies, D. W., C. B. Farmer, and D. D. LaPorte, Behavior of volatiles in Mars' polar areas: A model incorporating new experimental data, *J. Geophys. Res., 82*, 3815-3822, 1977.

Dollfus, A., New optical measurements of planetary diameters, IV., Size of the north polar cap of Mars, *Icarus, 18*, 142-155, 1973.

Fanale, F. P. , J. R. Salvail, W. B. Banerdt, and R. S. Saunders, Mars: The regolith-atmosphere-cap system and climate change, *Icarus, 50*, 381-407, 1982.

Fischbacher, G.E., L.J. Martin, and W.A. Baum, Martian polar cap boundaries, final report, part A contract 951547 to Jet Propul. Lab., Pasadena, Calif., Planet. Res. Center, Lowell Obs. Flagstaff, Ariz., May 1969.

Francois, L. M., J. C. G. Walker, and W. R. Kuhn, A numerical simulation of climate changes during the obliquity cycle on Mars, *J. Geophys. Res., 95*, 14,761-14,778, 1990.

Hess, S. L., J. A. Ryan, J. E. Tillman, R. M. Henry, and C. B. Leovy, The annual cycle of pressure on Mars measured by Viking Landers 1 and 2, *Geophys. Res. Lett., 7*, 197-200, 1980.

Hoffert, M. I., A. J. Callegari, C. T. Hsieh, and W. Z. Ziegler, Liquid water on Mars: An energy balance climate model for CO_2/H_2O atmospheres, *Icarus, 47*, 112-129, 1981.

Iwasaki, K., Y. Saito, and T. Akabane, Behavior of the Martian north polar cap, 1975-1978, *J. Geophys. Res., 84*, 8311-8316, 1979.

Iwasaki, K., Y. Saito, and T. Akabane, Martian north polar cap 1979-1980, *J. Geophys. Res., 87*, 10,265-10,269, 1982.

Iwasaki, K., Y. Saito, and T. Akabane, Martian north polar cap and haze 1981-1982, *Publ. Astron. Soc. Jpn., 36*, 347-356, 1984.

Iwasaki, K., Y. Saito, and T. Akabane, Interannual differences in the regressions of the polar caps of Mars, Mars: Evolution of its climate and atmosphere, *LPI Tech. Rep. 87-01*, pp. 57-59, Lunar and Planet. Inst., Houston, Tex., 1986.

Iwasaki, K., Y. Saito, T. Akabane, Y. Nakai, E. Panjaitan, I. Radiman, and S.D. Wiramiharja, Martian south polar cap 1986, *Vistas Astron., 31*, 141-146, 1988.

Iwasaki, K., Y. Saito, Y. Nakai, T. Akabane, E. Panjaitan, I. Radiman, and S. Wiramihardja, Martian south polar cap 1988, *J. Geophys. Res., 95*, 14,751-14,754, 1990.

Jakosky, B. M., and E. S. Barker, Comparison of ground-based and Viking orbiter measurements of Martian water vapor: Variability of the seasonal cycle, *Icarus, 57*, 322-334, 1984.

Jakosky, B. M., and R. M. Haberle, Year-to-year instability of the Mars south polar cap, *J. Geophys. Res., 95*, 1359-1365, 1990.

James, P.B., Recession of Martian north polar cap: 1977-1978 Viking observations, *J. Geophys. Res., 84*, 8332-8334, 1979.

James, P. B., Condensation phase of the Martian south polar cap (abstract), *Bull. Am. Astron. Soc., 15*, 846-847, 1983.

James, P. B., and K. Lumme, Martian south polar cap boundary: 1971 and 1973 data, *Icarus, 50*, 368-380, 1982.

James, P. B., and G. R. North, The seasonal CO_2 cycle on Mars: An application of an energy-balance climate model, *J. Geophys. Res., 87*, 10,271-10,283, 1982.

James, P. B., G. Briggs, J. Barnes, and A. Spruck, Seasonal recession of Mars' south polar cap as seen by Viking, *J. Geophys. Res., 84*, 2889-2922, 1979.

James, P. B., M. Pierce, and L. J. Martin, Martian north polar cap and circumpolar clouds: 1975-1980 telescopic observations, *Icarus, 71*, 306-312, 1987.

James, P. B., L.J. Martin, J. R. Hensen, and P. V. Birch, Seasonal recession of Mars' south polar cap in 1986, *J. Geophys. Res., 95*, 1337-1341, 1990.

Kieffer, H. H., Mars south polar spring and summer temperatures: A residual CO_2 frost, *J. Geophys. Res., 84*, 8263-8288, 1979.

Kieffer, H. H., S. C. Chase, Jr., T. Z. Martin, E. D. Miner, and F. D. Palluconi, Martian north pole summer temperatures: Dirty water ice, *Science, 194*, 1341-1343, 1976.

Kuhn, W. R., S. K. Atreya, and S. E. Postawko, The influence of ozone on Martian atmospheric temperature, *J. Geophys. Res., 84*, 8341-8342, 1979.

Leighton, R. B., and B. C. Murray, Behavior of carbon dioxide and other volatiles on Mars, *Science, 153*, 136-144, 1966.

Leovy, C. B., G. A. Briggs, A. T. Young, B. A. Smith, J. B. Pollack, E. N. Shipley, and R. L. Wildey, The Martian atmosphere: Mariner 9 television experiment progress report, *Icarus, 17*, 373-393, 1972.

Lindal, G. F., H. B. Hotz, D. N. Sweetnam, Z. Shippony, J. P. Brenkle, G. V. Hartsell, R. T. Spear, and W. H. Michael, Jr., Viking radio occultation measurements of the atmosphere and topography of Mars: Data acquired during 1 Martian year of tracking, *J. Geophys. Res., 84*, 8443-8456, 1979.

Lindner, B. L., The aeronomy and radiative transfer of the Martian atmosphere, Ph.D. dissertation, 470 pp., Univ. of Colo., Boulder, Aug. 1985.

Lindner, B. L., The Martian polar cap: Radiative effects of ozone, clouds, and airborne dust, *J. Geophys. Res., 95*, 1367-1379, 1990.

Lindner, B. L., Ozone heating in the Martian atmosphere, *Icarus, 93*, 354-361, 1991 .

Lindner, B. L., Sunlight penetration through the Martian polar caps: Effects on the thermal and frost budgets, *Geophys. Res. Lett., 19*, 1675-1678, 1992.

Martin, T. Z., and H. H. Kieffer, Thermal infrared properties of the Martian atmosphere, 2, The 15 micron band measurements, *J. Geophys. Res., 84*, 2843-2852, 1979.

Moreau, D., L.W. Esposito, and G. Brasseur, The chemical composition of the dust-free Martian atmosphere: Preliminary results of a two-dimensional model, *J. Geophys. Res., 96*, 7933-7945, 1991.

Narumi, Y., The seasonal variation of atmospheric pressure on Mars, in *Proceedings of the 13th Lunar and Planetary Symposium*, pp. 31-41, Institute of Space and Aeronautical Science, University of Tokyo, 1980.

North, G. R., R. F. Cahalan, and J. A. Coakley, Energy balance climate models, *Rev. Geophys., 19*, 91-124, 1981.

Paige, D. A., The annual heat balance of the Martian polar caps from Viking observations, Ph.D. dissertation, 207 pp., Calif. Inst. of Technol., Pasadena, May 1985.

Paige, D. A., and A. P. Ingersoll, Annual heat balance of Martian polar caps: Viking observations, *Science, 228*, 1160, 1985.

Paige, D. A., K. E. Herkenhoff, and B. C. Murray, Mariner 9 observations of the south polar cap of Mars: Evidence for residual CO_2 frost, *J. Geophys. Res., 95*, 1319-1335, 1990.

Pollack, J. B., D. S. Colburn, F. M. Flasar, R. Kahn, C. E. Carlston, and D. Pidek, Properties and effects of dust particles suspended in the Martian atmosphere, *J. Geophys. Res., 84*, 2929-2945, 1979.

Pollack, J. B., R. M. Haberle, J. Schaeffer, and H. Lee, Simulations of the general circulation of the Martian atmosphere, 1, Polar processes, *J. Geophys. Res., 95*, 1447-1474, 1990.

Sagan, C., O.B. Toon, and P.J. Gierasch, Climate change on Mars, *Science, 181*, 1045-1049, 1973.

Saunders, R. S., F. P. Fanale, T. J. Parker, J. B. Stephens, and S. Sutton, Properties of filamentary sublimation residuals from dispersions of clay in ice, *Icarus*, *66*, 94-104, 1986.

Svitek, T., and B. C. Murray, Penitentes on Mars? (abstract), *Bull. Am. Astron. Soc.*, *20*, 847-848, 1988.

Taylor, V. R., and L. L. Stowe, Reflectance characteristics of uniform Earth and cloud surfaces derived from Nimbus 7 ERB, *J. Geophys. Res.*, *89*, 4987-4996, 1984.

Toon, O. B., J. B. Pollack, W. Ward, J. A. Bums, and K. Bilski, The astronomical theory of climatic change on Mars, *Icarus*, *44*, 552-607, 1980.

Warren, S. G., W. J. Wiscombe, and J. F. Firestone, Spectral albedo and emissivity of CO_2 in Martian polar caps: Model results, *J. Geophys. Res.*, *95*, 14,714-14,741, 1990.

Woiceshyn, P. M., Global seasonal atmospheric fluctuations on Mars, *Icarus*, *22*, 325-344, 1974.

Wood, S.E., and D.A. Päige, Modeling the Martian seasonal CO_2 cycle. 1. Fitting the Viking Lander pressure curves, *Icarus*, *99*, 1-14, 1992.

B. L. Lindner, AER, Inc., 840 Memorial Drive, Cambridge, MA 02139.

(Received January 27, 1992;
revised October 26, 1992;
accepted December 17, 1992.)

The
LANETARY REPORT
e XIV Number 1 January/February 1994

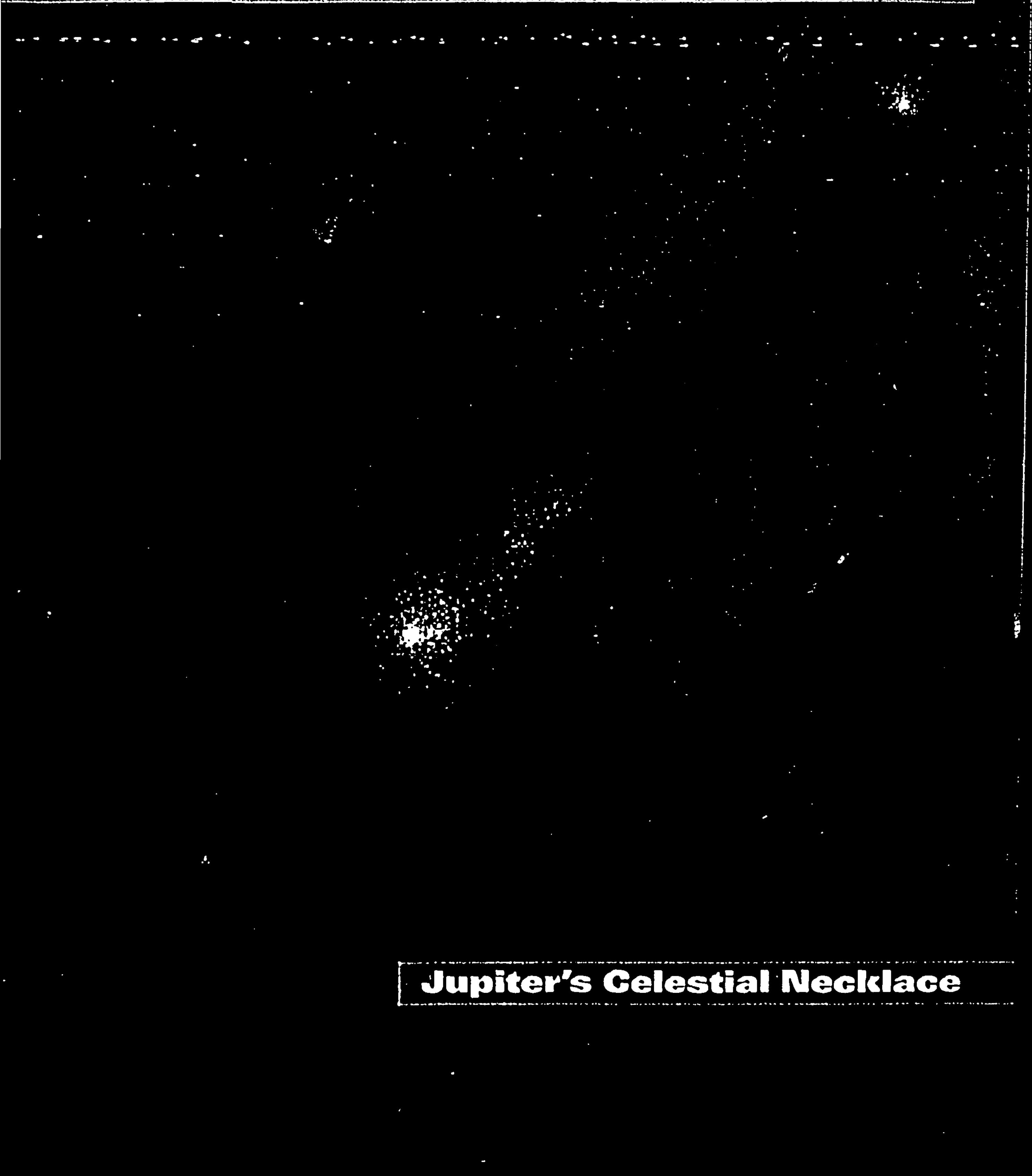

Jupiter's Celestial Necklace

the motion of a very rapidly moving object; for repetitive patterns such as the spokes of a wheel, the speed can be measured by adjusting the light's flash rate to mimic the time it takes for one spoke to advance exactly to the position of another. This effect would not apply here because sunlight has no such regular (or even irregular) flickering. Neither are the *Voyager* cameras susceptible to this sort of effect.

There is surely a lot that we don't understand about Saturn's spokes and about the rings in general. When *Cassini* arrives at Saturn in 2004, it will observe the flux of interplanetary material with its dust detector, observe the changes in the magnetic fields near the rings with charged-particle detectors, and observe the structure, formation, color and evolution of the spokes. It will discover whether the distribution of spokes varies with time and tilt of the rings, as might be expected based upon a meteoroid impact hypothesis.

Cassini will also answer many other questions about the rings: how the composition varies from dark, grayish material in the C ring and Cassini Division to bright, reddish material in the B and A rings; whether small moonlets reside in the many empty gaps in the rings (other than the one 10-kilometer object discovered recently in the A ring's Encke gap); whether new ring features have appeared or whether some of the features *Voyager* saw have since evolved into different forms.
—JEFF CUZZI, *NASA Ames Research Center*

Does Mars have an ozone layer similar to that of Earth? If so, are there fluctuations in the layer (presumably due to natural causes) similar to those resulting in the ozone hole(s) currently causing so much concern on Earth?
—Mike Cleary, Jefferson City, Missouri

Mars' ozone has been studied from Earth-based observatories and from Russian and American spacecraft, most notably *Mariner 9*. Mars does in fact have an "ozone layer" at equatorial and midlatitudes, much as Earth does.

In those regions, Mars' ozone concentrations are highest at an altitude of around 30 to 40 kilometers (19 to 25 miles), with a maximum concentration of about 0.5 parts per million (ppm). For comparison, ozone concentrations on Earth reach a maximum of about 5 ppm. However, the vertically mixed amount of ozone is many, many times less than it is on Earth.

Hence, while ozone on Earth shields the surface from much of the Sun's harmful ultraviolet radiation, the ozone on Mars does not. Furthermore, while the ozone in Earth's stratosphere exerts a strong control on the temperatures there, Mars' ozone exerts only a negligible control on the planet's atmospheric temperatures.

At Mars' poles in winter, ozone does not form a "layer," since it also exists in high quantities near the surface. The vertically integrated amount of ozone is higher at the poles than at equatorial latitudes in winter. Thus, ozone on Mars fluctuates much more than what we've observed on Earth, but for different reasons.

Earth's ozone hole is related in part to human-made chemicals that are not present on Mars. There, concentrations are more strongly influenced by the amount of water vapor, and the wide variability of water vapor on the planet results in a large fluctuation in the amount of ozone.

This explains why ozone on Mars is more abundant at the very cold wintertime poles, where water vapor is frozen out of the atmosphere. In fact, observations by *Mariner 9* in 1972 showed that ozone rose and fell in conjunction with the passage of meteorological cold fronts, due in part to the reduction in water vapor in colder air and in part to the obscuration of ozone by clouds and dust.

Our group is proposing to NASA that a balloon-borne ozone detector be sent to Mars to study this variability more closely, as a possible Discovery-class mission.
—B. LEE LINDNER, *Atmospheric and Environmental Research, Inc.*

Factinos

Examining the role of bubbles in the origin of life on Earth is one of the newest approaches to solving the scientific mystery that is probably second in importance only to the puzzle of how the universe itself began.

No one is saying that bubbles might explain everything. But a new theory receiving close attention suggests that the multitudes of bubbles forming on the surface of the primordial seas may have collected chemicals and concentrated them for synthesis into complex molecules. Eventually, through multistage reactions constantly repeated by uncounted generations of bubbles, the molecules grew in size and ambition, until they were ready for the transition to living, reproducing cells.

Louis Lerman, a geophysicist from Lawrence Berkeley Laboratory in California, is the originator of the concept. Biologists have said that the concept seems sound and is based on well-established physical principles, and is certainly worth detailed study. Sherwood Chang, a specialist in the origin of life at NASA's Ames Research Center, said, "Clearly the ocean-atmosphere interface is a dynamic environment worthy of much future study and simulation as a site for chemical evolution."

One attraction of the new hypothesis is that it offers a mechanism for a rapid chemical evolution. "Lerman is suggesting how the primordial soup might have been stirred up," said James P. Ferris, a chemist at Rensselaer Polytechnic Institute in Troy, New York, and editor of the journal *Origins of Life and Evolution of the Biosphere*.
—from John Noble Wilford in *The New York Times*

❖

For the first time, scientists have detected polycyclic aromatic hydrocarbons, an important family of organic molecules, in interplanetary dust. This dust may be some of the oldest matter in the solar system. The discovery gives weight to the theory that tiny dust particles from outer space helped seed Earth with the chemicals necessary for life to begin.

Two research teams collaborated on analyzing the dust, which was collected by a NASA aircraft. At Washington University in St. Louis, Robert M. Walker and colleagues measured the abundance of different isotopes of the same element and concluded that the dust did originate outside Earth. At Stanford University, a group including Simon J. Clemett and Richard N. Zare first vaporized, then ionized organic molecules in the dust. After using a mass spectrometer to sort the ions, the researchers concluded that they had indeed detected polycyclic aromatic hydrocarbons.
—from Ron Cowen in *Science News*

Planet. Space Sci., Vol. 00, No. 00, pp. 0000–0000, 1993
Printed in Great Britain.

0032–0633/93 \$5.00+0.00

Cooling the Martian atmosphere: the spectral overlap of the CO_2 15 μm band and dust

Bernhard Lee Lindner

AER, Inc., 840 Memorial Drive, Cambridge, MA 02139, U.S.A.

Received 5 May 1993; revised 6 September 1993; accepted 27 September 1993

Abstract—Careful consideration must be given to the simultaneous treatment of the radiative transfer of the CO_2 15 μm band and dust. Calculations for the Martian winter polar region show that a simple sum of separately calculated CO_2 cooling rates and dust cooling rates can easily result in a 30% error in the net cooling, particularly near the surface. CO_2 and dust hinder each other's ability to cool the atmosphere. Even during periods of low dust opacity, dust still reduces the efficacy of CO_2 at cooling the atmosphere. At the other extreme, when dust storms occur, CO_2 still significantly impedes the ability of dust to cool the atmosphere. Hence, both CO_2 and dust must be considered in radiative transfer models.

Introduction

CO_2 is the only gas which produces appreciable infrared cooling of the Martian troposphere (Goody and Belton, 1967; Crisp, 1990; Lindner, 1991; Savijarvi, 1991; Hourdin, 1992); hence, the transmission on Mars of the CO_2 15 μm band has been well studied (Gal'tsev and Osipov, 1979; Crisp, 1990; Lindner *et al.*, 1990a,b; Savijarvi, 1991; Hourdin, 1992). Airborne dust also produces appreciable cooling, even in periods other than global dust storms (e.g. Lindner, 1985, 1993). However, virtually all previous studies of Martian radiative cooling have ignored the presence of dust when calculating CO_2 cooling rates. The effect of dust–CO_2 spectral overlap (hereafter abbreviated as dust–CO_2 interaction) was studied by Kondrat'ev and Moscalenko (1975) and Egan *et al.* (1980) for the effect on line profiles, by Pallman (1983) for the near-surface boundary layer, by Pollack *et al.* (1979) for inverting data, and by Haberle *et al.* (1982) for circulation models. However, none of these studies published or discussed dust–CO_2 interaction. The importance of both CO_2 and dust in Martian radiative transfer requires a model capable of accurately handling the scattering by dust and the complex wavelength structure of CO_2. To simplify the problem, most prior work has studied CO_2 and dust radiative transfer separately and avoided their overlapping opacities. Here I examine the errors that can result from such a treatment.

Model

The discrete ordinate method of Stamnes *et al.* (1988) is used to treat the scattering, absorption and emission of monochromatic radiation through the Martian atmosphere. The exponential sum program of Evans *et al.* (1980) converts the banded wavelength structure of CO_2 to allow for monochromatic treatment (Freeman and Liou, 1979; Lindner, 1985; Lindner *et al.*, 1990a,b). The 15 μm band is broken into 16 subintervals to properly account for the multiple scattering (Lindner *et al.*, 1990a,b; Lacis and Oinas, 1991). Transmission functions for the 15.0 μm band of CO_2 are taken from the line-by-line model results of Gal'tsev and Osipov (1979). The transmission function, *Tr*, as a function of temperature *T*, pressure *P*, and CO_2 column abundance *U* is extrapolated from the Gal'tsev and Osipov results (subscript G) to temperatures below 200K by:

$$Tr(T,P,U) = 1-\{[1-Tr_G(200\mathrm{K},P,U)](T/200\mathrm{K})^{0.8}\}. \tag{1}$$

The exponential 0.8 is found when the temperature dependencies for the Pollack *et al.* (1981) transmission functions are recast in this form. Using a modified version of the FASCOD transmission model (Clough *et al.*, 1986), the accuracy of the transmission functions in equation (1) are confirmed for the range in temperature and pressure

Correspondence to: B. L. Lindner

(Note: my name is Lindner) n

present in the atmosphere to 40 km altitude (Lindner *et al.*, 1990a,b; Pollack *et al.*, 1990). Local thermodynamic equilibrium is assumed (Gierasch and Goody, 1967; Hourdin, 1992).

Dust opacities vary from 0.2 to 1.0 for conditions other than global dust storms (Pollack *et al.*, 1979). However, dust opacities over winter polar latitudes may be slightly less (e.g. Lindner, 1990). A Gaussian profile describes the vertical distribution of dust, being well mixed to 20 km altitude for conditions other than global dust storms (Anderson and Leovy, 1978; Zurek, 1982; Korablev *et al.*, 1993). The wavelength dependence of the dust opacity and the dust single-scattering albedo are given by Toon *et al.* (1977). Scattering of radiation by dust is represented by the Haze-L phase function (Toon *et al.*, 1977). Computational difficulties which accompany highly asymmetric phase functions are removed with the Delta-L method (Wiscombe, 1977). The emissivity of airborne dust is high and has been calculated as a function of wavelength from theory and observations (Toon *et al.*, 1977; Simpson *et al.*, 1981).

C

b2 Atmospheric composition is taken as 95% CO_2 (Owen *et al.*, 1977). Atmospheric composition may have been quite different in past epochs, with CO_2 being perhaps a minor constituent (e.g. Lindner and Jakosky, 1985), but this study focuses on the present epoch. Season-dependent CO_2 abundances (Hess *et al.*, 1980) are corrected for circulation-induced pressure gradient (Haberle *et al.*, 1979) and elevation (Lindal *et al.*, 1979). The surface pressure is 8 mbar at 57°N latitude in late winter. Atmospheric properties are zonally averaged and are assumed azimuthally independent. The region from the surface to 40 km altitude is broken into 20 layers, each 2 km thick, to account for vertical inhomogeneity. The temperature profile rises linearly with altitude from 150K at the surface to 160K at 10 km, and then falls linearly with altitude to 130K and 40 km, typical for winter polar conditions (Lindal *et al.*, 1979; Kieffer, 1979; Martin, 1984). The albedo of the polar cap is assumed to be zero (Kieffer, 1970; Smythe, 1975; Wiscombe and Warren, 1980). An average ice emissivity of 0.9 is adopted, with the wavelength dependence given in Ditteon and Kieffer (1979) and Hunt *et al.* (1980).

Results and discussion

Total atmospheric cooling rates owing to thermal emission by a vertical optical depth of dust, τ_v, of 0.2, and the contribution by various wavelength intervals are presented in Fig. 1 for winter polar conditions. The maximum cooling owing to dust below 30 km altitude occurs in the 12–18 μm wavelength interval. The strong dust cooling in the 12–18 μm range is owing to the cold temperature, to the high optical depth of dust at 12–18 μm (Toon *et al.*, 1977), and to the secondary maximum in dust emissivity at 12–18 μm (Toon *et al.*, 1977). Hence, CO_2 impedes the ability of dust to cool the atmosphere because CO_2 absorbs strongly in the 12–18 μm region where dust cools most effectively.

The presence of dust will affect CO_2 radiative transfer

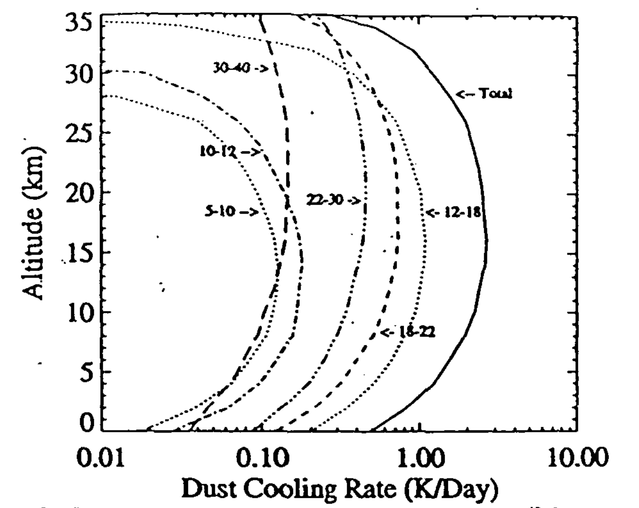

Fig. 1. Total infrared cooling rate by dust at winter polar latitudes (57°N latitude, $L_s = 343°$) as a function of altitude for dust vertical optical depth, τ_v, of 0.2, and the contribution from each wavelength interval from 5 to 40 μm (wavelength range of each bin is labeled in μm)

by increasing the optical depth, and absorbing light that is emitted by CO_2. Dust is particularly important in the radiative cooling in the line wings of CO_2. Line wings are important to cooling in that the strongly absorbing line center is often optically thick, which renders the line center ineffective at cooling (e.g. Lindner, 1993). Optically thin line wings cool effectively, in that photons emitted in the line wings can escape and cool the atmosphere. The presence of dust affects the line wings by absorbing emitted photons that would otherwise escape.

Hence, dust and CO_2 hinder each other's attempts to cool. Thus, simply adding dust cooling to CO_2 cooling is not accurate in those wavelength bands where both are important. This competition affects CO_2 cooling more than dust cooling. Dust cooling occurs over the entire infrared spectrum, which is mostly free of CO_2 absorption. However, CO_2 absorption and emission must always compete with the absorption by dust. Figure 2 shows that the cooling is overestimated up to 30% if dust and CO_2 cooling rates are computed separately and then summed. The effect is strongest near the surface where the optical depth is largest. CO_2 cooling is optically thick, making it very difficult for emitted photons to escape in the lowest 10 km. Some of the photons emitted by CO_2 line wings that would normally escape and cool are being absorbed by dust, which results in a lower cooling rate. CO_2 also absorbs some of the photons emitted by dust that would normally escape and cool.

The error induced by ignoring dust–CO_2 interaction is increased at higher dust loading (Fig. 3). Dust is now even more capable of choking off the escape of emitted photons, not only those of CO_2, but also photons emitted by dust itself. Dust–CO_2 interaction is highest near the surface for all three cases. The relative importance of the line wings for cooling is greater at lower altitudes. Since dust has its strongest effect on the line wings, dust–CO_2 interaction is strongest near the surface. Note that the errors do not change as much when dust opacity is changed from

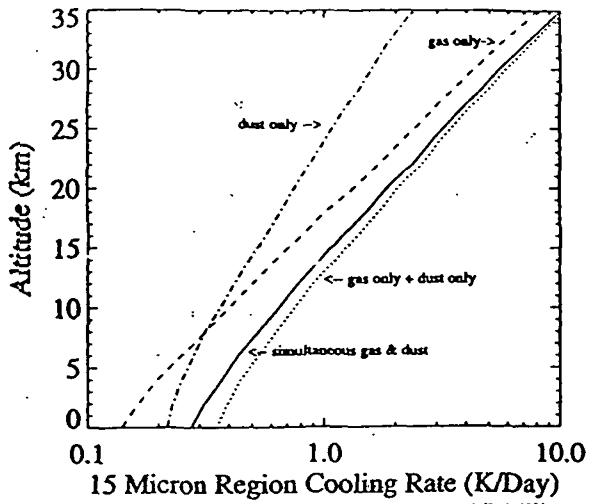

Fig. 2. Total 15 μm region (12–18 μm) cooling rates as a function of altitude for a pure CO_2 atmosphere (labeled "gas only") and for a pure dust ($\tau_v = 0.2$) atmosphere (labeled "dust only") at winter polar latitudes. Also shown are the cooling rates for a simple sum of the CO_2 only and dust only cooling rates (labeled "gas only + dust only"), and the cooling rates calculated when dust and CO_2 are treated simultaneously (labeled "simultaneous gas & dust")

$\tau_v = 0.5$ to 1.0 as they do when dust opacity is changed from $\tau_v = 0.2$ to 0.5 or from 0.0 to 0.2. This occurs because line wings are effective in optically thin media. Once large dust opacity is reached, further increases in dust opacity do not affect line wing optical depths as much.

Note that the error increases with dust optical depth, even when dust cooling exceeds CO_2 cooling. The explanation lies in the two-fold nature of dust–CO_2 interaction, and underlies the importance of its inclusion even for

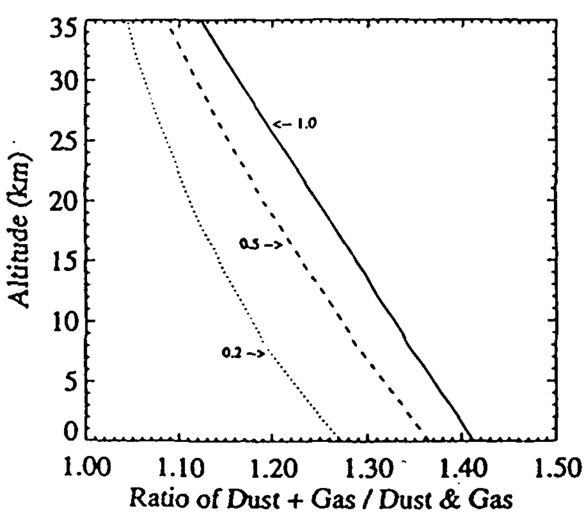

Fig. 3. Ratio of the 15μm region (12–18 μm) thermal cooling rates computed ignoring dust–CO_2 interaction (labeled "gas only+dust only" in Fig. 2) to those computed including dust–CO_2 interaction (labeled "simultaneous gas & dust" in Fig. 2) for τ_v(dust) of 0.2, 0.5 and 1.0 at winter polar latitudes. Hence, these curves represent the overestimation error of computing cooling rates in the 12–18 μm wavelength interval without proper simultaneous treatment of dust and CO_2, as a function of altitude and dust opacity

calculations for dust storm conditions. For low dust opacities, dust–CO_2 interaction involves the effect of dust in choking off emission in the line wings of the CO_2 15 μm band. However, for large dust opacities, it is CO_2 that is the parasite. For large dust opacities, dust cooling is dominant and as much as half of all dust cooling occurs in the 15 μm wavelength interval (Fig. 1). However, dust is unable to cool effectively in the 15 μm wavelength interval because emitted photons are quickly reabsorbed by CO_2. In fact, the parasitic effect of CO_2 grows as dust opacity increases, as shown in Fig. 3. The error reaches an asymptote at large dust opacities.

Summary and conclusions

As much as half of all atmospheric cooling owing to thermal emission by dust occurs in the 12–18 μm wavelength range. Since this is also the wavelength region where most cooling owing to thermal emission by CO_2 occurs, it is important to consider the spectral overlap between dust and CO_2. CO_2 infrared cooling and dust infrared cooling are both overestimated if CO_2 and dust cooling are computed separately and then summed. Indeed, if dust–CO_2 interaction is ignored, then the total 12–18 μm cooling is overestimated by almost 30% for minimal dust loading at winter polar latitudes. Furthermore, for one vertical optical depth of dust at winter polar latitudes, a simple sum of dust cooling and CO_2 cooling from 12–18 μm will overestimate the actual total 12–18 μm cooling by over 40% near the surface. Hence, dust–CO_2 interaction is important not only for calculating CO_2 cooling rates, since dust opacities overlap the CO_2 15 μm band, but also for calculating dust cooling rates, since the 15 μm band of CO_2 overlaps a significant portion of the infrared region where dust cooling is most effective. In other words, even when the Martian atmosphere is very dusty, when CO_2 cooling and heating rates are minor compared with dust (e.g. Lindner, 1993), the interaction of CO_2 will significantly affect the ability of dust to cool the atmosphere.

Acknowledgements. My thesis advisor, Gary Thomas, was invaluable in pointing out errors and improvements in the radiative transfer. Knut Stamnes and Warren Wiscombe are thanked for providing their computer codes. Anonymous reviewers are thanked for their insightful comments. This work was funded by NSF grant ATM 8305841 and NASA grants NASW-4614, NAGW-389 and NAGW-552.

References

Anderson, E. and Leovy, C., *Mariner* 9 television limb observations of dust and ice hazes on Mars. *J. Atmos. Sci.* 35, 723–734, 1978.

Clough, S. A., Kneizys, F. X. Sbettle, E. P. and Anderson, G. P., Atmospheric Radiation and transmission. *FASCOD2, Proc. Sixth Conf. on Atmospheric Radiation*, Williamsburg, Va, 1986

Crisp, D., Infrared radiative transfer in the dust-free Martian atmosphere. *J. geophys. Res.* 95, 14,577–14,588, 1990.

Ditteon, R. and Kieffer, H. H., Optical properties of solid carbon

dioxide: application to Mars. *J. geophys. Res.* 84, 8294–8300, 1979.
Egan, W. G., Fischbein, W. L. Smith, L. L. and Hilgeman, T., High-resolution Martian atmospheric modeling. *Icarus* 41, 166–174, 1980.
Evans, J. W., Gragg, W. B. and LeVeque, R. J., On the least squares exponential sum approximation with positive coefficients. *Math. Computat.* 34, 203–211, 1980.
Freeman, K. P. and Liou, K. N., Climatic effects of cirrus clouds. *Adv. Geophys.* 21, 231–287, 1979.
Gal'tsev, A. P. and Osipov, V. M., Spectral transmission functions of CO_2 for the conditions of the Martian atmosphere. *Bull. (Izv.) Acad. Sci. U.S.S.R. atmos, ocean. Phys.* 15, 767–769, 1979.
Gierasch, P. J. and Goody, R. M., An approximate calculation of radiative heating and radiative equilibrium in the Martian atmosphere. *Planet, Space Sci.* 15, 1465–1477, 1967.
Goody, R. and Belton, M. J. S., Radiative relaxation times for Mars. A discussion of Martian atmospheric dynamics. *Planet, Space Sci.* 15, 247–256, 1967.
Haberle, R. M., Leovy, C. B. and Pollack, J. B. A numerical model of the Martian polar cap winds. *Icarus* 39, 151–183, 1979.
Haberle, R. M., Leovy, C. B. and Pollack, J. B., Some effects of global dust storms on the atmospheric circulation of Mars. *Icarus* 50, 322–367, 1982.
Hess, S. L., Ryan, J. A., Tillman, J. E. Henry, R. M. and C. B. Leovy C. B., The annual cycle of pressure on Mars measured by *Viking* landers 1 and 2. *Geophys. Res. Lett.* 7, 197–200, 1980.
Hourdin, F., A new representation of the absorption by the CO_2 15 micron band for a Martian general circulation model. *J. geophys. Res.* 97, 18,319–18,335, 1992.
Hunt, G. E., Mitchell, E. A., Kieffer, H. H. and Ditteon, R., Scattering and absorption properties of carbon dioxide ice spheres in the region 360–4000 cm^{-1}. *J. Quant. Spectrosc. rad. Transfer* 24, 141–146, 1980.
Kieffer, H. H., Spectral reflectance of CO_2–H_2O frost. *J. geophys. Res.* 75, 501–509, 1970.
Kieffer, H. H., Mars South polar spring and summer temperatures: a residual CO_2 frost. *J. geophys. Res.* 84, 8263–8288, 1979.
Kondrat'ev, K. Ya., and Moscalenko, N. I., The spectral and spatial structure of a thermal radiation field under the conditions of Mars' turbid atmosphere. *Dokl. Akad. Nauk S.S.S.R.* 224, 316–319, 1975 (English translation: *Sov. Phys. Dokl.* 20, 593–594, 1976).
Korablev, O. I., Krasnopolsky, V. A., Rodin, A. V. and Chassefiere, E., Vertical structure of Martian dust measured by solar infrared occulatations from the *Phobos* spacecraft. *Icarus* 102, 76–87, 1993.
Lacis, A. A. and Oinas, V., A description of the correlated *k* distribution method for modeling nongray gaseous absorption, thermal emission, and multiple scattering in vertically inhomogenous atmospheres. *J. geophys. Res.* 96, 9027–9063, 1991.
Lindal, G. F., Hotz, H. B., Sweetnam, D. N., Shippony, Z., Brenkle, J. P., Hartsell, G. V., Spear, R. T. and Michael, W. H. Jr, Viking radio occulation measurements of the atmosphere and topography of Mars: data acquired during 1 Martian year of tracking. *J. geophys. Res.* 84, 8443–8456, 1979.
Lindner, B. L., The aeronomy and radiative transfer of the martian atmosphere. Ph.D. Dissertation, University of Colorado, Boulder, CO, 1985.
Lindner, B. L., The Martian polar cap: radiative effects of ozone, clouds, and airborne dust. *J. geophys. Res.* 95, 1367–1379, 1990.
Lindner, B. L., Ozone heating in the Martian atmosphere. *Icarus* 93, 354–361, 1991.
Lindner, B. L., Martian atmospheric radiation budget. *Pub. Astron. Soc. Japan*, submitted, 1993.
Lindner, B. L. and Jakosky, B. M., Martian atmospheric photochemistry and composition during periods of low obliquity. *J. geophys. Res.* 90, 3435–3440, 1985.
Lindner, B. L., Ackerman, T. P. and Pollack, J. B., An efficient and accurate technique to compute the absorption, emission, and transmission of radiation by the Martian atmosphere, in *Scientific Results of the NASA-sponsored Study Project on Mars: Evolution of Volcanism, Tectonics and Volatiles* (edited by S. C. Solomon, V. L. Sharpton and J. R. Zimbelman), p. 198–200. LPI Technical Report 90–06. Lunar and Planetary Institute, Houston, TX, 1990a.
Lindner, B. L., Ackerman, T. P., Pollack, J. B., Toon, O. B. and Thomas, G. E., Solar and I. R. radiation near the Martian surface: a parameterization for CO_2 transmittance, in *Lunar and Planetary Science* XXI, pp. 696–697. Lunar and Planetary Institute, Houston, TX, 1990b.
Martin, L. J., Clearing the Martian air: the troubled history of dust storms. *Icarus* 57, 317–321, 1984.
Owen, T., Biemann, K., Rushneck, D. R., Biller, J. E., Howarth, D. W. and Lafleur, A. L., The composition of the atmosphere at the surface of Mars. *J. geophys. Res.* 82, 4635–4639, 1977.
Pallman, A. J., The thermal structure of the atmospheric surface boundary layer on Mars as modified by the radiative effect of aeolian dust. *J. geophys. Res.* 88, 5483–5493, 1983.
Pollack, J. B., Colburn, D. S., Flasar, F. M., Kahn, R., Carlston, C. E. and Pidek, D., Properties and effects of dust particles suspended in the Martian atmosphere. *J. geophys. Res.* 84, 2929–2945, 1979.
Pollack, J. B., Leovy, C. B., Greiman, P. W. and Mintz, Y., A Martian general circulation experiment with large topography. *J. atmos. Sci.* 38, 3–29, 1981.
Pollack, J. B., Haberle, R. M., Schaeffer, J. and Lee, H., Simulations of the general circulation of the Martian atmosphere, 1. Polar processes. *J. geophys. Res.* 95, 1447–1474, 1990.
Savijarvi, H., Radiative fluxes on a dustfree Mars. *Beitr. Phys. Atmos.* 64, 103–112, 1991.
Simpson, J. P., Cuzzi, J. N., Erickson, E. F., Strecker, D. W. and Tokunaga, A. T., Mars: far-infrared spectra and thermal-emission models. *Icarus* 48, 230–245, 1981.
Smythe, W. D., Spectra of hydrate frosts: their application to the outer solar system. *Icarus* 24, 421–427, 1975.
Stamnes, K., Tsay, S., Wiscombe, W. and Jayaweera, K., Numerically stable algorithm for discrete-ordinate-method radiative transfer in multiple scattering and emitting media. *Apl. Optics* 27, 2502–2509, 1988.
Toon, O. B., Pollack, J. B. and Sagan, C., Physical properties of the particles composing the Martian dust storm of 1971–1972. *Icarus* 30, 663–696, 1977.
Wiscombe, W. J., The delta-*m* method: rapid yet accurate radiative flux calculations for strongly asymmetric phase functions. *J. atmos. Sci.* 34, 1408–1422, 1977.
Wiscombe, W. J. and Warren, S. G., A model for the spectral albedo of snow. I: pure snow. *J. atmos. Sci.* 37, 2712–2733, 1980.
Zurek, R. W., Martian great dust storms: an update. *Icarus* 50, 288–310, 1982.

1994023384

N94- 27887

Martian Atmospheric Radiation Budget

442632

Bernhard Lee Lindner

AER, Inc.

840 Memorial Drive

Cambridge, MA 02139

USA

Telephone:(617)349-2280

Fax:(617)661-6479

Submitted to Publications of the Astronomical Society of Japan

April 1993

Revised manuscript submitted October 1993

Second revision submitted January 1994

No. of Pages: 24

No. of Figures: 6

No. of Tables: 0

ABSTRACT

A computer model is used to study the radiative transfer of the martian winter-polar atmosphere. Solar heating at winter-polar latitudes is provided predominately by dust. For normal, low-dust conditions, CO_2 provides almost as much heating as dust. Most heating by CO_2 in the winter polar atmosphere is provided by the 2.7 μm band between 10 km and 30 km altitude, and by the 2.0 μm band below 10 km. The weak 1.3 μm band provides some significant heating near the surface. The minor CO_2 bands at 1.4, 1.6, 4.8 and 5.2 μm are all optically thin, and produce negligible heating. O_3 provides less than 10% of the total heating. Atmospheric cooling is predominantly thermal emission by dust, although CO_2 15 μm band emission is important above 20 km altitude.

Key Words: Mars, Radiative Transfer, Atmosphere, Planets

INTRODUCTION

While the past 20 years of spacecraft exploration have expanded our knowledge of the planet Mars, it seems more interesting problems exist today than ever before. At the heart of most of these mysteries is the winter polar atmosphere. Observations of the winter polar atmosphere have been limited by orbital constraints and darkness, and few models have been constructed to date. CO_2 and H_2O condensation commonly occur in the winter polar atmosphere of Mars, resulting in extensive cloudiness and a massive ice sheet. The structure and composition of the polar clouds as functions of latitude, altitude and season are poorly understood. Although observations of the southern polar hood are limited, it appears strikingly different from its northern counterpart, with much less coverage and different altitude structure (James, 1983; Christensen and Zurek, 1983; Martin and James, 1984; Akabane et al., 1990). The seasonal recession of the south polar cap (e.g., Iwasaki et al., 1990) cannot be accurately reproduced with energy balance models without consideration of atmospheric radiative effects (Narumi, 1980; James and North, 1982; Lindner, 1990; 1991a; 1992a; 1992b; 1993a), and the relative fraction of snow and frost in the cap is unknown (Pollack et al., 1990). Atmospheric dynamics at winter polar latitudes is also dependent on atmospheric heating and cooling (Haberle et al., 1979; 1982). Ozone abundances on Mars are also dependent on the radiative effects of dust (Lindner, 1988), and the observance of ozone on Mars is impaired by the radiative effects of dust (Lindner, 1992c).

Understanding the dominant radiative heating and cooling mechanisms in the winter polar atmosphere is crucial to solving many of these mysteries. While dynamical and latent heat mechanisms do provide as much as half of the atmospheric energy budget (Pollack et al., 1990), it is the radiative transfer mechanisms which drive the dynamical and latent heat mechanisms. In fact, due to the strong CO_2 heating and cooling, radiative processes are relatively more important in determining the temperature structure of the martian atmosphere than of the terrestrial atmosphere (e.g., Pollack et al., 1990). This work intends to establish the relative importance of O_3, CO_2 and dust in the radiative heating and cooling of the winter polar atmosphere of Mars, studying the importance of all wavelength bands. CO_2 was shown to be the only gas which produced appreciable infrared cooling at winter polar latitudes by Goody and Belton (1967), Crisp (1990), and Savijarvi(1991). Also, significant solar heating occurs in all the near-infrared (NIR) bands of CO_2 (Pollack et al., 1981; Lindner, 1985; Savijarvi,1991). Ozone was suggested to be an important contributor to the atmospheric temperature in the polar regions by Kuhn et al. (1979). However, the contribution of ozone to the atmospheric heat budget was later shown to be minor when compared to the contribution of dust (Lindner, 1991b). However, atmospheric heating due to dust absorption of solar radiation was shown to be important during dust storms by Gierasch and Goody (1972), Moriyama (1975), Zurek (1978), and Davies (1979). The importance of both CO_2 and dust in infrared radiative transfer, as well as the interaction between gas and dust, was demonstrated for certain cases by Kondrat'ev and Moscalenko (1975). The importance of both gas and dust in martian radiative transfer requires an advanced model capable of accurately handling the scattering by dust and the complex wavelength structure of carbon dioxide. To simplify the problem, most prior work has studied gas and dust radiative transfer separately and avoided their overlapping opacities, a technique which is inaccurate (Lindner, 1993b). To more properly assess the relative importance of dust and CO_2 in the thermal budget, this study treats them simultaneously.

MODEL

The discrete ordinate method of Stamnes et al. (1988) is used to treat the scattering, absorption and emission of monochromatic radiation through the martian atmosphere. The exponential sum program of Wiscombe and Evans (1977) and Evans et al. (1980) converts the banded wavelength structure of CO_2 to allow for monochromatic treatment (Lindner, 1985; 1993b; Lindner et al., 1990a,b). Lindner (1993b) clearly shows that errors as large as 50% occur when dust and CO_2 cooling and heating rates are computed separately and then summed. Hence, an approach such as the exponential sum technique which allows for simultaneous treatment of CO_2 and dust in the solution of the radiative transfer equation is necessary in order to properly assess their relative importance (Lindner, 1993b). Transmission functions for the 2.759, 4.301

and 14.93 μm bands of CO_2 (hereafter abbreviated as 2.7, 4.3, and 15.0, respectively) are taken from the line-by-line model results of Gal'tsev and Osipov (1979). The transmission function, Tr, as a function of temperature T, pressure P, and CO_2 column abundance U is extrapolated from the Gal'tsev and Osipov results (subscript G) to temperatures below 200 K by

$$Tr(T,P,U) = 1 - [(1 - Tr_G(200\ K, P, U))\ (T/200\ K)^Q] \tag{1}$$

The exponential Q is found to be 0.45, 0.3, and 0.8 for the 2.7, 4.3, and 15 μm bands, respectively, when the temperature dependencies for the Pollack et al. (1981) transmission functions are recast in this form. Using a modified version of the FASCOD transmission model (Clough et al., 1986), the accuracy of these transmission functions is confirmed, and transmission functions are obtained for the 1.316, 1.455, 1.600, 2.020, 4.840 and 5.200 μm bands of CO_2 (hereafter abbreviated as 1.3, 1.4, 1.6, 2.0, 4.8, and 5.2, respectively) covering the range in temperature and pressure present in the atmosphere to 40 km altitude (Lindner et al., 1990a,b). Additionally, ozone absorption cross-sections from 1500 Å to 3200 Å (Daumont et al., 1983; Freeman et al., 1984) and from 4000 Å to 8000 Å (Griggs, 1968) and ultraviolet (UV) cross-sections for CO_2 (Shemansky, 1972; Lewis and Carver, 1983), O_2 (Demore et al., 1988), H_2O (Thompson et al., 1963; Hudson, 1971), HO_2 (Demore et al., 1988) and H_2O_2 (Demore et al., 1988) are included [e.g., Lindner, 1988; 1991b].

Dust opacities vary from 0.2 to 1.0 for conditions other than global dust storms (Pollack et al., 1979; Lumme and James, 1984). However, dust opacities over winter polar latitudes may be slightly less [e.g., Lindner, 1990]. A gaussian profile describes the vertical distribution of dust, being well-mixed to 20 km altitude for conditions other than global dust storms (Anderson and Leovy, 1978; Zurek, 1982; Korablev et al., 1993). Dust storm conditions are not considered here because of the dramatic increase in dynamical processes during dust storms. The wavelength dependence of the dust opacity is given by Toon et al. (1977). The single scattering albedo of airborne dust as a function of wavelength is given by Zurek (1978; 1982) and Toon et al. (1977) for solar and infrared wavelengths, respectively, using a solar average of 0.9 (Clancy and Lee, 1991). Scattering of radiation by dust is represented by the Henyey-Greenstein phase function (Toon et al., 1977; Clancy and Lee, 1991). Computational difficulties which accompany highly asymmetric phase functions are removed with the Delta-M method (Wiscombe, 1977). The emissivity of airborne dust is high and has been calculated as a function of wavelength from theory and observations (Toon et al., 1977; Simpson et al., 1981). Dust optical properties in the near-IR (1-5 μm) are highly uncertain, hence making the calculated heating and cooling rates uncertain. However, as will be shown later, dust heating and cooling rates in the near-IR are minor, making the uncertainty in dust optical properties in the near-IR unimportant. Dust optical properties in the 15 μm region are also highly uncertain, and factor of 2 uncertainty in the computed cooling rates is quite possible. Clouds will also affect atmospheric radiative transfer. However, since the cloud opacity is highly variable (i.e. Briggs and Leovy, 1974), the cloud particle scattering properties are very uncertain, and even the composition of the clouds is unclear, the effect of clouds is highly speculative and variable. But clouds should affect atmospheric radiative transfer similarly to how dust does, since dust single scattering albedos are very high (Lindner, 1990; 1993a).

The Rayleigh scattering optical depth is computed as in Hansen and Travis (1974), using parameters appropriate for Mars. Solar fluxes are taken from Smith and Gottlieb (1974) and Rottman (1981), after adjusting for the eccentricity and orbital radius of Mars. Solar heating rates are diurnally averaged (e.g., Cogley and Borucki, 1976). Atmospheric properties are zonally averaged and assumed azimuthally-independent. The region from the surface to 40 km altitude is broken into 20 2-km-thick layers to account for vertical inhomogeneity. The improved Curtis-Godson approximation (Yamamoto et al., 1972; Ramanathan and Coakley, 1978) is used to treat vertical inhomogeneity at thermal wavelengths. The Chapman function is used to approximate the slant path in place of the secant function [e.g., Smith and Smith, 1972], because the winter polar atmosphere always has large solar zenith angles, and the secant function is in error for large angles.

Atmospheric composition is taken as 95% CO_2 (Owen et al., 1977; see also Kondrat'ev et al., 1973). Atmospheric composition may have been quite different in past epochs, with CO_2

being perhaps a minor constituent (e.g., Lindner and Jakosky, 1985; Lindner, 1993c), but this study focuses on the present epoch. Season-dependent CO_2 abundances (Hess et al., 1980) are corrected for circulation-induced pressure gradients (Haberle et al., 1979) and elevation (Jakosky and Farmer, 1982; Lindal et al., 1979). The surface pressure is 8 mbar at 57°N latitude in late winter, which is when the maximum O_3 column abundance of 57 µm-atm was observed (Barth et al., 1973). The altitude dependence of O_3 is based on model results (Lindner, 1988).

As this study uses late northern winter conditions ($L_s = 343°$), the surface is covered by somewhat dirty ice with an albedo of 0.5 (Kieffer, 1979; James and Lumme, 1982). [Ls, the solar longitude, is a seasonal index; Ls of 0°, 90°, 180°, 270°, correspond to northern spring equinox, summer solstice, autumnal equinox, and winter solstice, respectively]. The wavelength dependence of the ice albedo is taken from Hapke et al. (1981) and Warren and Wiscombe (1980). The infrared (5.4 - 100 µm) albedo of the polar cap is assumed to be zero (Kieffer, 1970; Smythe, 1975; Wiscombe and Warren, 1980). An average ice emissivity of 0.9 is adopted, with the wavelength dependence given in Ditteon and Kieffer (1979) and Hunt et al. (1980). The temperature profile rises linearly with altitude from 150K at the surface to 160K at 10 km, and then falls linearly with altitude to 130 K and 40 km, typical for winter polar conditions (Lindal et al., 1979; Kieffer, 1979; Martin, 1984). Atmospheric temperatures are poorly known above 30 km altitude, and therefore results above that altitude are speculative and are not presented here. Local thermodynamic equilibrium is assumed (Gierasch and Goody, 1967; Uplinger et al., 1984; Hourdin, 1992).

RESULTS AND DISCUSSION

Figure 1 presents the ozone, carbon dioxide, and dust heating rates, and the carbon dioxide and dust cooling rates, for late winter ($L_s = 343°$) conditions at 57°N latitude with 0.2 vertical optical depths, τ_v, of dust (averaged over the solar spectrum). The net heating and net cooling are virtually identical at all altitudes. Because thermal emission is a strong function of the temperature and heating is virtually independent of temperature, less than a 10K adjustment in the assumed temperature profile will yield a perfect balance of heating and cooling. These modifications would still be consistent with observations of temperature (Lindal et al., 1979). Because the variation in dust with altitude is not well understood, the discrepancy could also be due to the assumed altitude profile of dust. Indeed, the assumed temperature profile could be correct, and the dust profile could be extracted by obtaining a balance between heating and cooling. Note that in addition to radiative cooling, energy could also go into condensation. In fact, clouds are often observed at these latitudes and seasons. Clouds would also change heating and cooling rates by increasing the flux (and heating) up high, and decreasing flux (and heating) in the lower 10 km.

While the near equality of heating and cooling rates means that meridional and vertical heat transport may not be required to explain the observed winter polar temperatures, it certainly does not rule out any meridional or vertical heat transport. Indeed, vertical heat transport could also be responsible for the low cooling rates at 20-30 km altitude. Observations do show some day to day variability, which could be due to changes in dynamical heat transport, or to pockets of high ozone or dust concentrations which would change radiative heating and cooling. However, maximum dynamical heating rates are of the order lK/day, with typical winter polar heating rates much smaller (Gadian, 1978; Pollack et al., 1981). While this could be significant near the surface, it becomes less so at higher altitudes.

The relative importance of gas and dust is clearly seen in Figure 1. Dust heating is the major source of heating at all altitudes, particularly above 20 km. Ozone provides approximately 10% of the total heating at all altitudes. 57 μm atmospheres of ozone are used, the maximum observed by Mariner 9 (Barth et al., 1973). [1 μm atmosphere = 2.69 x 10^{15} cm^{-2}]. Smaller ozone abundances will reduce the importance, but not dramatically. This contradicts earlier work by Kuhn et al. (1979) which showed ozone to be a more significant source of heating. However, Kuhn et al. (1979) ignored the heating by dust, which is clearly incorrect (Lindner, 1991b). Indeed, 0.2 vertical optical depths of dust represent the minimum amount of dust observed (Leovy et al., 1972; Pollack et al., 1979; Thorpe, 1981; Zurek, 1981). Larger dust loading will provide greater heating. Ozone heating is almost the same as that of the NIR bands of CO_2, at all altitudes. This occurs because the major CO_2 bands are saturated at the large solar zenith angles in the winter polar atmosphere.

Figure 1 can also be used to show what would happen to the thermal structure for the case of no dust. CO_2 and O_3 heating is triple CO_2 cooling near the surface, while CO_2 cooling is triple CO_2 and O_3 heating at 30 km altitude. This means that a dust-free atmosphere would be warmer near the surface and cooler at 30 km to allow for a balance between heating and cooling. Higher lapse rates were found in other dust-free studies as well (e.g., Gierasch and Goody, 1968).

Cooling rates are also dominated by dust. Dust cooling is greater than CO_2 15 μm band cooling from the surface to 25 km altitude, with CO_2 cooling dominant above this altitude. Note that cooling is not dependent on latitude, but on temperature. Hence the relative importance of dust cooling to CO_2 cooling is approximately the same at all winter polar latitudes.

The dominant ozone heating occurs at 2700 Å, with appreciable contributions from 2200 Å to 3100 Å (Lindner, 1991b). The Chappuis bands (4000 - 7000 Å) provide over 10% of the total ozone heating near the surface. CO_2, O_2, H_2O, HO_2, and H_2O_2 produce minor heating of the winter polar atmosphere at UV wavelengths, although CO_2 and O_2 UV heating is appreciable above 30 km altitude (Lindner, 1991b). H_2O, HO_2, and H_2O_2 number densities are too low for any appreciable UV heating.

CO_2 solar heating rates at near-infrared (NIR) wavelengths at 57°N latitude are computed for each CO_2 band, as shown in Figure 2. Most heating by CO_2 in the winter polar atmosphere is provided by the 2.7 μm band between 10 km and 30 km altitude, and by the 2.0 μm band below 10 km. The weak 1.3 μm band provides some significant heating near the surface. The minor CO_2 bands at 1.3, 1.4, 1.6, 4.8 and 5.2 μm are all optically thin, and produce negligible heating. The 2.0 μm band is more strongly absorbing than these minor bands and becomes optically thick at 10 km altitude, which results in a decreasing heating rate with a decrease in altitude below 10 km. The 2.7 μm band is stronger yet, and becomes optically thick at 20 km altitude. The 4.3 μm and 15 μm bands are very efficient, and are optically thick even at 30 km altitude. 15 μm band heating is surprisingly strong, despite the low solar flux at infrared wavelengths. The explanation lies in the large bandwidth (from 12 to 19 μm) and the efficient absorption over the band width.

In addition to being heated from absorption of solar radiation by O_3 and CO_2, the martian atmosphere is also heated by absorption of solar radiation by dust. As dust optical depths are not as strongly wavelength dependent as CO_2 and O_3 optical depths, the altitude dependence of dust heating is virtually the same for all wavelengths (Fig. 3). The strongest heating occurs in the visible where the maximum in solar flux occurs.

Atmospheric cooling rates due to thermal emission by 0.2 vertical optical depths of dust are presented in Figure 4. The maximum cooling occurs at 10 km altitude. Cooling is not as efficient in the lowest 5 km for two reasons. The temperature profile is inverted, with a maximum near 5-10 km altitude. Thus the near-surface atmosphere absorbs more radiation relative to its emission than does the atmosphere at 10 km altitude. Furthermore, the larger optical depths near the surface do not allow the emitted thermal radiation to escape the layer as easily as at higher altitudes.

The maximum cooling due to dust below 30 km altitude occurs in the 12-18 μm wavelength interval. This is due to the cold temperatures at winter polar latitudes. The overlap of strong dust cooling in the 12-18 μm interval with the strong cooling by CO_2 in the 15 μm band (12-19 μm) is particularly important, as discussed by Lindner (1993b). Hence, to properly account for both dust and CO_2 cooling, they must be treated simultaneously (Lindner, 1993b), unlike what is usually done. Significant cooling due to dust also occurs at wavelengths longer than 18 μm. Cooling by dust at wavelengths shorter than 12 μm is inefficient due to the cold winter polar temperatures. (Recall that the peak Planck emission occurs at longer wavelengths for colder temperatures.)

Cooling due to CO_2 near the surface occurs mostly in the wings of the 15 μm band, those parts of the 15 μm band where neither absorption nor emission is efficient. Photons emitted near the surface in the center of the 15 μm band (the strongly absorbing parts of the band) are rapidly re-absorbed. Hence, the cooling is smaller at lower altitudes (see Fig. 1) due to the inability of photons to escape and cool the atmosphere. Photons in the line center can escape to space more easily at higher altitudes, explaining the higher cooling rates there. Cooling to the surface also occurs, and is included in all calculations. However, in order to cool to the surface, photons must pass through large optical depths. Cooling to the surface is only important right near the surface.

Cooling rates in the 4.3 μm band of CO_2 increase from 10^{-6} K/Mars day at the surface to 3×10^{-4} K/Mars day at 30 km. Hence, cooling in the 4.3 μm band of CO_2 is about 10^{-3}% of the total cooling via CO_2. Clearly, 4.3 μm band cooling is not an important process in the winter polar atmosphere of Mars. The 4.3 μm cooling rate has the same altitude behavior as the 15 μm cooling rate. As with the 15 μm band, the line center is optically thick near the surface and all emitted photons are quickly reabsorbed, preventing effective line-center cooling in the 4.3 μm band. 4.3 μm cooling would be larger at warmer latitudes, as thermal emission would shift to shorter wavelengths. However, 4.3 μm band cooling will never be an important cooling source in the martian atmosphere. The 4.3 μm band and other NIR bands are important cooling processes in the Earth's atmosphere.

The heating and cooling rates for a late winter ($L_s = 343°$) atmosphere at 57° N latitude with more dust ($\tau_v = 0.5$) are shown in Fig. 5. Comparing Fig. 1 and Fig. 5, we see that dust heating and cooling rates increase at higher dust opacities, at all altitudes. Clearly, dust heating and cooling dominates over that of gas, except possibly for CO_2 cooling above 30 km altitude. As $\tau_v = 0.5$ was not unusual during the Viking mission, dust heating and cooling would dominate for most winter polar latitudes and seasons. Dust heating and cooling at larger dust loadings is even more dominant. During global dust storms (τ_v~3), heating and cooling by O_3 and CO_2 will be negligible compared to that of dust. However, dynamical transport of heat increases during dust storms.

For τ_v (dust) = 0.5, meridional and vertical heat transport may be even less important than for the $\tau_v = 0.2$ case. Based on observational and modeling evidence, meridional and vertical winds do not change much between the 0.2 and 0.5 cases (Haberle et al., 1982). Therefore, radiative equilibrium may be a more valid assumption at $\tau_v = 0.5$ because total radiative heating and cooling rates are twice as large for τ_v (dust) = 0.5, and are greater than 3 K/Mars day at almost all altitudes.

Heating and cooling rates are well balanced in the lower 20 km of the atmosphere in Fig. 5. Above 20 km the assumed temperatures are incorrect. Temperatures closer to 140 K at 30 km altitude would give a better balance between the heating and cooling rates above 20 km. Indeed, the inability of dust cooling to keep up with dust heating at higher dust loadings in addition to heat transport is the explanation for the higher atmospheric temperatures observed during global dust storms. The explanation lies in the negative feedback of larger dust loadings, in that larger opacities decrease the ability of photons to escape. CO_2 cooling also becomes less effective at higher dust loadings due to dust-gas interaction (Lindner, 1993b).

Obviously, higher dust loading results in increased dust heating rates. The higher optical depth chokes off some light from reaching lower altitudes, which explains why the increases in the heating rate for higher dust optical depths are not as large at the surface as at higher altitudes. Cooling rates for 0.5 vertical optical depths of dust are twice the cooling rates for $\tau_v = 0.2$. While the optical depth is 2.5 times as large, cooling rates are only 2.2 times larger. This is because two negative feedbacks exist in that larger optical depths also hinder the ease of escape for emitted photons, and in that larger optical depths increase the thermal flux which increases absorption and heating. The thermal heating at altitudes above 25 km also increases. The heating above 25 km increases because the upward thermal flux is larger for $\tau_v = 0.5$, which results in larger absorption in the upper atmosphere, while the thermal emission above 25 km remains the same.

The phenomenon of thermal heating is also partly responsible for the low lapse rates in the martian atmosphere. Because dust and CO_2 are both radiatively active in the infrared, the atmosphere near the surface is able to cool very effectively, and keep near-surface temperatures low. But the high thermal fluxes are also causing a heating as they are absorbed by the other regions of the atmosphere. Any part of the atmosphere that is too cold will be heated by both solar and thermal flux. Higher dust loading increases both solar and thermal heating more effectively than thermal cooling. This results in more isothermal conditions as the dust loading increases, as is observed.

Figure 6 shows the heating and cooling rates deeper in the winter polar region at 70°N latitude for the same season for normal, low-dust conditions. The cooling rates are the same as at 57°N latitude (Figure 1), because the same temperature profile is used. The same temperatures are used at both latitudes to illustrate latitude-dependent changes in the heating rates. The lower solar fluxes at 70°N latitude (due to the larger solar zenith angle) result in lower heating rates. The atmospheric heating and cooling is approximately equal near the surface and above 20 km. However, the assumed temperature inversion is too strong for radiative equilibrium for 70°N latitude conditions, as the cooling at 10 km is twice the heating. Slightly lower temperatures in the 5-10 km range would provide a better balance between heating and cooling, and would agree with observational evidence (Lindal et al., 1979). Dynamics could be relatively more important at transporting heat at 70°N latitude because the heating rates are lower. However, observations and dynamical modeling indicate that the atmosphere is even more stable against motion at these latitudes which would lower heat transport (Haberle et al., 1979).

The excess cooling could also go into condensation, rather than in changing the temperature (Pollack et al., 1990). Indeed, optically thick clouds are frequently observed in the 5-10 km altitude range. As the atmospheric temperature near the surface is already at the CO_2 condensation temperature, the clouds at this latitude will be at least partly composed of CO_2 ice. Clouds would also alter the heating rate profile by shifting the location of solar flux through scattering.

Comparing Fig. 1 and Fig. 6 shows that the relative importance of O_3 to CO_2 heating is virtually the same at 70°N latitude as it is at 57°N latitude. However, both O_3 and CO_2 heating are less important relative to dust. CO_2 heating occurs mostly in bands which are optically thick. At higher latitudes, the larger solar zenith angles only serve to decrease the transmission in these already optically-thick bands and hence decrease their relative importance. O_3 is less important to the heat budget at 70°N latitude due to the lower O_3 abundances there (Barth et al., 1973; Lane et al., 1973; Lindner, 1991b). The same general altitude and wavelength behavior in heating and cooling is seen at 70°N latitude as at 57°N latitude. Therefore, while dust heating is less at higher latitudes due to the decreased solar flux, the importance of dust heating relative to gas heating has increased.

The large solar zenith angle Θ at 70°N latitude increases the effective optical depth ($\tau = \tau_v/\cos\Theta$) of dust, which increases the absorption of solar flux, and hence increases the heating. The larger solar zenith angle also decreases the solar flux, and hence decreases the heating. In an optically-thin medium, these effects would cancel and the heating would be the same at 70°N latitude as at 57°N latitude. However, the 0.2 vertical optical depths of dust yield an effective optical depth of 1.7 at 70°N latitude. Thus, the dust is actually choking off the solar-flux, which decreases the heating rate relative to 57°N latitude. The lower heating at the surface is due to the large optical-depth of dust.

CO_2 NIR heating at 70°N latitude is half that at 57°N latitude. The general behavior of each band at 70°N latitude is similar to that at 57°N latitude, although the bands saturate at higher altitudes. Consequently, the 4.3 and 15 μm bands are less important at 70°N latitude, and the 2.0 and 2.7 μm bands are less important near the surface. The minor bands (1.3, 1.4, 1.6, 4.8 and 5.2 μm) are optically thin at 70°N latitude, as at 57°N latitude. The heating in all bands is reduced at 70°N latitude, due to the lower solar flux (via the larger solar zenith angle). Comparing the results of 57°N latitude and 70°N latitude, it is apparent that CO_2 NIR heating would be markedly higher at equatorial latitudes, due to the increased solar flux, and the larger contributions by the saturated 2.0, 2.7, 4.3 and 15 μm bands. Hence, the relative importance of dust and CO_2 will shift in the favor of CO_2 at more equatorward latitudes. O_3 heating will not be important at equatorial and mid-latitudes because negligible ozone abundances exist there (Barth et al., 1973). Total heating rates will increase with decreasing latitude due to the decrease in the solar zenith angle. The net result is higher atmospheric temperatures with decreasing latitude, which is in fact observed.

SUMMARY AND CONCLUSIONS

Heating in the winter polar atmosphere of Mars is provided mostly by dust at visible wavelengths, especially for high dust loading, or at high latitudes. CO_2 NIR heating is always less than dust heating at 57°N latitude during late winter, but is comparable to dust heating at low altitudes for minimal dust loading. CO_2 NIR heating is more important at equatorial latitudes, and less important at high latitudes. Most CO_2 heating comes from the 2.7 μm band above 10-20 km altitude, with most heating by the 2.0 μm band below. 1.3 μm band heating is appreciable near the surface. The importance of minor CO_2 bands requires their inclusion in models of polar winter winds and surface energy balance. Ozone heating is only 10% of the total heating at 57°N latitude, and is even less at other latitudes due to lower ozone abundances. Ozone heating was suggested to be important to the polar heat budget by Kuhn et al. (1979), but the importance of dust heating was ignored by Kuhn et al. Heating by CO_2, O_2, H_2O, HO_2 and H_2O_2 is negligible at ultraviolet wavelengths below 30 km altitude.

CO_2 15 μm band cooling is the dominant source of cooling at high altitudes for low dust abundances, but is ineffective near the surface. CO_2 4.3 μm band cooling is negligible. Dust cooling is the dominant source of cooling at winter polar latitudes under most conditions, with the largest dust cooling in the 12-18 μm wavelength range. Dust cooling increases at higher dust loadings; however dust cooling does not increase as fast as dust heating, due to several negative feedbacks. As a result, atmospheric temperatures rise with increasing dust opacity, in agreement with observations. The warmest winter polar temperatures occur during global dust storms, when the largest dust opacity exists. However, whether the high temperatures at polar latitudes during global dust storms are due primarily to radiative processes or dynamical heat transport is uncertain. Radiative effects of dust have little effect on the overall recession of the polar cap (Lindner, 1990).

Radiative processes are responsible for the low lapse rates in the martian atmosphere. Significant dust and gas heating occurs at all altitudes, damping out inhomogeneities in temperature. Any region of the atmosphere which is significantly colder than the rest of the atmosphere is warmed not only by solar flux but also by the absorption of the large thermal flux. Large lapse rates are quickly eliminated by solar and infrared heating. As atmospheric dust loading increases, the atmosphere becomes more isothermal due to the increased solar and thermal heating, particularly at higher altitudes. Ignoring dust altogether leads to the opposite situation. CO_2 cools ineffectively near the surface, but cools readily at high altitudes, which leads to stronger lapse rates in the dust-free atmosphere.

Acknowledgments

My thesis advisor, Gary Thomas, was invaluable in pointing out errors and improvements in the radiative transfer. Knut Stamnes and Warren Wiscombe are thanked for providing their computer codes. The reviewers are thanked for insightful comments on this manuscript. This work was funded by NSF grant ATM 8305841 and NASA grants NASW-4614, NAGW-389 and NAGW-552.

REFERENCES

Akabane, T., K. Iwasaki, Y. Saito, and Y. Narumi, Blue clearing of Syrtis Major at the 1982 Opposition, J. Geophys. Res., 95, 14649-14655, 1990.

Anderson, E. and C. Leovy, Mariner 9 television limb observations of dust and ice hazes on Mars, J. Atmos. Sci., 35, 723734, 1978.

Barth, C.A., C.W. Hord, A.I. Stewart, A.L. Lane, M.L. Dick and G.P. Anderson, Mariner 9 Ultraviolet experiment: Seasonal variation of ozone on Mars, Science, 179, 795-796, 1973.

Briggs, G.A. and Leovy, C.B., Mariner 9 observations of the Mars north polar hood, Bull. Amer. Met. Soc., 55, 278-296, 1974.

Christensen, P.R. and R.W. Zurek, Martian water-ice clouds: Location and seasonal variation, Bull. Amer. Astron. Soc., 15, 847, 1983.

Clancy, R.T., and S.W. Lee, A new look at dust and clouds in the Mars atmosphere: Analysis of emission-phase-function sequences from global Viking IRTM observations, Icarus, 93, 135-158, 1991.

Clough, S.A., F.X. Kneizys, E.P. Shettle, and G. P. Anderson, Atmospheric Radiation and Transmission, FASCOD2, Proceedings of the Sixth Conference on Atmospheric Radiation, Williamsburg, Virginia, 1986

Cogley, A.C. and W.J. Borucki, Exponential approximations for daily average solar heating or photolysis, J. Atmos. Sci., 33, 1347-1356, 1976.

Crisp, D., Infrared radiative transfer in the dust-free martian atmosphere, J. Geophys. Res., 95, 14577-14588, 1990.

Daumont, D., J. Brion and J. Malicet, Measurement of total atmospheric ozone: Consequences entailed by new values of ozone absorption cross-sections at 223 K in the 310-350 nm spectral range, Planet. Space Sci., 31, 1229-1234, 1983.

Davies, D.W., Effects of dust on the heating of Mars surface and atmosphere, J. Geophys. Res., 84, 8289-8293, 1979.

DeMore, W.B., J.J. Margitan, M.J. Molina, R.T. Watson, D.M. Golden, R.F. Hampson, M.J. Kurylo, C.J. Howard, and A.R. Ravishankara, Chemical kinetics and photochemical data for use in stratospheric modeling, evaluation no. 7, JPL Publication 85-67, Jet Propulsion Laboratory, Pasadena, California, 1985.

Ditteon, R. and H.H. Kieffer, Optical properties of solid carbon dioxide: Application to Mars, J. Geophys. Res., 84, 8294-8300, 1979.

Evans, J.W., W.B. Gragg and R.J. LeVeque, On the least squares exponential sum approximation with positive coefficients, Math. of Computat., 34, 203-211, 1980.

Freeman, D.E., K. Yoshino, J.R. Esmond and W.H. Parkinson, High resolution absorption cross-section measurements of ozone at 195 K in the wavelength region 240-350 nm, Planet. Space Sci., 32, 239-248, 1984.

Gadian, A.M., The dynamics of and the heat transfer by baroclinic eddies and large-scale stationary topographically forced long waves in the martian atmosphere, Icarus, 33, 454-465, 1978.

Gal'tsev, A.P. and V.M. Osipov, Spectral transmission functions of CO2 for the conditions of the martian atmosphere, Bull. (Izv.), Acad. Sci. USSR, Atmos. Ocean. Phys., 15, 767-769, 1979.

Gierasch, P.J. and R.M. Goody, An approximate calculation of radiative heating and radiative equilibrium in the martian atmosphere, Planet. Space Sci., 15, 1465-1477, 1967.

Gierasch, P.J. and R.M. Goody, A study of the thermal and dynamical structure of the martian lower atmosphere, Planet. Space Sci., 16, 615-646, 1968.

Gierasch, P.J. and R.M. Goody, The effect of dust on the temperature of the martian atmosphere, J. Atmos. Sci., 29, 400 - 402, 1972.

Goody, R. and M.J.S. Belton, Radiative relaxation times for Mars. A discussion of martian atmospheric dynamics, Planet. Space Sci., 15, 247-256, 1967.

Griggs, M., Absorption coefficients of ozone in the ultraviolet and visible regions, J. Chem. Phys., 49, 857-859, 1968.

Haberle, R.M., C.B. Leovy and J.B: Pollack, A numerical model of the martian polar cap winds, Icarus, 39, 151-183, 1979.

Haberle, R.M., C.B. Leovy and J.B. Pollack, Some effects of global dust storms on the atmospheric circulation of Mars, Icarus, 50, 322-367, 1982.

Hansen, J.E. and L.D. Travis, Light scattering in planetary atmospheres, Space Science Reviews, 16, 527-610, 1974.

Hapke, B., E. Wells, J. Wagner and W. Partlow, Far-UV, Visible, and Near-IR reflectance spectra of frosts of H_2O, CO_2, NH , and SO_2, Icarus, 47, 361-367, 1981.

Hess, S.L., J.A. Ryan, J.E. Tillman, R.M. Henry and C.B. Leovy, The annual cycle of pressure on Mars measured by Viking Landers 1 and 2, Geophys. Res. Lett., 7, 197-200, 1980.

Hourdin, F., A new representation of the absorption by the CO2 15 micron band for a martian general circulation model, J. Geophys. Res., 97, 18319-18335, 1992.

Hudson, R.D., Critical review of ultraviolet photoabsorption cross sections for molecules of astrophysical and aeronomic interest, Rev. Geophys. Space Phys., 9, 305-406, 1971.

Hunt, G.E., E.A. Mitchell, H.H. Kieffer and R. Ditteon, Scattering-and absorption properties of carbon dioxide ice spheres in the region 360-4000 cm^{-1}, J. Quant. Spectrosc. Radiat. Transfer, 24, 141-146, 1980.

Iwasaki, K., Y. Saito, Y. Nakai, and T. Akabane, Martian south polar cap 1988, J. Geophys. Res., 95, 14751-14754, 1990.

Jakosky, B.M. and C.B. Farmer, The seasonal and global behavior of water vapor in the Mars atmosphere: Complete global results of the Viking atmospheric water detector experiment, J. Geophys. Res., 87, 2999-3019, 1982.

James, P.B., Condensation phase of the martian south polar cap, Bull. Amer. Astron. Soc., 15, 846-847, 1983.

James, P.B. and K. Lumme, Martian south polar cap boundary: 1971 and 1973 data, Icarus, 50, 368-380, 1982.

James, P.B. and G.R. North, The seasonal CO_2 cycle on Mars: An application of an energy balance climate model, J. Geophys. Res., 87, 10271-10283, 1982.

Kieffer, H.H., Spectral reflectance of CO2-H2O frosts, J. Geophys. Res., 75, 501-509, 1970.

Kieffer, H.H., Mars south polar spring and summer temperatures: A residual CO_2 frost, J. Geophys. Res., 84, 8263-8288, 1979.

Kondrat'ev, K.Ya., and N.I. Moscalenko, The spectral and spatial structure of a thermal radiation field unde the conditions of Mars' turbid atmosphere, Dokl. Akad. Nauk SSSR, 224, 316-319, 1975. (English translation: Sov. Phys. Dokl., 20, 593-594, 1976).

Kondrat'ev, K.Ya., Yu.M.Timofeev, O.M. Pokrovskii and T.A. Dvorovik, Determination of vertical temperature profile in the atmosphere of Mars from Mariner 9 infrared thermal radiation measurements, Dokl. Akad. Nauk SSSR, 211, 801-803, 1973. (English translation: Sov. Phys. Dokl., 18, 509-510, 1974).

Korablev, O.I., V.A. Krasnopolsky, A.V. Rodin, and E. Chassefiere, Vertical structure of martian dust measured by solar infrared occulatations from the Phobos spacecraft, Icarus, 102, 76-87, 1993.

Kuhn, W.R., S.K. Atreya and S.E. Postawko, The influence of ozone on martian atmospheric temperature, J. Geophys. Res., 84, 8341-8342, 1979.

Lane, A.L., C.A. Barth, C.W. Hord and A.I. Stewart, Mariner 9 ultraviolet spectrometer experiment: Observations of ozone on Mars, Icarus, 18, 102-108, 1973.

Leovy, C.B., G.A. Briggs, A.T. Young, B.A. Smith, J.B. Pollack, E.N. Shipley and R.L. Wildey, The martian atmosphere: Mariner 9 television experiment progress report, Icarus, 17, 373-393, 1972.

Lewis, B.R. and J.H. Carver, Temperature dependence of the carbon dioxide photoabsorption cross section between 1200 and 1970 Angstroms, J. Quant. Spectrosc. Radiat. Transfer, 30, 297-309, 1983.

Lindal, G.F., H.B. Hotz, D.N. Sweetnam, Z. Shippony, J.P. Brenkle, G.V. Hartsell, R.T. Spear and W.H. Michael, Jr., Viking radio occultation measurements of the atmosphere and topography of Mars: Data acquired during 1 martian year of tracking, J. Geophys. Res., 84, 8443-8456, 1979.

Lindner, B. L., The aeronomy and radiative transfer of the martian atmosphere, Ph.D. Dissertation, 470 pp., University of Colorado, Boulder, 1985.

Lindner, B. L., Ozone on Mars: The effects of clouds and airborne dust, Planet. Space Sci., 36, 125-144, 1988.

Lindner, B. L., The martian polar cap: Radiative effects of ozone, clouds, and airborne dust, J. Geophys. Res., 95, 1367-1379, 1990.

Lindner, B. L., Why is the north polar cap on Mars different than the south polar cap?, Summaries, International Symposium on the Physics and Chemistry of Ice, p. 120-121, held in Sapporo Japan, Sept. 1-6, 1991a.

Lindner, B. L., Ozone heating in the martian atmosphere, Icarus, 93, 354-361, 1991b.

Lindner, B. L., Sunlight penetration through the martian polar caps: Effects on the thermal and frost budgets, Geophys. Res. Lett., 19, 1675-1678, 1992a.

Lindner, B. L., CO_2-ice on Mars: Theoretical simulations, in Physics and Chemistry of Ice, N. Maeno and T. Hondoh, ed.s, pp. 225-228, Hokkaido University Press, Sapporo, 1992b.

Lindner, B. L., Does UV instrumentation effectively measure ozone abundance?, in Workshop on innovative instrumentation for the in situ study of atmosphere-surface interactions on Mars, B. Fegley, Jr. and H. Waenke, ed.s, pp. 10-11, LPI Tech. Rep. #92-07, Part 1, Lunar and Planetary Institute, Houston, Texas, 1992c.

Lindner, B. L., The hemispherical asymmetry in the martian polar caps, J. Geophys. Res., 98, 3339-3344, 1993a.

Lindner, B. L., Cooling the martian atmosphere: The spectral overlap of the CO2 15 micron band and dust, accepted by Planet. Space Sci., 1993b.

Lindner, B. L., Comment on "Mars secular obliquity change due to the seasonal polar caps" by David Parry Rubincam, submitted to J. Geophys. Res., 1993c.

Lindner, B. L. and B. M. Jakosky, Martian atmospheric photochemistry and composition during periods of low obliquity, J. Geophys. Res., 90, 3435-3440, 1985.

Lindner, B. L., T. P. Ackerman, and J. B. Pollack, An efficient and accurate technique to compute the absorption, emission, and transmission of radiation by the martian atmosphere, in Scientific results of the NASA-sponsored study project on Mars: Evolution of volcanism, tectonics and volatiles, S.C. Solomon, V.L. Sharpton, and J.R. Zimbelman, ed.s, p. 198-200, LPI Tech. Rpt. 90-06, 322 pp., Lunar and Planetary Institute, Houston, Texas, 1990a.

Lindner, B. L., T. P. Ackerman, J. B. Pollack, O. B. Toon, and G. E. Thomas, Solar and IR radiation near the martian surface: A parameterization for CO_2 transmittance, In Lunar and Planetary Science XXI, pp. 696-697, Lunar and Planetary Institute, Houston, Texas, 1990b.

Lumme K. and P.B. James, Some photometric properties of the martian south polar cap region during the 1971 apparition, Icarus, 58, 363-376, 1984.

Martin, L.J., North polar hood observations during martian dust storms, Icarus, 26, 341-352, 1975.

Martin, L.J., Clearing the martian air: The troubled history of dust storms, Icarus, 57, 317-321, 1984.

Martin, L.J. and P.B. James, Mars 1984: The transition from polar hood to surface-cap (abstract), Bull. Amer. Astron. Soc., 16, 673, 1984.

Moriyama, S., Effects of dust on radiation transfer in the martian atmosphere. II. Heating due to absorption of the visible solar radiation and importance of radiative effects of dust on the Martian meteorological phenomena, J. Meteorl. Soc. Japan, 53, 214-221, 1975.

Narumi, Y., The seasonal variation of atmospheric pressure on Mars, in Proceedings of the 13th Lunar and Planetary Symposium, pp. 31-41, Institute of Space and Aeronautical Science, University of Tokyo, 1980.

Owen, T., K. Biemann, D.R. Rushneck, J.E. Biller, D.W. Howarth, and A.L. Lafleur, The composition of the atmosphere at the surface of Mars, J. Geophys. Res., 82, 4635-4639, 1977.

Pollack, J.B., D.S. Colburn, F.M. Flasar, R. Kahn, C.E. Carlston and D. Pidek, Properties and effects of dust particles suspended in the martian atmosphere, J. Geophys. Res., 84, 2929-2945, 1979.

Pollack, J.B., C.B. Leovy, P.W. Greiman and Y. Mintz, A martian general circulation experiment with large topography, J. Atmos. Sci., 38, 3-29, 1981.

Pollack, J.B., R.M. Haberle, J. Schaeffer, and H. Lee, Simulations of the general circulation of the martian atmosphere, 1, Polar processes, J. Geophys. Res., 95, 1447-1474, 1990.

Ramanathan, V. and J.A. Coakley, Jr., Climate modeling through radiative-convective models, Rev. Geophys. Space Phys., 16, 465-489, 1978.

Rottman, G.J., Rocket measurements of the solar spectral irradiance during solar minimum, 1972-1977, J. Geophys. Res., 86, 6697-6705, 1981.

Savijarvi, H., Radiative Fluxes on a dustfree Mars, Beitr. Phys. Atmosph., 64, 103-112, 1991.

Shemansky, D.E., Carbon dioxide extinction coefficient 1700-3000 Angstroms, J. Chem. Phys., 56, 1582-1587, 1972.

Simpson, J.P., J.N. Cuzzi, E.F. Erickson, D.W. Strecker, and A.T. Tokunaga, Mars: Far-infrared spectra and thermal-emission models, Icarus, 48, 230-245, 1981.

Smith, E.V.P. and D.M. Gottlieb, Solar flux and its variations, Space Sci. Rev., 16, 771-802, 1974.

Smith, F.L., III, and C. Smith, Numerical evaluation of Chapman's grazing incidence integral ch(X,X), J. Geophys. Res., 77, 3592-3597, 1972.

Smythe, W.D., Spectra of hydrate frosts: Their application to the outer solar system, Icarus, 24, 421-427, 1975.

Stamnes, K., S. Tsay, W. Wiscombe, and K. Jayaweera, Numerically stable algorithm for discrete-ordinate-method radiative transfer in multiple scattering and emitting media, App. Optics, 27, 2502-2509, 1988.

Thompson, B.A., P. Harteck and R.R. Reeves, Jr., Ultraviolet absorption coefficients of CO_2, CO, O_2, H_2O, N_2O, NH_3, NO, SO_2, and CH_4 between 1850 and 4000 Angstroms, J.

Geophys. Res., 68, 6431-6436, 1963.

Thorpe, T.E., Mars atmospheric opacity effects observed in the northern hemisphere by Viking orbiter imaging, J. Geophys. Res., 86, 11419-11429, 1981.

Toon, O.B., J.B. Pollack and C. Sagan, Physical properties of the particles composing the martian dust storm of 1971-1972, Icarus, 30, 663-696, 1977.

Uplinger, W.G., G.A. Ely, T.C. James and J.B. Kumer, Martian horizon radiance profiles (abstract), EOS, 65, 982, 1984.

Warren, S.G. and W.J. Wiscombe, A model for the spectral albedo of snow. II: Snow containing atmospheric aerosols, J. Atmos. Sci., 37, 2734-2745, 1980.

Wiscombe, W.J., The delta-m method: Rapid yet accurate radiative flux calculations for strongly asymmetric phase functions, J. Atmos. Sci., 34, 1408-1422, 1977.

Wiscombe, W.J. and J.W. Evans, Exponential-sum fitting of radiative transmission functions, J. Computational Phys., 24, 416-444, 1977.

Wiscombe, W.J. and S.G. Warren, A model for the spectral albedo of snow. I: Pure snow, J. Atmos. Sci., 37, 2712-2733, 1980.

Yamamoto, G., M. Aida and S. Yamamoto, Improved Curtis-Godson approximation in a non-homogeneous atmosphere, J. Atmos. Sci., 29, 1150-1155, 1972.

Zurek, R.W., Solar heating of the martian dusty atmosphere, Icarus, 35, 196-208, 1978.

Zurek, R.W., Inference of dust opacities for the 1977 martian great dust storms from Viking Lander 1 pressure data, Icarus, 45, 202-215, 1981.

Zurek, R.W., Martian great dust storms: An update, Icarus, 50, 288-310, 1982.

Figure Captions

Figure 1. Total atmospheric radiative heating and cooling as a function of altitude on Mars at 57°N latitude with τ_v (dust) = 0.2. Also shown is the contribution by CO_2, O_3 and dust.

Figure 2. Total solar heating rates for CO_2 as a function of altitude and the contribution by each CO_2 band (labeled by wavelength in μm) at 57°N latitude (a) and 70°N latitude (b).

Figure 3. Total radiative heating rate as a function of altitude due to absorption of solar radiation by dust ($\tau_v = 0.2$) and the contribution from each wavelength bin from 0 to 5 microns (bins labeled on figure in μm).

Figure 4. Total infrared radiative cooling rate by dust as a function of altitude for $\tau_v = 0.2$, and the contribution from each wavelength interval from 5 to 40 μm (wavelength range of each bin is labeled in μm).

Figure 5. As in Figure 1 except for τ_v (dust) = 0.5.

Figure 6. As in Figure 1 except at 70°N latitude for τ_v (dust) = 0.2

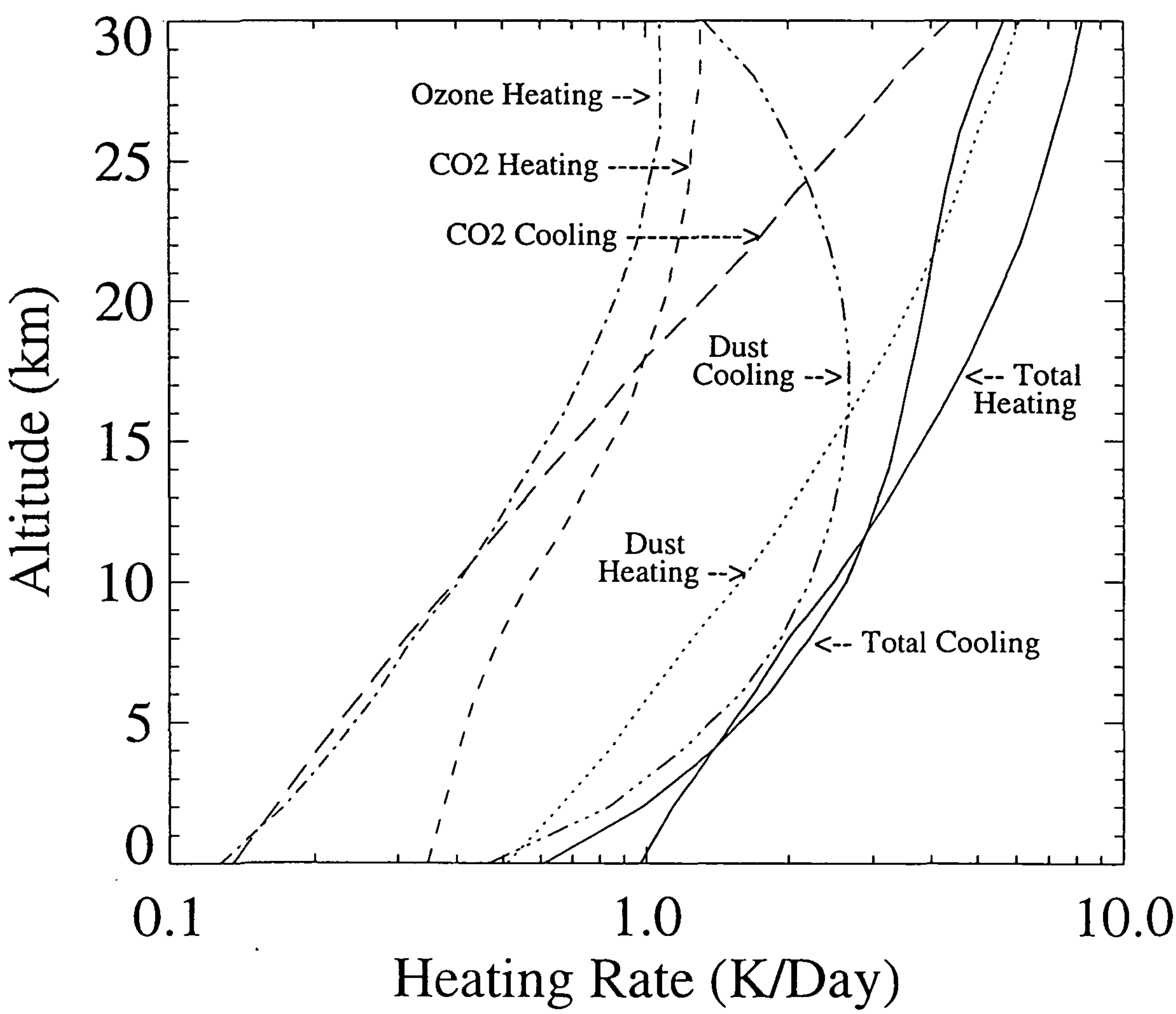
Ozone Heating -->
CO2 Heating -------->
CO2 Cooling ---------->
Dust
Cooling -->
<-- Total
Heating
Dust
Heating -->
<-- Total Cooling
30
25
20
15
10
5
0
Altitude (km)
0.1
1.0
10.0
Heating Rate (K/Day)

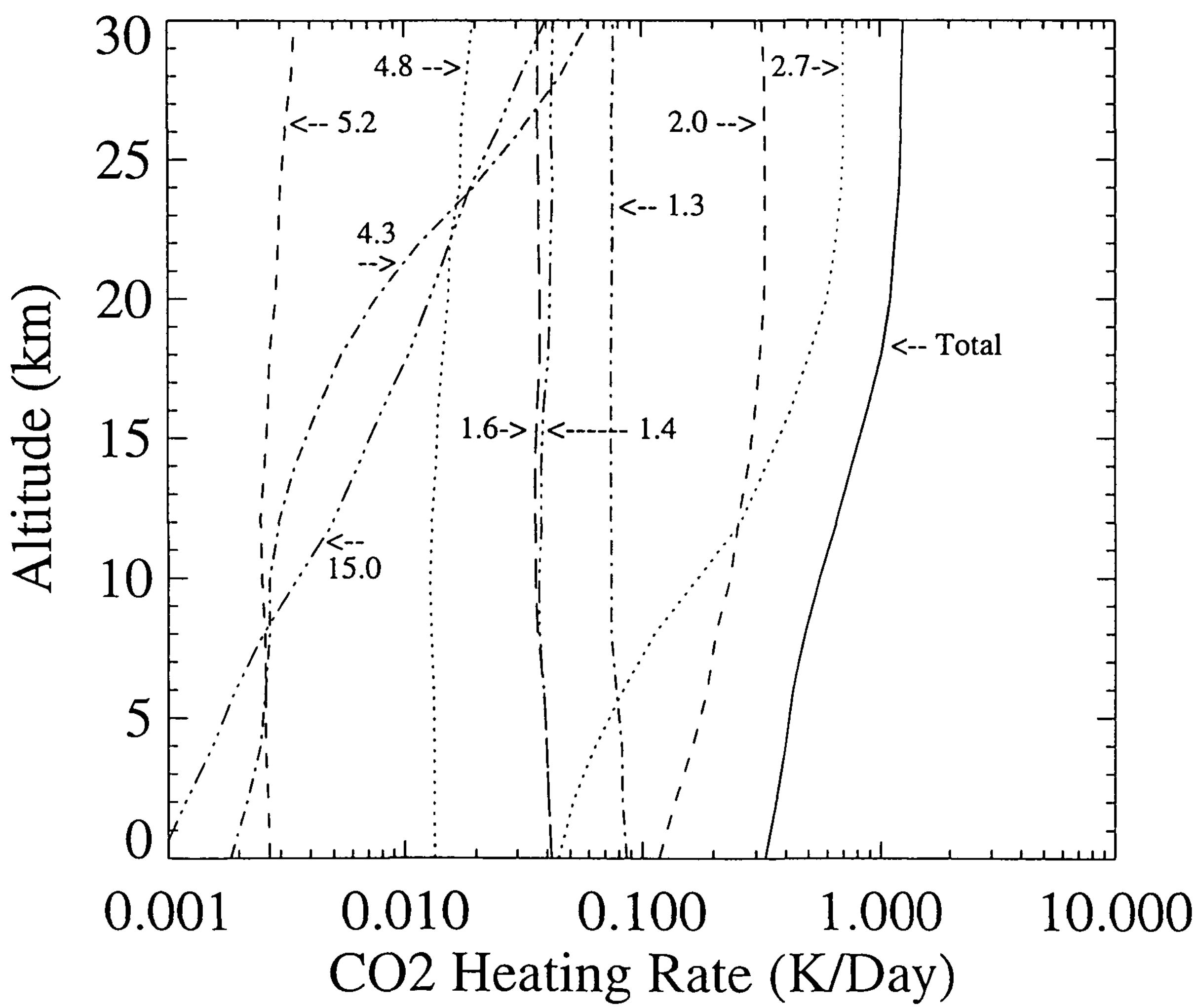

Altitude (km)
CO2 Heating Rate (K/Day)
0.001
0.010
0.100
1.000
10.000
0
5
10
15
20
25
30
4.8 -->
<-- 5.2
4.3
-->
<--
15.0
1.6->
<------ 1.4
<-- 1.3
2.0 -->
2.7->
<-- Total

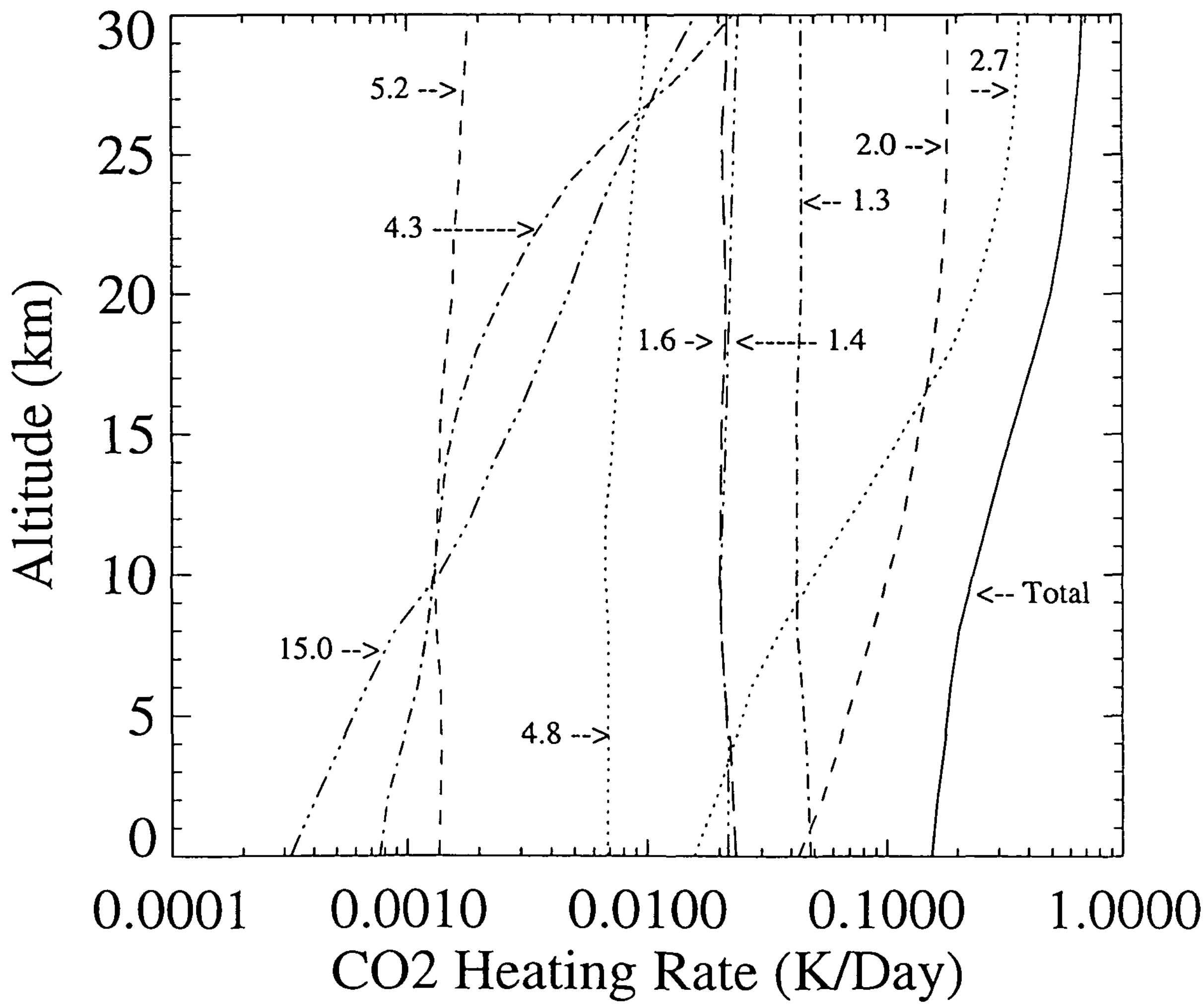

30
25
20
15
10
5
0
Altitude (km)
0.0001
0.0010
0.0100
0.1000
1.0000
CO2 Heating Rate (K/Day)
5.2 -->
4.3 -->
15.0 -->
4.8 -->
1.6 ->
<-- 1.4
<-- 1.3
2.0 -->
2.7 -->
<-- Total

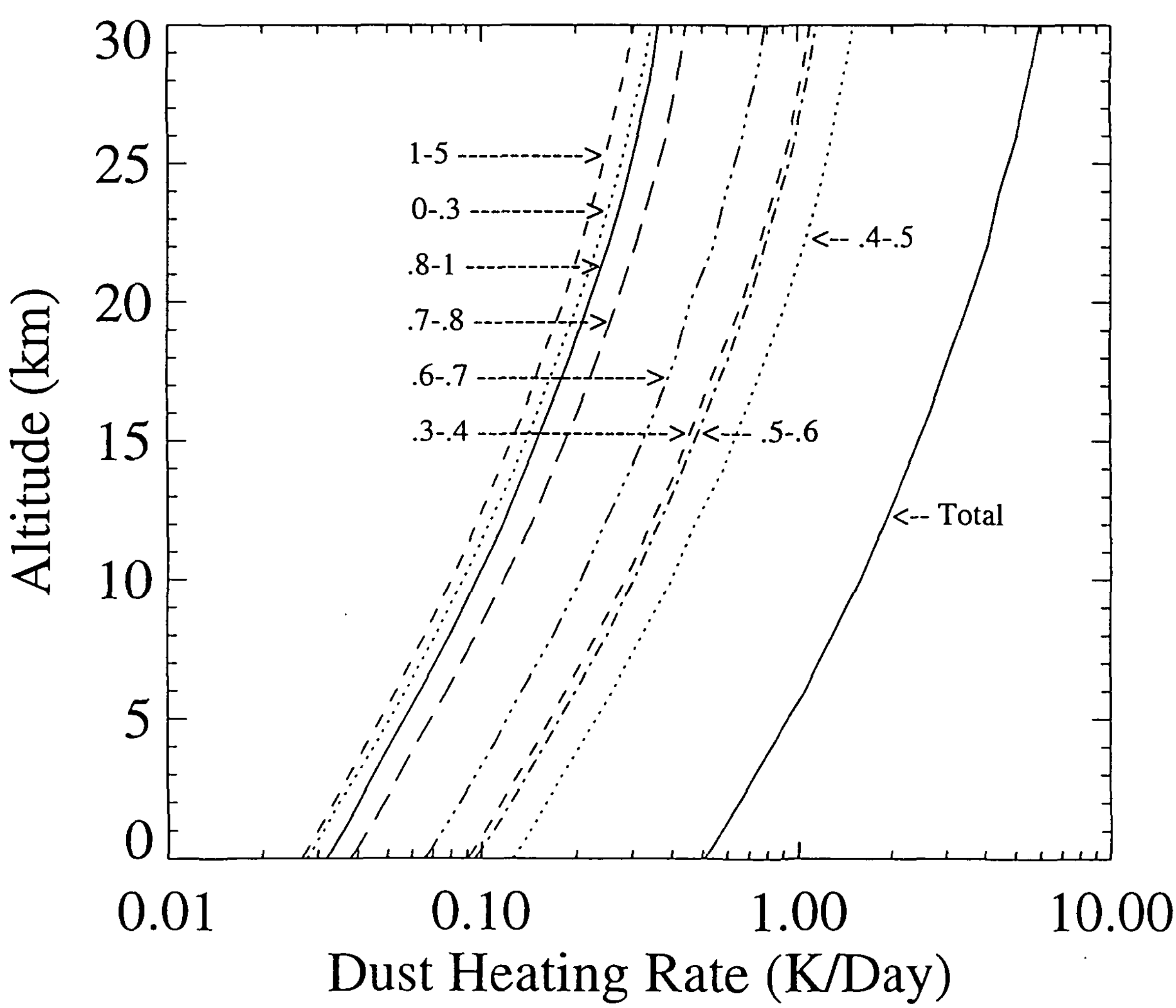

Altitude (km)
30
25
20
15
10
5
0
0.01
0.10
1.00
10.00
Dust Heating Rate (K/Day)
1-5
0-.3
.8-1
.7-.8
.6-.7
.3-.4
.4-.5
.5-.6
Total

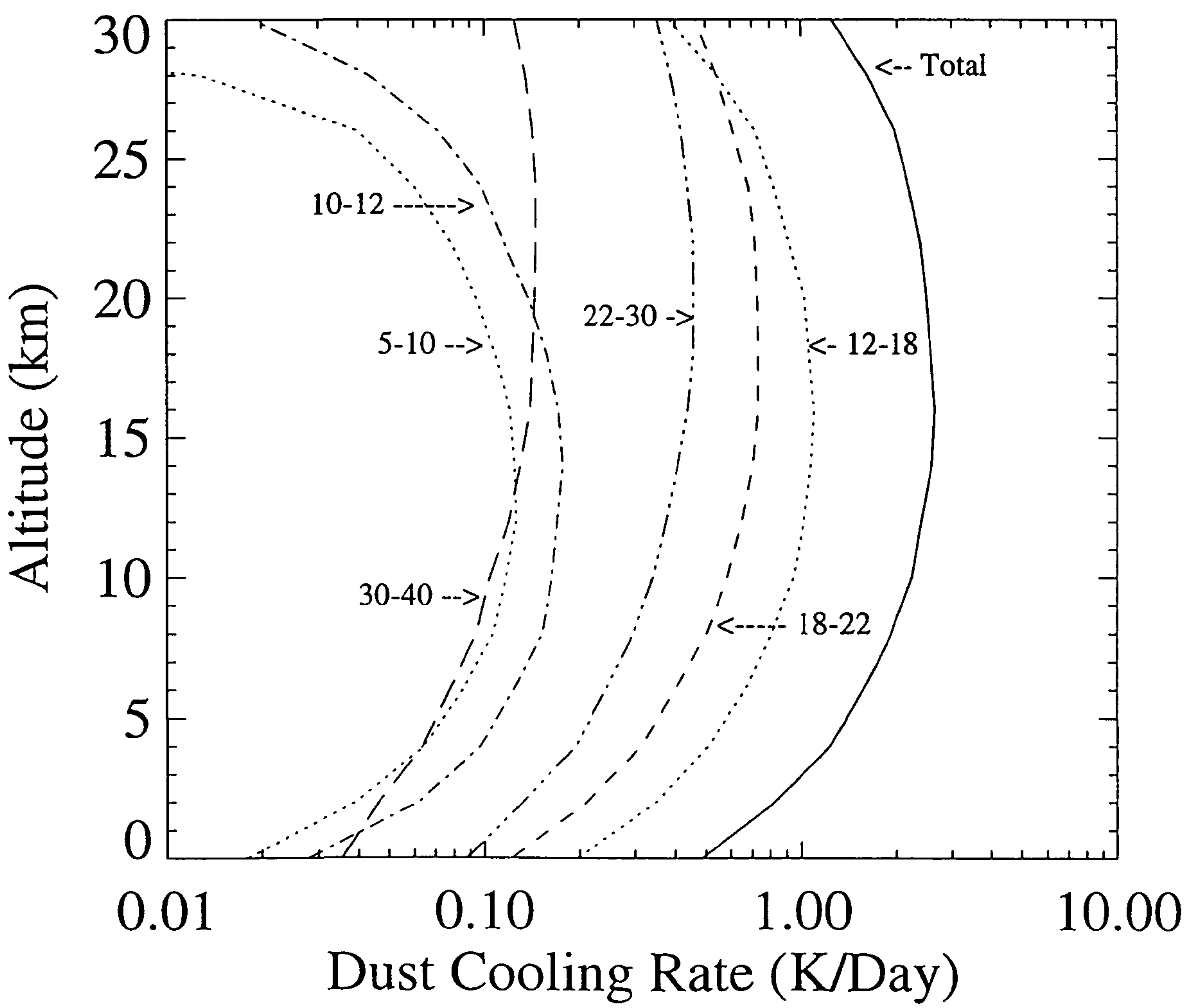

30
25
20
15
10
5
0
Altitude (km)
0.01
0.10
1.00
10.00
Dust Cooling Rate (K/Day)
<-- Total
10-12 -------->
5-10 -->
22-30 ->
<- 12-18
30-40 -->
<------ 18-22

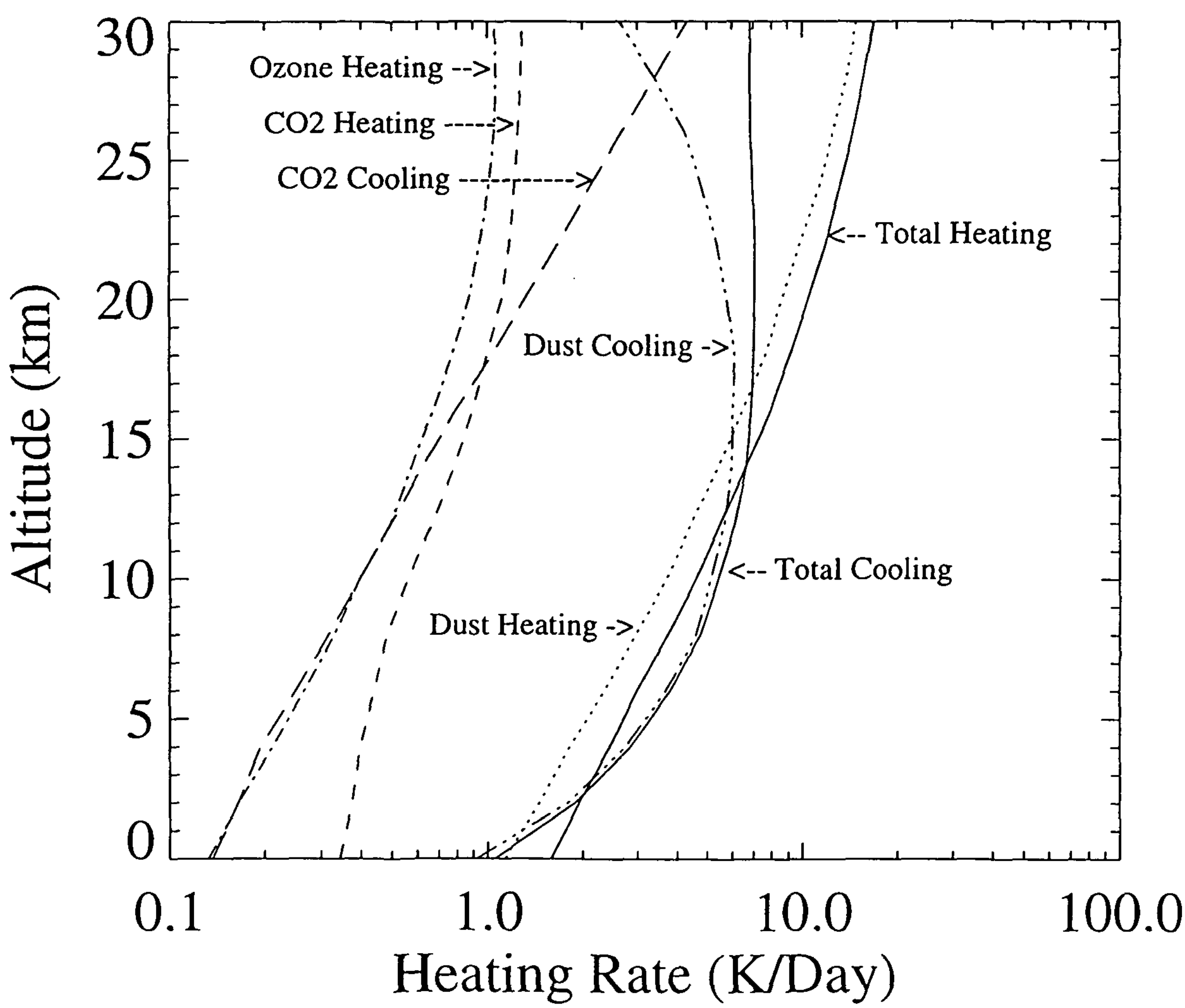

Ozone Heating -->
CO2 Heating ----->
CO2 Cooling ------------>
<-- Total Heating
Dust Cooling ->
<-- Total Cooling
Dust Heating ->
30
25
20
15
10
5
0
Altitude (km)
0.1
1.0
10.0
100.0
Heating Rate (K/Day)

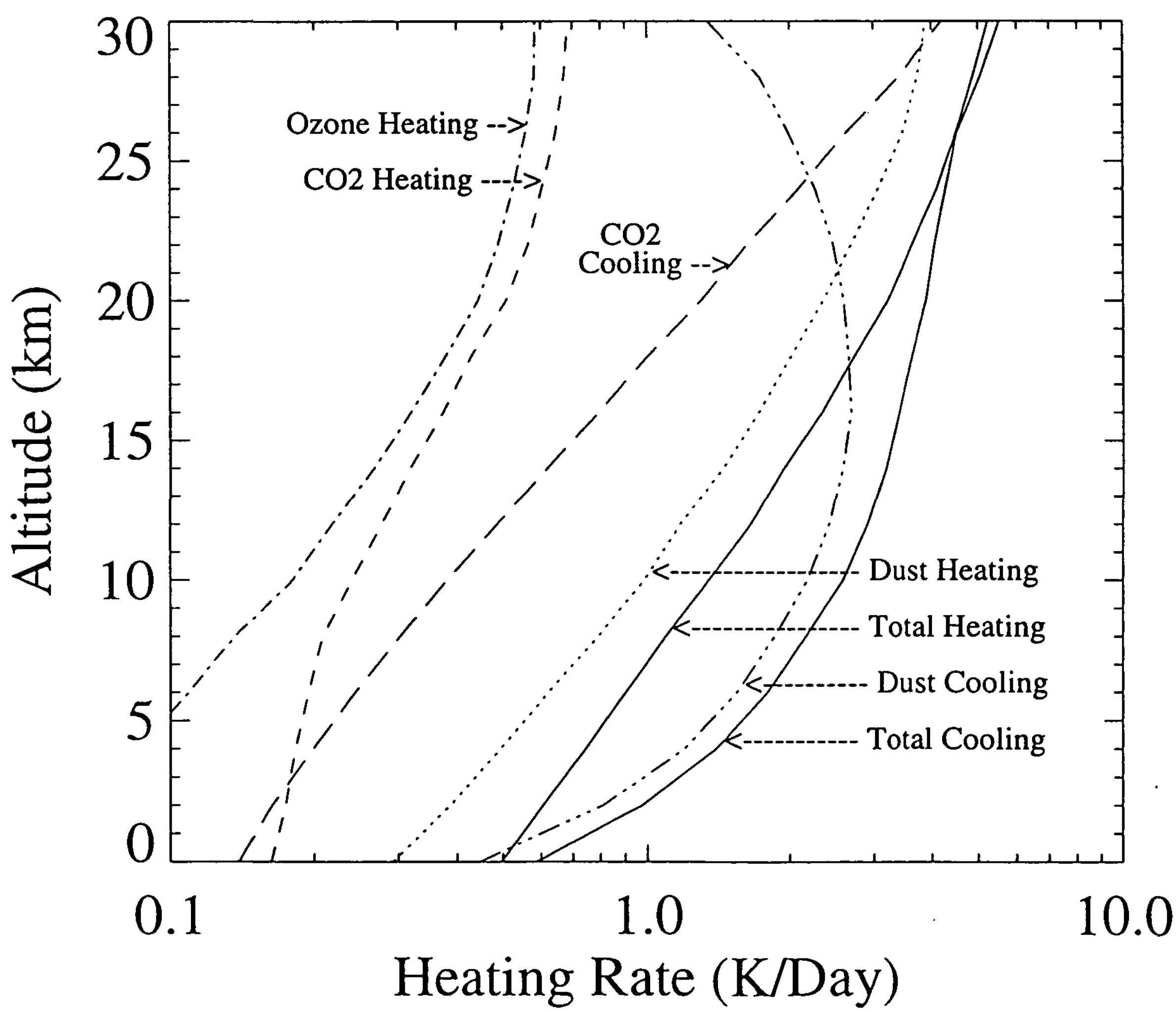
Ozone Heating -->
CO2 Heating --->
CO2
Cooling -->
Dust Heating
Total Heating
Dust Cooling
Total Cooling
30
25
20
15
10
5
0
Altitude (km)
0.1
1.0
10.0
Heating Rate (K/Day)

1994023385

N94-27888

MARS OZONE: MARINER 9 REVISITED

442634

Bernhard Lee Lindner

Atmospheric and Environmental Research, Inc.

840 Memorial Drive

Cambridge, Massachusetts 02139 USA

Telephone: (617)349-2280

Fax: (617)661-6479

Submitted to Geophys. Res. Lett.

Dec. 1993

No. of Pages: 12

No. of Figures: 3

No. of Tables: 0

ABSTRACT: The efficacy of the UV spectroscopy technique used by Mariner 9 to remotely measure ozone abundance at Mars is discussed. Previously-inferred ozone abundances could be underestimated by as much as a factor of 3, and much of the observed variability in the ozone abundance could be due to temporal and spatial variability in cloud and dust amount.

INTRODUCTION

Ozone is a key to understanding atmospheric chemistry on Mars. Over 20 photochemical models of the martian atmosphere have been published, and O_3 is often used as a benchmark for these models (e.g., Lindner, 1988; Shimazaki, 1989; Krasnopolsky, 1993). O_3 abundance has been inferred from instrumentation on several spacecraft, with the most complete coverage provided by Mariner 9 (Barth et al., 1973; Lane et al., 1973; Wehrbein et al., 1979). The Mariner 9 UV spectrometer scanned from 2100 to 3500 Angstroms with a spectral resolution of 15 Angstroms and an effective field-of-view of approximately 300 km^2. The only atmospheric absorption in the 2000 to 3000 Å wavelength region was previously assumed to come from the Hartley band system of ozone (Barth et al., 1973; Lane et al. 1973), which has an opacity of order unity at winter polar latitudes (Lindner, 1988). Therefore the amount of ozone was inferred by fitting this absorption feature with laboratory data of ozone absorption, as shown in Fig. 1 (Lane et al., 1973). Mars O_3 shows strong seasonal and latitudinal variation, with column abundances ranging from 0.2 μm-atm at equatorial latitudes to 60 μm-atm over northern winter polar latitudes (1 μm-atm is a column abundance of 2.689×10^{15} molecules cm^{-2}). However, the O_3 abundance is never great enough to significantly affect atmospheric temperatures (Lindner, 1991; 1993a) or surface temperatures and frost amounts (Lindner, 1990; 1992; 1993b). Figure 2 (Barth, 1985) shows some of the previously-inferred O_3 abundances.

MODELING PROCEDURE

A radiative transfer computer model is used to re-examine the Mariner 9 UV spectra. The discrete ordinate method of Stamnes et al. (1988) is used to treat the scattering and absorption of monochromatic radiation through the martian atmosphere. O_3 absorption cross-sections from 2000 Å to 3200 Å are included (Daumont et al., 1983; Freeman et al, 1984). Ultraviolet absorption cross-sections for CO_2, O_2, H_2O, HO_2 and H_2O_2 are negligible (e.g., Lindner, 1988; 1991;1993b). The Rayleigh scattering optical depth is computed as in Hansen and Travis (1974), using parameters appropriate for Mars. Atmospheric composition is taken as 95% CO_2 (Owen et al., 1977). The altitude dependence of O_3 is based on model results (Lindner, 1988).

Atmospheric properties are zonally averaged and assumed azimuthally-independent. The region from the surface to 40 km altitude is broken into twenty 2-km-thick layers to account for vertical inhomogeneity. The Chapman function is used to approximate the slant path in place of the secant function (Smith and Smith, 1972), because the winter polar atmosphere always has large solar zenith angles, and the secant function is in error for large angles. This work examines 57°N latitude in late winter ($L_S = 343°$), which is when the maximum O_3 column abundance was observed (Barth et al, 1973; Lane et al., 1973). [L_S, the solar longitude, is a seasonal index; L_S of 0°, 90°, 180°, 270°, correspond to northern spring equinox, summer solstice, autumnal equinox, and winter solstice, respectively]. The surface is covered by ice with an albedo of 0.6 (Warren and Wiscombe, 1980; Hapke et al., 1981; James and Lumme, 1982; Warren et al., 1990; Lindner, 1993a). The altitude profile of temperature rises linearly from 150K at the surface to 160K at 10 km, and then falls linearly with altitude to 130 K at 40 km, typical for winter polar conditions (Lindal et al., 1979; Kieffer, 1979).

Dust opacities varied from 0.2 to 1.0 for conditions other than global dust storms during the Mariner 9 and Viking observations (Briggs and Leovy, 1974; Pollack et al., 1979; Lumme and James, 1984), although dust opacities over winter polar latitudes may be slightly less [e.g., Lindner, 1990]. Dust opacity varies with wavelength (Zurek, 1978; 1982). The vertical distribution of dust is well-mixed to 20 km altitude (Anderson and Leovy, 1978; Zurek, 1982; Korablev et al., 1993). The single scattering albedo of airborne dust has a solar average of 0.9 (Clancy and Lee, 1991), but is only 0.6 in the 2000 Å to 3000 Å range (Pang et al., 1976; Thorpe, 1977). Scattering of radiation by dust is represented by the Henyey-Greenstein phase function, with an asymmetry parameter of 0.55 (Clancy and Lee, 1991). Typical cloud and fog opacities of 1.0 are taken from theory (Kulikov and Rykhletskii, 1983) and observations (Moroz, 1976; Pollack et al., 1977; Clancy and Lee, 1991), although large seasonal and latitudinal variations exist (Briggs and Leovy, 1974). A single-scattering albedo for cloud particles of 1.0 is taken from observations (Clancy and Lee, 1991). The Henyey-Greenstein phase function with asymmetry parameter of 0.55 is also used to describe the scattering by clouds (Clancy and Lee, 1991). Computational difficulties which accompany highly asymmetric phase functions are removed with the Delta-L method (Wiscombe, 1977).

RESULTS AND DISCUSSION

Using a constant mixing ratio for O_3 (e.g., Wehrbein, 1979; Lindner, 1988) and no chemical or radiative interaction between O_3 and clouds/dust, Fig. 3 shows that when typical amounts of dust and cloud are present that significant underestimation of O_3 abundance occurs. A factor of 3 times as much O_3 is needed to generate the same spectrum the spacecraft would measure for a cloudy, dusty atmosphere as for a clear atmosphere. If the scattering properties of martian clouds and dust were well known, then their appearance would not be a problem, as a model would be capable of retrieving the O_3 abundance. However, these properties are not well known, which raises doubts about the effectiveness of the UV reflectance spectroscopy technique for measuring O_3 abundance on Mars. The simulations shown in Fig. 3 are repeated for a range in solar zenith angle (50°-90°), ground albedo (0.3-0.8), altitude distribution of O_3, satellite viewing geometries, dust scattering properties, and cloud, dust and O_3 abundances. A factor of 3 underestimation is typical, with greater underestimation for high ground albedo or high dust opacities. Even if scattering by clouds is properly accounted for (as previously done with Mariner 9 data reduction in [4]), masking by dust can easily result in factor of 2 underestimation. Results are not strongly dependent on solar zenith angle.

Spatial and temporal variability in temperature and water vapor have been claimed to account for the scatter of the data points in Fig. 2 (Barth and Dick, 1974). A decrease in temperature results in a decrease in water vapor, assuming the atmosphere is saturated. A decreased water vapor abundance decreases the availability of odd hydrogen (H, OH, and HO_2), which converts CO and O into CO_2 catalytically, decreasing the abundance of O needed to form O_3. However, water vapor is a small source of odd hydrogen in the winter polar atmosphere compared to H_2, and may not account for most of the variability in Fig. 2 (Lindner, 1988). Masking by clouds and dust may also account for some of the observed O_3 variability, because the nature and opacity of the clouds and dust at winter polar latitudes change significantly spatially and temporally. As the maximum O_3 abundance resides near the surface (Lindner, 1988), spacecraft must be able to observe through the entire cloud and dust abundance in order to measure the total O_3 column abundance. If reflectance spectroscopy is used, as on Mariner 9, then the cloud and the airborne dust must be traversed twice; first by the incoming solar flux down to the surface, and then once again upon reflection from the surface out to the spacecraft. In addition, the large solar zenith angles at winter polar latitudes mean several times the vertical opacity of cloud and dust must be traversed. Indeed, part of the observed latitudinal variation in O_3 abundance in Fig. 2 may be due to the inability of the spacecraft to observe through the increasing effective optical depths as one goes poleward.

By using a photochemical model which included multiple scattering of solar radiation, Lindner (1988) showed that the absorption and scattering of solar radiation by clouds and dust should actually increase O_3 abundances at winter polar latitudes. Hence, regions with high dust and cloud abundance could contain high O_3 abundances (heterogeneous chemistry effects have yet to be fully understood [Atreya and Blamont, 1990; Krasnopolsky, 1993]). It is quite possible that the maximum O_3 column abundance observed by Mariner 9 of 60μm-atm is common. In fact, larger quantities may exist in some of the colder areas with optically thick clouds and dust. As the Viking period often had more atmospheric dust loading than did that of Mariner 9, the reflectance spectroscopy technique may even have been incapable of detecting the entire O_3 column abundance during much of the Mars year that Viking observed, particularly at high latitudes. The behavior of O_3 is virtually unknown during global dust storms, in polar night, and within the polar hood, leaving large gaps in our understanding.

Other possibilities for measuring O_3 abundance include solar occultation (Blamont et al., 1989), IR observations in the 9.6 μm O_3 absorption band (Espanek et al., 1991), and observations of the O_2 dayglow at 1.27 μm, produced by photolysis of O_3 (Traub et al., 1979). However, further studies of these other techniques are required, especially as regards the effects of clouds and dust.

ACKNOWLEDGMENTS. I thank Knut Stamnes for providing the radiative transfer program, and NASA's MSATT Program for support (contract NASW-4614).

REFERENCES

Anderson, E. and Leovy, C., Mariner 9 television limb observations of dust and ice hazes on Mars, *J. Atmos. Sci.*, **35**, 723-734, 1978.

Atreya, S.K. and Blamont, J.E., Stability of the martian atmosphere: Possible role of heterogenous chemistry, *Geophys. Res. Lett.*, **17**, 287-290, 1990.

Barth, C.A., Photochemistry of the atmosphere of Mars, in *The Photochemistry of Atmospheres. Earth, other Planets, and Comets*, ed. Levine, J., Academic Press, Orlando, Fla., 1985.

Barth, C.A. and Dick, M.L., Ozone and the polar hood of Mars, *Icarus*, **22**, 205-211, 1974.

Barth, C.A. C.W. Hord, A.I. Stewart, A.L. Lane, M.L. Dick and G.P. Anderson, Mariner 9 Ultraviolet experiment: Seasonal variation of ozone on Mars, *Science*, **179**, 795-796, 1973.

Blamont, J.E., E. Chassefiere, J.P. Goutail, B. Mege, M. Nunes-Pinharanda, G. Souchon, V.A. Krasnopolsky, A.A. Krysko and V.I. Moroz, Vertical profiles of dust and ozone in the martian atmosphere deduced from solar occultation measurements, *Nature*, **341**, 600-603, 1989.

Briggs, G.A. and Leovy, C.B., Mariner 9 observations of the Mars north polar hood, *Bull. Amer. Met. Soc.*, **55**, 278-296, 1974.

Clancy, R.T. and Lee, S.W., A new look at dust and clouds in the Mars atmosphere: Analysis of emission-phase-function sequences from global Viking IRTM observations, *Icarus*, **93**, 135-158, 1991.

Daumont, D., Brion, J. and Malicet, J., Measurement of total atmospheric ozone: Consequences entailed by new values of ozone absorption cross-sections at 223 K in the 310-350 nm spectral range, *Planet. Space Sci.*, **31**, 1229-1234, 1983.

Espanek, F., M.J. Mumma, T. Kostiuk, and D. Zipoy, Ground based infrared measurements of the global distribution of O3 in the atmosphere of Mars, *Icarus*, **92**, 252-262, 1991.

Freeman, D.E., K. Yoshino, J.R. Esmond and W.H. Parkinson, High resolution absorption cross-section measurements of ozone at 195 K in the wavelength region 240-350 nm, *Planet. Space Sci.*, **32**, 239-248, 1984.

Hansen, J.E. and Travis, L.D., Light scattering in planetary atmospheres, *Space Science Reviews*, **16**, 527-610, 1974.

Hapke, B., E. Wells, J. Wagner and W. Partlow, Far-UV, Visible, and Near-IR reflectance spectra of frosts of H_2O, CO_2, NH , and SO_2, *Icarus*, **47**, 361-367, 1981.

James, P.B. & Lumme, K., Martian south polar cap boundary: 1971 and 1973 data, *Icarus*, **50**, 368-380, 1982.

Kieffer, H.H., Mars south polar spring and summer temperatures: A residual CO_2 frost, *J. Geophys. Res.*, **84**, 8263-8288, 1979.

Korablev, O.I., V.A. Krasnopolsky, A.V. Rodin, and E. Chassefiere, Vertical structure of martian dust measured by solar infrared occulatations from the Phobos spacecraft, *Icarus*, **102**, 76-87, 1993.

Krasnopolsky, V.A., Photochemistry of the martian atmosphere (mean conditions), *Icarus*, **101**, 313-332, 1993.

Kulikov, Yu.N. and Rykhletskii, M.V., Modeling of the vertical distribution of water in the atmosphere of Mars, *Astron. Vestnik*, **17**, 144-152, 1983. (English translation: *Solar System Res.*, **17**, 112-118, 1983.)

Lane, A.L., Barth, C., Hord,C. and Stewart, A.I., Mariner 9 ultraviolet spectrometer experiment: Observations of ozone on Mars, *Icarus*, **18**, 102-108, 1973.

Lindal, G.F., H.B. Hotz, D.N. Sweetnam, Z. Shippony, J.P. Brenkle, G.V. Hartsell, R.T. Spear and W.H. Michael, Jr., Viking radio occultation measurements of the atmosphere and topography of Mars: Data acquired during 1 martian year of tracking, *J. Geophys. Res.*, **84**, 8443-8456, 1979.

Lindner, B.L., Ozone on Mars: The effects of clouds and airborne dust, *Planet. Space Sci.*, **36**, 125-144, 1988.

Lindner, B.L., The martian polar cap: Radiative effects of ozone, clouds, and airborne dust, *J. Geophys. Res.*, **95**, 1367-1379, 1990.

Lindner, B.L., Ozone heating in the martian atmosphere, *Icarus*, **93**, 354-361, 1991.

Lindner, B.L., Sunlight penetration through the martian polar caps: Effects on the thermal and frost budgets, *Geophys. Res. Lett.*, **19**, 1675-1678, 1992.

Lindner, B.L., The hemispherical asymmetry in the martian polar caps, *J. Geophys. Res.*, **98**, 3339-3344, 1993a.

Lindner, B.L., Martian atmospheric radiation budget, submitted to *Publ. Astron. Soc. Japan*, 1993b.

Lumme K. and James, P.B., Some photometric properties of the martian south polar cap region during the 1971 apparition, *Icarus*, **58**, 363-376, 1984.

Moroz, V.I., Clouds on Mars: Some results from observations on Mars 3, *Kosmich. Issled.*, **14**, 406-416, 1976. (English translation: *Cosmic Res.*, **14**, 364-372, 1976).

Owen, T., K. Biemann, D.R. Rushneck, J.E. Biller, D.W. Howarth, and A.L. Lafleur, The composition of the atmosphere at the surface of Mars, *J. Geophys. Res.*, **82**, 4635-4639, 1977.

Pang, K., J. M. Ajello, C.W. Hord, and W.G. Egan, Complex refractive index of martian dust: Mariner 9 UV observations, *Icarus*, **27**, 55-67, 1976.

Pollack, J.B., D. Colborn, R. Kahn, J. Hunter, W. Van Camp, C.E. Carlston and M.R. Wolf, Properties of aerosols in the Martian atmosphere as inferred from Viking Lander imaging data, *J. Geophys. Res.*, **82**, 4479-4496, 1977.

Pollack, J.B., D.S. Colburn, F.M. Flasar, R. Kahn, C.E. Carlston and D. Pidek, Properties and effects of dust particles suspended in the martian atmosphere, *J. Geophys. Res.*, **84**, 2929-2945, 1979.

Shimazaki, T., Photochemical stability of CO2 in the martian atmosphere: Reevaluation of the eddy diffusion coefficient and role of water vapor, *J. Geomag. Geoelectr.*, **41**, 273-301, 1989.

Smith, F.L., III, and Smith, C., Numerical evaluation of Chapman's grazing incidence integral ch(X,X), *J. Geophys. Res.*, **77**, 3592-3597, 1972.

Stamnes, K., S. Tsay, W. Wiscombe, and K. Jayaweera, Numerically stable algorithm for discrete-ordinate-method radiative transfer in multiple scattering and emitting media, *App. Optics*, **27**, 2502-2509, 1988.

Thorpe, T.E., Viking orbiter observations of atmospheric opacity during July-November 1976, *J. Geophys. Res.*, **82**, 4151-4159, 1977.

Traub, W.A., N.P. Carleton, P. Connes and J.F. Noxon, 1979: The latitudinal variation of O2 dayglow and O3 abundance on Mars, *Astrophys. J.*, **229**, 846-850, 1979.

Warren, S.G. and Wiscombe, W.J., A model for the spectral albedo of snow. II: Snow containing atmospheric aerosols, *J. Atmos. Sci.*, **37**, 2734-2745, 1980.

Warren, S.G., W.J. Wiscombe, and J.F. Firestone, Spectral albedo and emissivity of CO2 in martian polar caps: model results, *J. Geophys. Res.*, **95**, 14717-14741, 1990.

Wehrbein, W.M., C.W. Hord, and C.A. Barth, Mariner 9 UV Spectrometer Experiment: Vertical distribution of ozone on Mars, *Icarus*, **38**, 288-299, 1979.

Wiscombe, W.J., The delta-m method: Rapid yet accurate radiative flux calculations for strongly asymmetric phase functions, *J. Atmos. Sci.*, **34**, 1408-1422, 1977.

Zurek, R.W., Solar heating of the martian dusty atmosphere, *Icarus*, 35, 196-208, 1978.

Zurek, R.W., Martian great dust storms: An update, *Icarus*, **50**, 288-310, 1982.

FIGURE CAPTIONS

Figure 1. Ultraviolet spectrum measured by Mariner 9 at 57°N latitude on orbit 144 (taken from Lane et al., 1973). To enhance the O_3 absorption feature, this spectrum was divided by one obtained at 20°N latitude on orbit 144, where O_3 abundances are minimal.

Figure 2. Measurements of the O_3 column abundance previously inferred from the Mariner 9 UV spectrometer data during the northern winter, L_s = 330-360°, in the northern hemisphere (taken from Barth, 1985).

Figure 3. Synthetic spectra as would be observed by spacecraft for atmospheres with no cloud or dust and 30 µm-atm O_3 (solid line), vertical opacities of dust and cloud of 0.3 and 1.0, respectively, and 30 µm-atm of O_3 (dashed line), and vertical opacities of dust and cloud of 0.3 and 1.0, respectively, and 100 µm-atm of O_3 (dotted line). All cases assume a solar a zenith angle of 75° (typical for winter polar observations), and a polar cap albedo of 0.6.

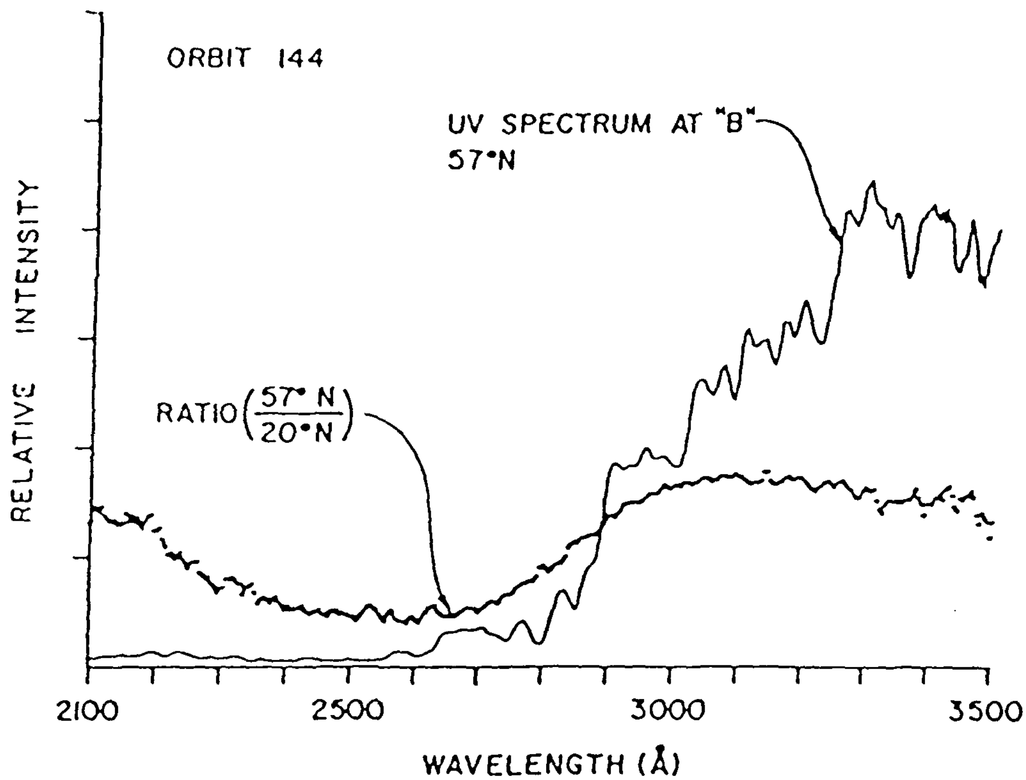

ORBIT 144
UV SPECTRUM AT "B" 57°N
RATIO (57° N / 20° N)
RELATIVE INTENSITY
2100
2500
3000
3500
WAVELENGTH (Å)

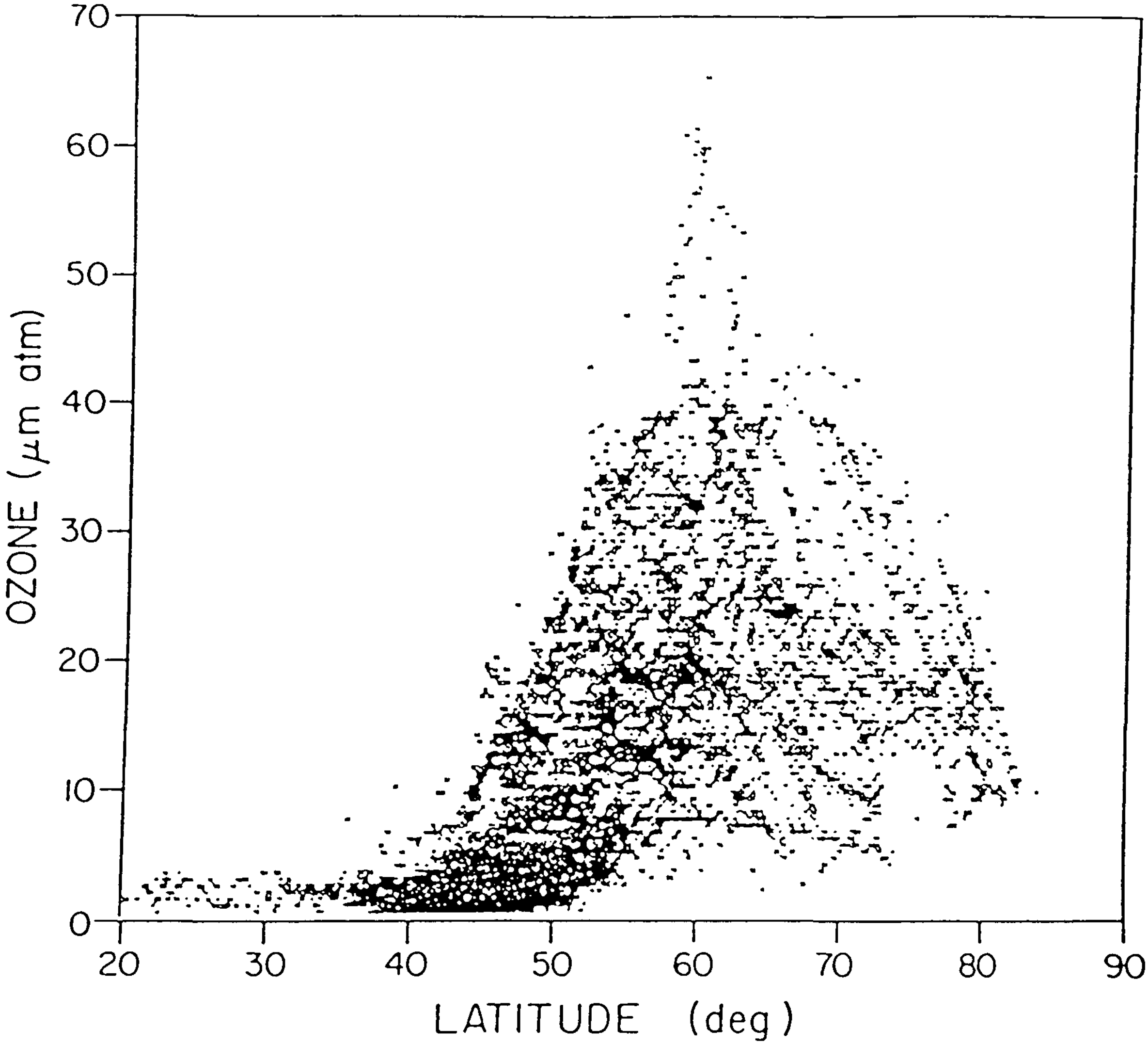
70
60
50
40
30
20
10
0
OZONE (μm atm)
20
30
40
50
60
70
80
90
LATITUDE (deg)

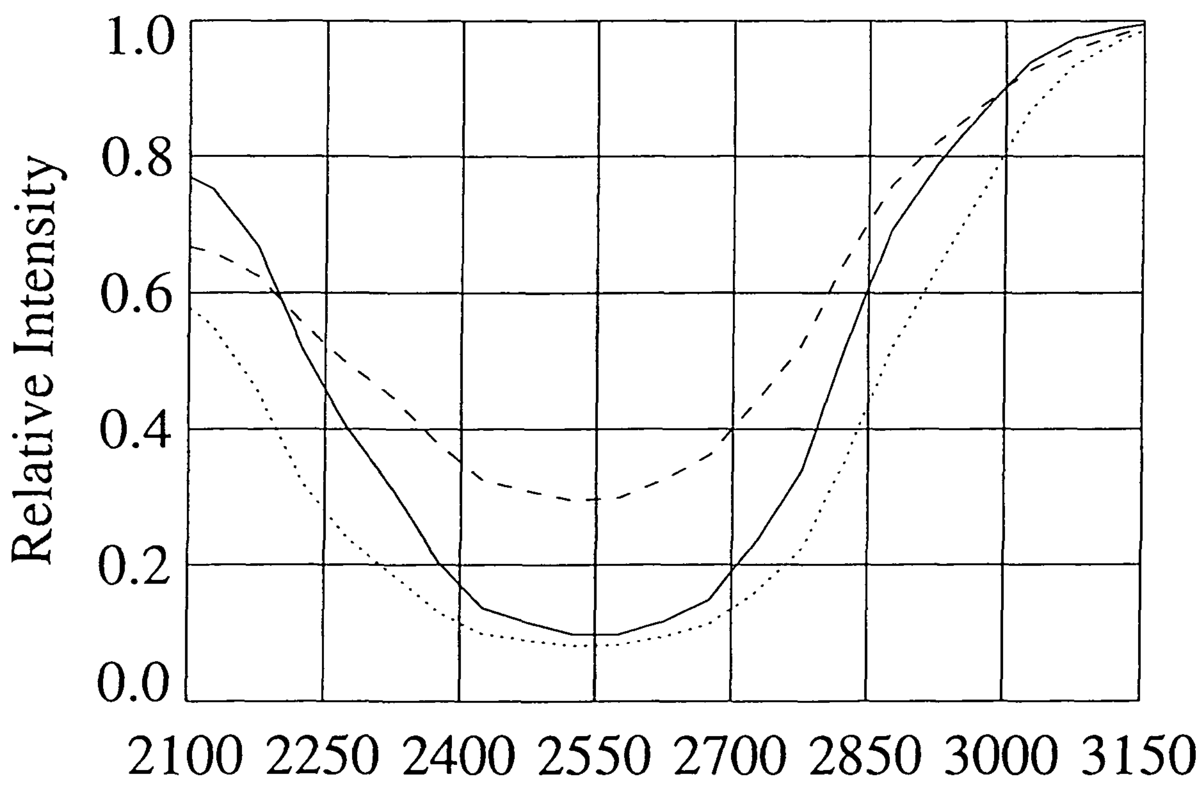
1.0
0.8
0.6
0.4
0.2
0.0
Relative Intensity
2100 2250 2400 2550 2700 2850 3000 3150
Wavelength (in Angstroms)

Comment on

"Mars secular obliquity change due to the seasonal polar caps"

by David Parry Rubincam

Bernhard Lee Lindner

AER, Inc.

840 Memorial Drive

Cambridge, MA 02139

(617) 349-2280

Submitted to *J. Geophys. Res.*

April 15, 1993

No. of pages: 6

No. of figures: 0

No. of tables: 0

Rubincam (1992) has splendidly shown that the martian obliquity is dependent on the seasonal polar caps. In particular, Rubincam analytically derived this dependence, and showed that the change in obliquity is directly proportional to the seasonal polar cap mass. Specifically, Rubincam showed

$$dT/dt = 3 \times 10^{-10}\, M(t)/M(0) \qquad \text{degrees / Earth year} \tag{1}$$

where T is the obliquity and M is the mass of the seasonal polar caps, with time t of 0 being the present. This expression assumes uniformly thick spherical caps with identical angular radii of 45°. However even if a very different polar cap mass distribution is used, Rubincam estimates the total uncertainty in the constant in Equation (1) to be less than a factor of 2. Using the current mass of the seasonal polar cap as typical over geologic time, Rubincam calculates that the amount that the obliquity would secularly change is only 1.4°. Considering that the current obliquity of Mars is 25°, Rubincam concludes that seasonal friction does not appear to have changed Mars' climate significantly.

Using a computer model for the evolution of the martian atmosphere, Haberle et al. (1992a, b) have made a convincing case for the possibility of huge polar caps, about ten times the mass of the current polar caps, which exist for a significant fraction of the planet's history. Given the large uncertainties in input parameters and in the model itself, the results must be regarded as speculative. Also, the Haberle et al. results have been unable to favor or rule out a large polar cap scenario versus a small polar cap scenario.

Nonetheless, even just the possibility of massive polar caps makes the Rubincam paper more noteworthy. Since Rubincam showed that the effect of seasonal friction on obliquity is directly proportional to polar cap mass, a scenario with a ten-fold increase in polar cap mass over a significant fraction of the planet's history would result in a secular increase in Mars' obliquity of perhaps 10° (using Equation 1). Hence, the Rubincam conclusion of an insignificant contribution to Mars' climate by seasonal friction may be incorrect. Furthermore, if seasonal friction is an important consideration in the obliquity of Mars, this would significantly alter the predictions of past obliquity as presented by

Ward (1973; 1974; 1979), Murray et al. (1973), Ward et al. (1979), Rubincam (1990), Chao and Rubincam (1990), Bills (1990), Ward and Ruby (1991), Touma and Wisdom (1993), and Laskar and Robutel (1993). That in turn would significantly alter the predictions of past climate which are based on obliquity predictions (Sagan et al., 1973; Ward et al., 1974; Toon et al., 1980; Fanale et al., 1982; Pollack and Toon, 1982; Francois et al., 1990). The mechanics of the polar cap system also depend on obliquity (Leighton and Murray, 1966; James and North, 1982; Lindner, 1990; 1992; 1993; Wood and Paige, 1992.) If obliquities were often much smaller than at present, that could have implications for past atmospheric composition (Lindner and Jakosky, 1985).

Given the enormity of the implications, the work of Rubincam should be given more attention and study. Perhaps further modeling of obliquity could be used to rule out the possibility of large polar caps for extended times, which would assist modeling of atmospheric evolution. Similarly, modeling of atmospheric evolution should be given more attention and study because of the implications for obliquity history, and therefore climate history.

Acknowledgement: The author is indebted to the NASA MSATT program for support (Contract NASW-4614).

REFERENCES

Bills, B. G., The rigid body obliquity history of Mars, *J. Geophys. Res., 95,* 14137-14153, 1990.

Chao, B. F., and D. P. Rubincam, Variations of Mars gravitational field and rotation due to seasonal CO_2 exchange, *J. Geophys. Res., 95,* 14755-14760, 1990.

Fanale, F. P., J. R. Salvail, W. B. Banerdt, and R. S. Saunders, Mars: The regolith-atmosphere-cap system and climate change, *Icarus, 50,* 381-407, 1982.

Francois, L. M., J. C. G. Walker, and W. R. Kuhn, A numerical simulation of climate changes during the obliquity cycle on Mars, *J. Geophys. Res., 95,* 14761-14778, 1990.

Haberle, R. M., D. Tyler, C. P. McKay, and W. Davis, Evolution of the martian atmosphere: The role of the polar caps, in *Workshop on the Polar Regions of Mars: Geology, Glaciology, and Climate History,* Clifford, S.M., A.D. Howard, W.S.B. Paterson, eds, pp. 10-11, LPI Tech. Rpt. 92-08, Part I, Lunar and Planetary Institute, Houston, Texas, 1992a.

Haberle, R. M., D. Tyler, C. P. McKay, and W. L. Davis, Evolution of Mars' Atmosphere: Where has the CO_2 gone? *Bull. Amer. Astron. Soc., 24,* 1015-1016, 1992b.

James, P. B., and G. R. North, The seasonal CO_2 cycle on Mars: An application of an energy-balance climate model, *J. Geophys. Res., 87,* 10271-10283, 1982.

Laskar, J., and P. Robutel, The chaotic obliquity of the planets, *Nature, 361,* 608-612, 1993.

Leighton, R. B., and B. C. Murray, Behavior of carbon dioxide and other volatiles on Mars, *Science, 153,* 136-144, 1966.

Lindner, B. L., The martian polar cap: Radiative effects of ozone, clouds, and airborne dust, *J. Geophys. Res., 95,* 1367-1379, 1990.

Lindner, B. L., Sunlight penetration through the martian polar caps: Effects on the thermal and frost budgets, *Geophys. Res. Lett., 19*, 1675-1678, 1992.

Lindner, B. L., The hemispherical asymmetry in the martian polar caps, *J. Geophys. Res.*, *98*, 3339-3344, 1993.

Lindner, B. L., and B. M. Jakosky, Martian atmospheric photochemistry and composition during periods of low obliquity, *J. Geophys. Res., 90*, 3435-3440, 1985.

Murray, B. C., W. R. Ward, and S. C. Yeung, Periodic insolation variations on Mars, *Science, 180*, 638-640, 1973.

Pollack, J. B., and O. B. Toon, Quasi-periodic climate changes on Mars: A Review, *Icarus, 50*, 259-287, 1982.

Rubincam, D. P., Mars: Change in axial tilt due to climate?, *Science, 248*, 720-721, 1990.

Rubincam, D. P., Mars secular obliquity change due to the seasonal polar caps, *J. Geophys. Res., 97*, 2629-2632, 1992.

Sagan, C., O. B. Toon, and P. J. Gierasch, Climate change on Mars, *Science, 181*, 1045-1049, 1973.

Toon, O. B., J. B. Pollack, W. Ward, J. A. Burns, and K. Bilski, The astronomical theory of climate change on Mars, *Icarus, 44*, 552-607, 1980.

Touma, J., and J. Wisdom, The chaotic obliquity of Mars, *Science, 259*, 1294-1297, 1993.

Ward, W. R., Large scale variations in the obliquity of Mars, *Science, 181*, 260-262, 1973.

Ward, W. R. Climatic variations on Mars. I. Astronomical theory of insolation, *J. Geophys. Res., 79*, 3375-3386, 1974.

Ward, W. R., Present obliquity oscillations on Mars: Fourth-Order accuracy in orbital *e* and *I*, *J. Geophys. Res., 84*, 237-241, 1979.

Ward, W. R., and D.J. Ruby, Resonant obliquity of Mars?, *Icarus, 94*, 160-164, 1991.

Ward, W. R., B. C. Murray, and M. C. Malin, Climatic variations on Mars. 2. Evolution of carbon dioxide atmosphere and polar caps, *J. Geophys. Res.*, *79*, 3387-3395, 1974.

Ward, W. R., J. A. Burns, and O. B. Toon, Past obliquity oscillations of Mars: The role of the Tharsis uplift, *J. Geophys. Res.*, *84*, 243-259, 1979.

Wood, S. E., and D. A. Paige, Modeling the martian seasonal CO_2 cycle. I Fitting the Viking Lander pressure curves, *Icarus, 99,* 1-14, 1992.

19940023386

N94-27889

442636

WHY IS THE NORTH POLAR CAP ON MARS DIFFERENT THAN THE SOUTH POLAR CAP?

Bernhard Lee Lindner, Atmospheric and Environmental Research, Inc.
840 Memorial Drive, Cambridge, Mass. 02139-3794, USA

Introduction. One of the most puzzling mysteries about the planet Mars is the hemispherical asymmetry in the polar caps. Every spring the seasonal polar cap of CO_2 recedes until the end of summer, when only a small part, the residual polar cap, remains. During the year that Viking observed Mars, the residual polar cap was composed of water ice in the northern hemisphere [Kieffer et al., Science, 194, 1341, 1976] but was primarily carbon dioxide ice in the southern hemisphere [Kieffer, J. Geophys. Res., 84, 8263, 1979]. Scientists have sought to explain this asymmetry by modeling observations of the latitudinal recession of the polar cap and seasonal variations in atmospheric pressure (since the seasonal polar caps are primarily frozen atmosphere, they are directly related to changes in atmospheric mass). These models reproduce most aspects of the observed annual variation in atmospheric pressure fairly accurately. Furthermore, the predicted latitudinal recession of the northern polar cap in the spring agrees well with observations, including the fact that the CO_2 ice is predicted to completely sublime away. However, these models all predict that the carbon dioxide ice will also sublime away during the summer in the southern hemisphere, unlike what is observed. This paper will show how the radiative effects of ozone, clouds, and airborne dust, light penetration into and through the polar cap, and the dependence of albedo on solar zenith angle affect CO_2 ice formation and sublimation, and how they help explain the hemispherical asymmetry in the residual polar caps. These effects have not been studied with prior polar cap models.

Ozone, Clouds, and Airborne Dust. Since O_3 is more prevalent in the northern hemisphere than in the southern hemisphere, O_3 was suggested as a cause for the hemispherical asymmetry in the residual polar caps by Kuhn et al. (J. Geophys. Res., 84, 8341, 1979). However, Lindner (submitted to Icarus, 1991) has shown that O_3 has a minor effect on the atmospheric temperature, and hence on the infrared radiation which strikes the polar cap, and Lindner (J. Geophys. Res., 95, 1367, 1990) has shown that O_3 absorbs less than 1% of the total solar radiation absorbed by the polar cap. Thus, O_3 is not an important consideration in the polar cap energy budget.

Lindner (1990) has computed the solar and thermal flux striking the polar cap of Mars for various ozone, dust, and cloud abundances and for three solar zenith angles. These calculations have been inserted in the polar-cap models of Lindner (Eos Trans. AGU, 67, 1078, 1986) and Jakosky and Haberle (J. Geophys. Res., 95, 1359, 1990). Vertical optical depths of dust and cloud ranging from zero to 1 cause little change in the total flux absorbed by the polar cap near its edge but increase the absorbed flux significantly as one travels poleward. Observed hemispherical asymmetries in dust abundance, cloud cover, and surface pressure combine to cause a significant hemispherical asymmetry in the total flux absorbed by the residual polar caps, which helps to explain the dichotomy in the residual polar caps on Mars.

Light Penetration. Penetration of solar radiation into the cap itself is included in my polar cap model, based on the theoretical work of Clow (Icarus, 72, 95, 1987). I find that the inclusion of light penetration slightly decreases the albedo needed in the model to keep CO_2-ice year-round at the south pole by on the order of 1%. The required albedo is decreased because some solar radiation is used to heat the subsurface, and not all of this heat is transported back to the surface. Overall, I conclude that penetration of light into the polar cap has only a small effect on the polarcap energy budget.

Albedo and the Solar Zenith Angle. Warren et al. (J. Geophys. Res., 95, 14717, 1990) has computed the dependence of the albedo of the martian polar caps on solar zenith angle, and these calculations have been included in my polar cap model. Since the albedo of ice increases and becomes more forward scattering at higher solar zenith angles, and since the solar zenith angle becomes higher as one approaches the pole, the albedo is greatest at the pole. This decreases absorption of sunlight, hence increasing survivability of CO_2 ice. In fact, this increases the survivability of ice enough to offset the decrease in survivability of ice due to the radiative effects of clouds and dust.

Discussion. The combination of the effects of solar zenith angle on albedo and the radiative effects of clouds and dust act to extend the lifetime of CO_2 ice on the south pole relatively more than on the north pole, explaining the hemispherical asymmetry in the residual polar caps without the need of a hemispherical asymmetry in polar cap albedo. Another positive aspect this solution is that neither the inclusion of solar zenith angle effects on ice albedo nor the radiative effects of clouds and dust should appreciably change model predictions of the annual cycle of pressure or polar cap recession equatorward of 75° latitude, since approximately 90% of the seasonal CO_2 frost is equatorward of 80° latitude. Hence, the good model agreement noted by prior researchers to the seasonal cycle in atmospheric pressure and to the recession of the polar cap equatorward of 80° latitude is retained.

MARS SEASONAL CO_2-ICE LIFETIMES AND THE ANGULAR DEPENDENCE OF ALBEDO

Bernhard Lee Lindner, AER, 840 Memorial Drive, Cambridge MA 02139 USA

The albedo of the polar caps on Mars brightens appreciably at high solar zenith angle (Warren et al., J. Geophys. Res., 95, 14717, 1990), an effect not included in prior polar-cap energy-balance models. This decreases absorption of sunlight by the polar cap, hence decreasing sublimation of CO_2 ice. Lindner (J. Geophys. Res., 95, 1367, 1990) has shown that the radiative effects of clouds and airborne dust will increase sublimation of CO_2 ice over that predicted by prior polar-cap energy-balance models. Furthermore, observations hint that more clouds may exist in the northern hemisphere, which Lindner (1990) has shown would sublime CO_2 ice more quickly in the north than in the south. I show here that the effects of the solar zenith angle dependence of albedo and the radiative effects of clouds and dust offset each other, but act to extend the lifetime of CO_2 ice on the south pole more than on the north pole, possibly explaining the observed hemispherical asymmetry in the residual polar caps without the need of a hemispherical asymmetry in polar-cap albedo required by prior models. Another positive aspect of this solution is that neither the inclusion of the solar zenith angle dependence of albedo nor the radiative effects of clouds and dust should appreciably change prior model agreement with observations of the annual cycle of surface pressure and the recession of the polar caps equatorward of 75° latitude.

- LINDNER, Bernhard Lee, Ph.D., Atmospheric and Environmental Research, Inc., 840 Memorial Drive, Cambridge, MA 02139 USA

- The Climate of Mars Symposium, Symposium M13
- Oral presentation preferred
- 1 overhead projector

SIMULATIONS OF THE SEASONAL POLAR CAPS ON MARS

Bernhard Lee Lindner, Atmospheric and Environmental Research, Inc., 840 Memorial Drive, Cambridge, Mass. 02139-3794, USA

Introduction. One of the most puzzling mysteries about the planet Mars is the hemispherical asymmetry in the polar caps. Every spring the seasonal polar cap of CO_2 recedes until the end of summer, when only a small part, the residual polar cap, remains. During the year that Viking observed Mars, the residual polar cap was composed of water ice in the northern hemisphere [Kieffer et al., Science, 194, 1341, 1976] but was primarily carbon dioxide ice in the southern hemisphere [Kieffer, J. Geophys. Res., 84, 8263, 1979]. Scientists have sought to explain this asymmetry by modeling observations of the latitudinal recession of the polar cap and seasonal variations in atmospheric pressure (since the seasonal polar caps are primarily frozen atmosphere, they are directly related to changes in atmospheric mass). These models reproduce most aspects of the observed annual variation in atmospheric pressure fairly accurately. Furthermore, the predicted latitudinal recession of the northern polar cap in the spring agrees well with observations, including the fact that the CO_2 ice is predicted to completely sublime away. However, these models all predict that the carbon dioxide ice will also sublime away during the summer in the southern hemisphere, unlike what is observed. This paper will show how the radiative effects of ozone, clouds, and airborne dust, light penetration into and through the polar cap, and the dependence of albedo on solar zenith angle affect CO_2 ice formation and sublimation, and how they help explain the hemispherical asymmetry in the residual polar caps. These effects have not been studied with prior polar cap models.

Ozone, Clouds, and Airborne Dust. Since O_3 is more prevalent in the northern hemisphere than in the southern hemisphere, O_3 was suggested as a cause for the hemispherical asymmetry in the residual polar caps by Kuhn et al. (J. Geophys. Res., 84, 8341, 1979). However, Lindner (submitted to Icarus, 1991) has shown that O_3 has a minor effect on the atmospheric temperature, and hence on the infrared radiation which strikes the polar cap, and Lindner (J. Geophys. Res., 95, 1367, 1990) has shown that O_3 absorbs less than 1% of the total solar radiation absorbed by the polar cap. Thus, O_3 is not an important consideration in the polar cap energy budget.

Lindner (1990) has computed the solar and thermal flux striking the polar cap of Mars for various ozone, dust, and cloud abundances and for three solar zenith angles. These calculations have been inserted in the polar-cap model of Lindner (Eos Trans. AGU, 67, 1078, 1986). Vertical optical depths of dust and cloud ranging from zero to 1 cause little change in the total flux absorbed by the polar cap near its edge but increase the absorbed flux significantly as one travels poleward. Observations hint that hemispherical asymmetries in dust abundance and cloud cover exist, and these would combine to cause a significant hemispherical asymmetry in the total flux absorbed by the residual polar caps, which helps to explain the dichotomy in the residual polar caps.

Light Penetration. Penetration of solar radiation into the cap itself is included in the polar cap model of Jakosky and Haberle (J. Geophys. Res., 95, 1359, 1990), based on the theoretical work of Clow (Icarus, 72, 95, 1987). Lindner and Jakosky (B.A.A.S., 22, 1060, 1990) find that the inclusion of light penetration slightly decreases the albedo needed in the model to keep CO_2-ice year-round at the south pole by on the order of 1%. The required albedo is decreased because some solar radiation is used to heat the subsurface, and not all of this heat is transported back to the surface. Overall, we conclude that penetration of light into the polar cap has only a small effect on the polarcap energy budget.

Albedo and the Solar Zenith Angle. Warren et al. (J. Geophys. Res., 95, 14717, 1990) have computed the dependence of the albedo of the martian polar caps on solar zenith angle, and these calculations have been included in my polar cap model. Since the albedo of ice increases and becomes more forward scattering at higher solar zenith angles, and since the solar zenith angle becomes higher as one approaches the pole, the albedo is greatest at the pole. This decreases absorption of sunlight, hence increasing survivability of CO_2 ice. In fact, this increases the survivability of ice enough to offset the decrease in survivability of ice due to radiative effects of clouds and dust.

Discussion. The combination of the effects of solar zenith angle on albedo and the radiative effects of clouds and dust act to extend the lifetime of CO_2 ice on the south pole relatively more than on the north pole, possibly explaining the hemispherical asymmetry in the residual polar caps without the need of a hemispherical asymmetry in polar cap albedo. This does not imply that a hemispherical asymmetry in polar cap albedo does not exist, but that one is not necessary.

Observations of the regression of the polar caps and the annual cycle in atmospheric pressure are reproduced fairly well by the model, as shown in the figures, although further improvement is needed. When CO_2 ice is retained at the south pole, the model predictions of the annual cycle in atmospheric pressure have a phase shift relative to the data, no matter what model input parameters are used. We are investigating other processes not included in prior polar cap models.

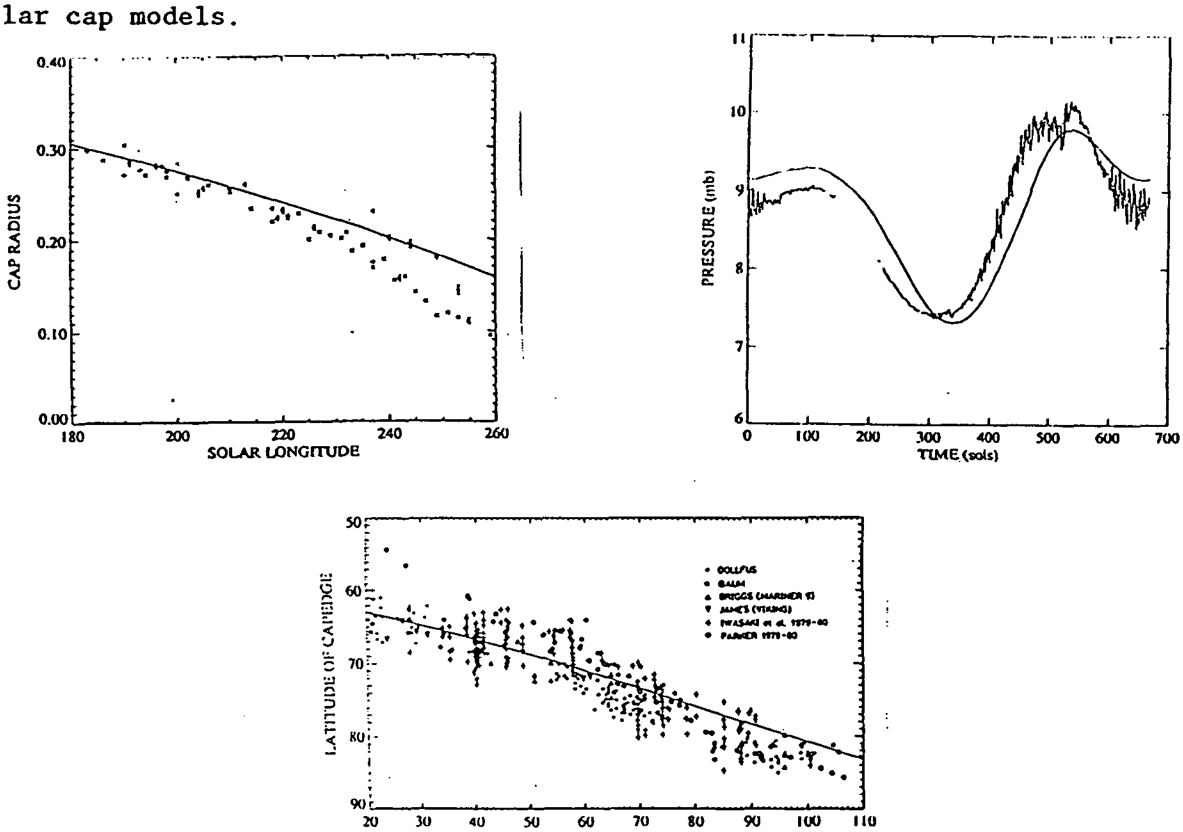

Comparison of the model to atmospheric pressure (upper right), south polar cap regression (upper left), and north polar cap regression (bottom)

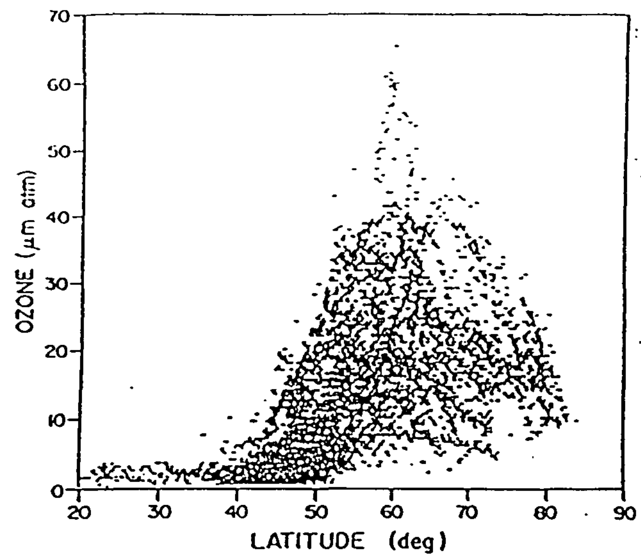

Fig. 1. Measurements of the O_3 column abundance inferred from the Mariner 9 UV spectrometer data during the northern winter, L_S = 330–360, in the northern hemisphere (see [2]).

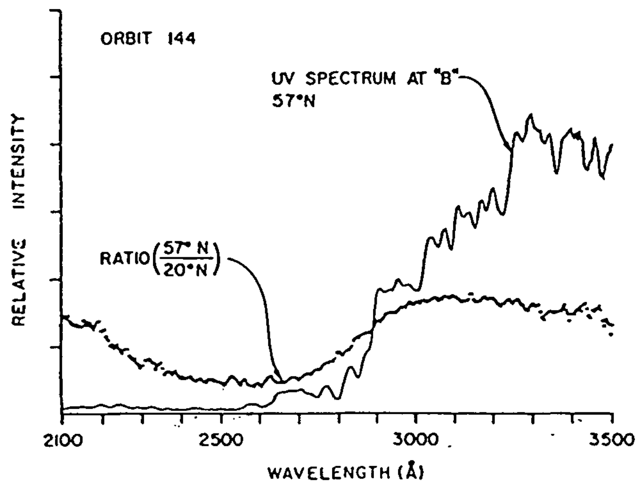

Fig. 2. Ultraviolet spectrum measured by Mariner 9 at 57N latitude on orbit 144. To enhance the O_3 absorption feature, this spectrum was divided by one obtained at 20N latitude on orbit 144, where O_3 abundances are minimal [1].

DOES UV INSTRUMENTATION EFFECTIVELY MEASURE OZONE ABUNDANCE? Bernhard Lee Lindner, AER, 840 Memorial Drive, Cambridge MA 02139, USA.

Measurements of O_3 on Mars provide significant information about the chemistry and composition of the atmosphere [1], including long-term changes [2]. The most extensive and accurate data were inferred from the Mariner 9 UV spectrometer experiment, some of which are reproduced in Fig. 1. Mars O_3 shows strong seasonal and latitudinal variation, with column abundances ranging from 0.2 μm-atm at equatorial latitudes to 60 μm-atm over the northern winter polar latitudes [1] (1 μm-atm is a column abundance of 2.689×10^{15} molecules cm^{-2}).

The Mariner 9 UV spectrometer scanned from 2100 to 3500 Å in one of its two spectral channels every 3 s with a spectral resolution of 15 Å and an effective field-of-view of approximately 300 km^2. Measurements were made for almost half a martian year, with winter and spring in the northern hemisphere and summer and fall in the southern hemisphere. The detectability limit of the spectrometer was approximately 3 μm-atm of ozone. The process used by earlier investigators to extract the ozone abundance from the observed Mariner 9 spectra is as follows [1]. Each spectrum was filtered to remove spurious data points, then compared to the solar flux spectrum and shifted slightly in wavelength in order to compensate for any systematic shift in the wavelength calibration of the spectrometer. Incoming solar radiation was assumed to undergo Rayleigh scattering by CO_2 and Mie scattering by the polar hood, and to be reflected by a wavelength-independent surface albedo. The only atmospheric absorption in the 2000- to 3000-Å region was assumed to come from the Hartley band system of ozone, and therefore the amount of ozone was inferred by fitting this absorption feature with laboratory data of ozone absorption, as shown in Fig. 2. O_3 absorption of sunlight is not strong enough to affect atmospheric temperature on Mars [3], and hence cannot be inferred from temperature measurements.

I use a radiative transfer model based on the discrete ordinate method to calculate synthetic radiance spectra. Figure 3 shows that when typical amounts of dust and cloud are present, significant underestimation of O_3 occurs. A factor of 3 times as much O_3 is needed to generate the same spectrum as for a clear atmosphere. If

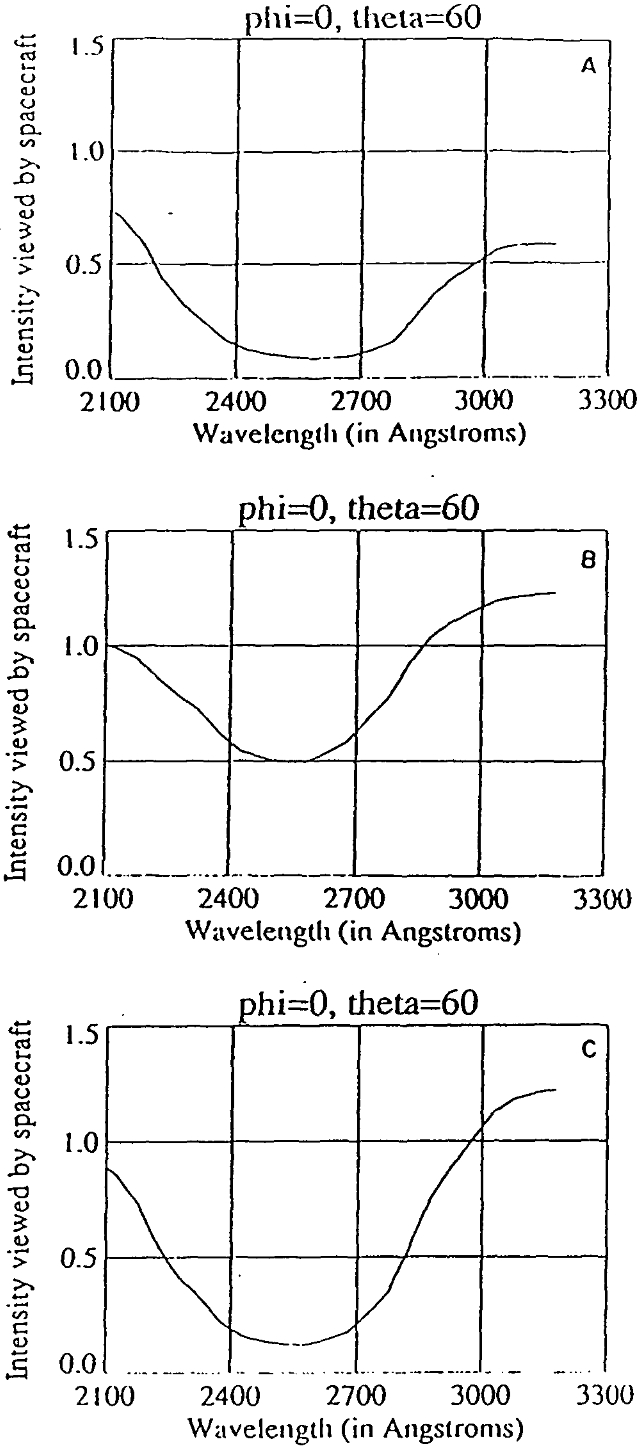

Fig. 3. Synthetic spectra as would be observed by spacecraft for atmospheres with (a) no cloud or dust and 30 mm-atm O_3, (b) vertical opacities of dust and cloud of 0.3 and 1.0 respectively and 30 mm-atm of O_3, and (c) vertical opacities of dust and cloud of 0.3 and 1.0 respectively and 100 mm-atm of O_3. All cases assume a solar zenith angle of 75 (typical for winter polar observations) and viewing angle of 60, with azimuth angle of 0 (typical for Mariner 9). Polar cap albedo of 0.6.

the scattering properties of martian clouds and dust were well known, then their appearance would not be a problem, as a model would be capable of retrieving the O_3 abundance. However, these properties are not well known, which raises doubts about the effectiveness of the current UV spectroscopy technique used to measure O_3.

Spatial and temporal variability in temperature and water vapor have been claimed to account for the scatter of the data points in Fig. 1 [4]. A decrease in temperature would result in a decrease in water vapor, if saturated as expected at prevalent temperatures. A decreased water vapor abundance decreases the availability of odd hydrogen, which converts CO and O into CO_2 catalytically, decreasing the abundance of O needed to form O_3. However, water vapor is a small source of odd hydrogen in the winter polar atmosphere, and may not account for most of the variability in Fig. 1 [5]. Masking by clouds and dust may also account for some of the observed O_3 variability, because the nature and opacity of the clouds and dust in the polar hood change dramatically in latitude and even on a day-to-day basis. As the maximum O_3 abundance resides near the surface [5], spacecraft must be able to observe through the entire cloud and dust abundance in order to actually see the total O_3 column abundance. If reflectance spectroscopy is used, as on Mariner 9, then the cloud and the airborne dust must be traversed twice, first by the incoming solar flux down to the surface and then once again upon reflection from the surface out to the spacecraft. In addition, the large solar zenith angles at winter polar latitudes mean several times the vertical opacity of cloud and dust must be traversed. Indeed, part of the observed latitudinal variation in O_3 in Fig. 1 may be due to the inability of the spacecraft to observe through the increasing effective optical depths as one goes poleward.

The UV spectrometer on Mariner 9 was incapable of penetrating the dust during dust storms [1]; the single-scattering albedo and phase function of airborne dust and cloud ice are not known to the degree required to extract the small UV signal reflected up from near the surface. The reflectance spectroscopy technique would also have difficulty detecting the total column abundance of O_3 in cases where large dust abundances exist together with the polar hood, especially at high latitudes where large solar zenith angles magnify those optical depths; yet these cases would contain the maximum O_3 based on theoretical results [5]. It is quite possible that the maximum O_3 column abundance observed by Mariner 9 of 60 μm-atm is common. In fact, larger quantities may exist in some of the colder areas with optically thick clouds and dust. As the Viking period often had more atmospheric dust loading than did that of Mariner 9, the reflectance spectroscopy technique may even have been incapable of detecting the entire O_3 column abundance during much of the Mars year that Viking observed, particularly at high latitudes.

Acknowledgments: I acknowledge support under contract NASW-4614.

References: [1] Lane A. L. et al. (1973) *Icarus, 18*, 102–108. [2] Lindner B. L. and Jakosky B. M. (1985) *JGR, 90*, 3435–3440. [3] Lindner B. L. (1991) *Icarus, 93*, 354–361. [4] Barth C. A. and Dick M. L. (1974) *Icarus, 22*, 205–211. [5] Lindner B. L. (1988) *Planet. Space Sci., 36*, 125–144.

How well is martian ozone inferred with reflectance spectroscopy?

Bernhard Lee Lindner

AER, 840 Memorial Drive, Cambridge, MA 02139 (617)349-2280

The Mariner 9 UV spectrometer scanned from 2100 to 3500 Angstroms in one of its two spectral channels every 3 seconds with a spectral resolution of 15 Angstroms and an effective field-of-view of approximately 300 km^2. The only gaseous absorption in the 2000 to 3000 Angstrom region was assumed to come from the Hartley band system of ozone, and therefore the amount of ozone was inferred by fitting this absorption feature with laboratory data of ozone absorption[1]. Mars O_3 as inferred from these spectra shows strong seasonal and latitudinal variation, with column abundances ranging from 0.2 μm-atm at equatorial latitudes to 60 μm-atm over the northern winter polar latitudes [1]. The detectability limit of the spectrometer was approximately 3 μm-atm.

I use a radiative transfer model based on the discrete ordinate method to calculate synthetic radiance spectra. When typical amounts of dust and cloud are present, significant underestimation of O_3 occurs. A factor of 3 times as much O_3 is needed to generate the same spectrum for cloudy, dusty atmospheres as for a clear atmosphere. If the scattering properties of martian clouds and dust were well known, then their appearance would not be a problem, as a model would be capable of retrieving the O_3 abundance. However, these properties are not well known, which raises doubts about the effectiveness of the current UV spectroscopy technique used to measure O_3.

Spatial and temporal variability in temperature and water vapor account have been claimed to account for the scatter of the data points [2]. However, water vapor is a small source of odd hydrogen in the winter polar atmosphere, and may not account for most of the variability [3]. Masking by clouds and dust may also account for some of the observed O_3 variability, because the nature and opacity of the clouds and dust in the polar hood change dramatically in latitude and even on a day-to-day basis. As the maximum O_3 abundance resides near the surface [3], spacecraft must be able to observe through the entire cloud and dust abundance in order to actually see the total O_3 column abundance. If reflectance spectroscopy is used, as on Mariner 9, then the cloud and the airborne dust must be traversed twice; first by the incoming solar flux down to the surface, and then once again upon reflection from the surface out to the spacecraft. In addition, the large solar zenith angles at winter polar latitudes mean several times the vertical opacity of cloud and dust must be traversed; yet these cases would contain the maximum O_3, based on theoretical results [3]. Indeed, part of the observed latitudinal variation in O_3 may be due to the inability of the spacecraft to observe through the increasing effective optical depths as one goes poleward. It is quite possible that the maximum O_3 column abundance observed by Mariner 9 of 60μm-atm is common. In fact, larger quantities may exist in some of the colder areas with optically thick clouds and dust [3]. As the Viking period often had more atmospheric dust loading than did that of Mariner 9, the reflectance spectroscopy technique may even have been incapable of detecting the entire O_3 column abundance during much of the Mars year that Viking observed, particularly at high latitudes.

I acknowledge support under contract NASW-4614.

[1] Lane A.L. et al. (1973) Icarus, 18, 102-108.
[2] Barth C.A. and Dick M.L. (1974) Icarus, 22, 205-211.
[3] Lindner B.L. (1988) Planet. Space Sci., 36, 125-144.

DIVISION FOR PLANETARY SCIENCES ABSTRACT FORM

Run.No.______ Sess.No.______
FOR EDITORIAL USE ONLY

Martian Polar Cap Seasonal Regression Simulations

B.L. Lindner (AER)

A model of the energy balance of the polar caps of Mars has been created which includes the radiative effects of clouds and dust (Lindner, J. Geophys. Res., 95, 1367-1379, 1990) and allows ice albedo to vary with age, latitude, hemisphere and solar zenith angle. The model reproduces polar cap regression data very well, including the survival of CO_2 frost at the south pole and not the north pole, and reproduces the general trend in the Viking Lander pressure data, although further improvement is needed.

The solar zenith angle dependence of ice albedo is not an important consideration over most of the polar cap, but is an important consideration at the pole. Therefore, energy balance studies of the residual polar caps should include the solar zenith angle dependence to ice albedo.

Hemispherical asymmetries in cloud and dust abundance could result in the survival of seasonal CO_2 ice through summer in the south and not in the north, in agreement with observations. Thus, the CO_2 ice observed in the summertime polar cap in the south could be of recent origin, although a permanent CO_2 polar cap cannot be ruled out.

This work was supported by NASA grants NASW-4444 and NASW-4614.

ORAL PAPER ☒ POSTER PAPER ☐

PAPER PRESENTED BY Bernhard Lee Lindner
(Please Print, Must be First Author)

SPECIAL INSTRUCTIONS:
Would appreciate speaking after 10 a.m.

First Author's Address - Print
AER, Inc.; 840 Memorial Drive, Cambridge, MA 02139

E-mail ______

Signature of First Author

Signature of Introducing Member, If Author is a Nonmember

Phone: 617-349-2280

Membership Status (Presenter):

DPS-AAS Member ☒ Non-Member ☐ Student ☐

Is your abstract especially newsworthy, and if so, would you be willing to prepare a news release and be available for interviews with reporters?

Yes ☐ No ☒ Maybe ☐

DPS Category No. 4 (From list on separate page)

Abstracts must conform to the AAS style as described on the back of this form. Abstract original must be typed or glued directly onto this form. The charge for publication of this abstract in the *Bulletin of the American Astronomical Society* will be included in the registration fee for this meeting.

Deadline for receipt of abstract: July 13, 1992

SUBMIT ORIGINAL AND FIVE COPIES TO:

DPS Abstracts
Lunar and Planetary Institute
Publications Services Department
3600 Bay Area Road
Houston, TX 77058-1113

For Editorial Use Only
BAAS VOL ______ NO ______ 19

Abstract Submitted for the Division for Planetary Sciences Munich Meeting

Date Submitted July 1, 1992 Form Version 2/92

LPSC XXI, 598–599. [6] Kargel J. S. and Strom R. G. (1991) *LPSC XXII*, 683–684. [7] Carr M. H. (1984) In *The Geology of the Terrestrial Planets* (M. H. Carr, ed.), 231–232, NASA SP-469. [8] Parker T. J. et al. (1986) *NASA TM-88383*, 468–470. [9] Parker T. J. and Gorsline D. S. (1992) *LPSC XXIII*, 1031–1032. [10] Tanaka K. L and Scott D. H. (1987) *Geologic Map of the Polar Regions of Mars*, U.S. Geol. Surv. Misc. Inv. Ser. Map I-1802-C. [11] Ruff S. W. and Greeley R. (1990) *LPSC XXI*, 1047–1048. [12] Metzger S. M. (1991) *LPSC XXII*, 891–892. [13] Metzger S. M. (1992) *LPSC XXIII*, 901–902.

IS CO_2 ICE PERMANENT? Bernhard Lee Lindner, Atmospheric and Environmental Research, Inc., 840 Memorial Drive, Cambridge MA 02139, USA.

Carbon dioxide ice has been inferred to exist at the south pole in summertime [1,2], but Earth-based measurements in 1969 of water vapor in the martian atmosphere suggest that all CO_2 ice sublimed from the southern polar cap and exposed underlying water ice [3]. This implies that the observed summertime CO_2 ice is of recent origin.

However, Fig. 1 shows that theoretical models of the energy budget of the surface that simulate the formation and dissipation of CO_2 ice have been unable to preserve seasonal CO_2 ice at the south pole and still obtain agreement with observations of the polar cap regression and the annual cycle in atmospheric pressure [4–10]. This implies that either these models improperly treat the energy budget or that CO_2 ice from an earlier time is exposed in summer.

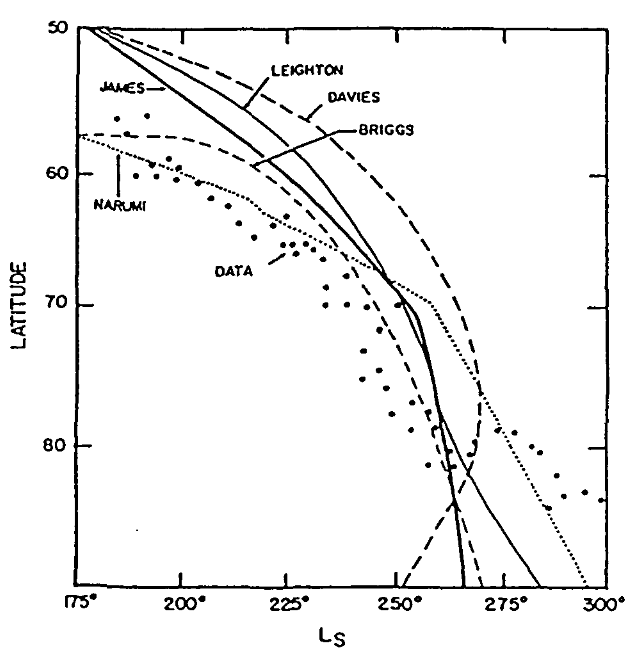

Fig. 1. The seasonal recession of the south polar cap as observed over the last 20 years [22] and as predicted by models [4,6–9]. (The aerocentric longitude of the Sun, L_s, is the seasonal index; L_s = 0°, 90°, 180°, and 270° correspond to northern spring equinox, summer solstice, autumnal equinox, and winter solstice respectively.)

An exact comparison to data is difficult, considering that the edge of the polar cap is usually patchy and ill defined [18,19], in large part due to terrain that is not included in any polar cap model. The edge of the polar cap is also diurnally variable since ice frequently forms at night and sublimes during the day. There is also some year-to-year variability in polar cap regression [20,21].

Several processes have been examined that might retain the good agreement to observations of the annual cycle in atmospheric pressure and to overall polar cap regression, and yet allow for better agreement at the south pole, without requiring old CO_2 ice. The radiative effects of ozone were suggested as important [11], but were shown numerically to be unimportant [12,13]. However, the radiative effects of clouds and dust [12] and the dependence of frost albedo on solar zenith angle [14,15] do allow for better agreement at the pole while maintaining good agreement to overall polar cap regression and the atmospheric pressure cycle [16]. Penetration of sunlight through the seasonal ice also has a marginal positive effect on CO_2 ice stability at the pole itself because it allows some solar radiation that would otherwise sublime overlying CO_2 seasonal ice to sublime ice within the residual polar cap [17].

Figures 2 and 3 show my model predictions for polar cap regression compared to observations. Before solar longitude of 250°, south polar cap regression is predicted to be similar to that predicted by earlier models (compare to Fig. 1). However, the new model retains CO_2 ice year round at the

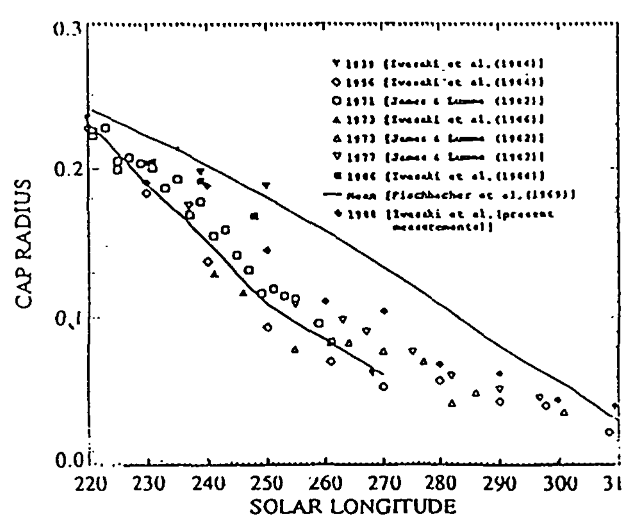

Fig. 2. The regression of the south polar cap, as observed for various years (taken from [23]) and as simulated by my model (thin line), as a function of the aerocentric longitude of the Sun (L_s). The cap radius is that which would be measured on a polar stereographic projection of the south polar region; the units of the radius are fractions of the planetary radius of Mars.

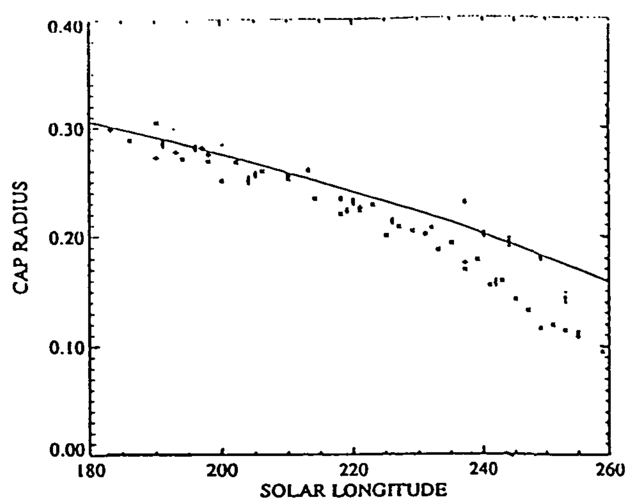

Fig. 3. The regression of the south polar cap, as observed in 1986 (solid circles), 1971 (crosses), and 1977 (plus signs) (taken from [21]) and as simulated by my model (thin line), as a function of the aerocentric longitude of the Sun (L_s). Two-sigma error bars are indicated for the 1986 data; the errors are smaller for the denser 1971 data and for the 1977 Viking data.

south pole. Unfortunately, the model does overpredict polar cap extent in early southern summer (see Fig. 2).

In summary, it appears possible to construct an energy balance model that maintains seasonal CO_2 ice at the south pole year round and still reasonably simulates the polar cap regression and atmospheric pressure data. This implies that the CO_2 ice observed in the summertime south polar cap could be seasonal in origin, and that minor changes in climate could cause CO_2 ice to completely vanish, as would appear to have happened in 1969 [3]. However, further research remains before it is certain whether the CO_2 ice observed in the summertime south polar cap is seasonal or is part of a permanent reservoir.

Acknowledgments. I acknowledge support by NASA contracts NASW 4444 and NASW 4614, under the Planetary Atmospheres Program and the Mars Data Analysis Program.

References: [1] Kieffer H. H. (1979) *JGR, 84,* 8263–8288. [2] Paige D. A. et al. (1990) *JGR, 95,* 1319–1335. [3] Jakosky B. M. and Barker E. S. (1984) *Icarus, 57,* 322–334. [4] Leighton R. B. and Murray B. C. (1966) *Science, 153,* 136–144. [5] Cross C. A. (1971) *Icarus, 15,* 110–114. [6] Briggs G. A. (1974) *Icarus, 23,* 167–191. [7] Davies D. W. et al. (1977) *JGR, 82,* 3815–3822. [8] Narumi Y. (1980) *Proceedings of the 13th Lunar and Planetary Symposium,* 31–41, Inst. Space Aeronaut. Sci., Univ. of Tokyo. [9] James P. B. and North G. R. (1982) *JGR, 87,* 10271–10283. [10] Lindner B. L. (1985) Ph.D. dissertation, Univ. of Colorado, Boulder, 470 pp. [11] Kuhn W. R. et al. (1979) *JGR, 84,* 8341–8342. [12] Lindner B. L. (1990) *JGR, 95,* 1367–1379. [13] Lindner B. L. (1991) *Icarus, 93,* 354–361. [14] Lindner B. L. (1991) In *International Union of Geodesy and Geophysics General Assembly XX, IAMAP Program and Abstracts,* 309, RM-Druck- and Verlagsgesellschaft, Graz, Austria. [15] Lindner B. L. (1992) In *Physics and Chemistry of Ice* (N. Maeno and T. Hondoh, eds.), 225–228, Hokkaido Univ., Sapporo. [16] Lindner B. L. (1992) *LPI Tech. Rpt. 92-02,* 76–77. [17] Lindner B. L. (1992) *GRL, 19,* 1675–1678. [18] Leovy C. B. et al. (1972) *Icarus, 17,* 373–393. [19] Christensen P. R. and Zurek R. W. (1983) *Bull. Am. Astron. Soc., 15,* 847. [20] Iwasaki K. et al. (1990) *JGR, 95,* 14751–14754. [21] James P. B. et al. (1990) *JGR, 95,* 1337–1341. [22] James P. B. and Lumme K. (1982) *Icarus, 50,* 368–380. [23] Iwasaki K. et al. (1990) *JGR, 95,* 14751–14754.

THE INTERANNUAL VARIABILITY OF POLAR CAP RECESSIONS AS A MEASURE OF MARTIAN CLIMATE AND WEATHER: USING EARTH-BASED DATA TO AUGMENT THE TIME LINE FOR THE MARS OBSERVER MAPPING MISSION. L. J. Martin[1] and P. B. James[2], [1]Lowell Observatory, 1400 West Mars Hill Road, Flagstaff AZ 86001, USA, [2]Department of Physics and Astronomy, University of Toledo, Toledo OH 43606, USA.

Seasonal Cycles of Dust, Water, and CO_2: The recessions of the polar ice caps are the most visible and most studied indication of seasonal change on Mars. Strong, if circumstantial, evidence links these recessions to the seasonal cycles of CO_2, water, and dust. These phenomena and their interactions will be the subject of an MSATT workshop next year titled "Atmospheric Transport on Mars." Briggs and Leovy [1] have shown from Mariner 9 observations that the atmospheric polar hoods of the fall and winter seasons are at least partially water ice clouds. Around the time of the vernal equinox, this water ice may precipitate onto the surface that includes CO_2 frosts. The sublimation of the outer edge of the seasonal cap begins about this same time, and we begin to observe its recession. During the recession of the north cap we also observe cirumpolar clouds that are believed to be formed by water vapor from the subliming cap [2]. Some observations suggest that at least part of the sublimed water and/or CO_2 reforms as surface ice toward the cap's interior. This "new" ice is probably the bright component of the polar caps that is seen on Earth-based observations. This would explain the south cap's appearance as that of a shrinking donut during its recession [3]. Near the edge of the shrinking cap, dust activity is also evident on the Viking images [4]. This may result from off-cap winds generated from sublimation and/or dust that might be released from within or beneath the ices. It has been found that all of Mars' major dust storms that have been observed to date occurred during the broad seasons when either the north or south polar cap was receding [5]. There are short seasonal periods around the beginning and ending of cap recessions when no major dust

Physical Science

The Abundance of Ozone on Mars. BERNHARD LEE LINDNER (AER)

The most extensive data on martian ozone (O_3) come from Mariner 9 observations. The Mariner 9 UV spectrometer scanned from 2100 to 3500 Angstroms with a spectral resolution of 15 Angstroms. O_3 column abundances inferred from these spectra show strong seasonal and latitudinal variability, ranging from 0.2 μm-atm at equatorial latitudes to 60 μm-atm over northern winter polar latitudes. Unlike Earth, these O_3 amounts do not significantly affect atmospheric temperature (1). I use a radiative transfer model based on the discrete ordinate method to calculate synthetic radiance spectra from 2100 to 3500 Angstroms. A factor of three times as much O_3 is needed to generate the same spectrum for typically observed cloudy, dusty atmospheres as for a clear atmosphere. If the scattering properties of martian clouds and dust were well known, then their appearance would not be a problem, as a model would be capable of retrieving the O_3 abundance. However, these properties are not well known, which raises doubts about the effectiveness of the UV spectroscopy technique used to measure O_3 abundances with Mariner 9, and about the accuracy of previously inferred O_3 abundances (cloud and dust effects were largely ignored in earlier analysis). While scattering and absorption of sunlight by clouds and dust seriously affect UV spectroscopy, scattering and absorption of sunlight by clouds and dust does not seriously affect O_3 abundance on Mars (2). I acknowledge support under NASA contract NASW-4614.

1. B.L. Lindner, *Icarus*, **93**, 354 (1991).
2. B.L. Lindner, *Planet. Space Sci.*, **36**, 125 (1988).

Bernhard Lee Lindner
AER Inc.
840 Memorial Drive
Cambridge, MA 02139
U.S.A.
(617)349-2280
(617)661-6479

Douglas W. Johnson
AER Inc.
000018216853#AS 09/18/92 M 3792 3

ATMOSPHERIC CHEMISTRY ON MARS

B.L. Lindner (Atmospheric and Environmental Research Inc., 840 Memorial Drive, Cambridge, MA 02139; 617-349-2280; fax:617-661-6479)

The current state of our knowledge of atmospheric chemistry on Mars will be reviewed, and differences with the Earth will be highlighted. Improvements in modeling work have shown that the excessively high atmospheric mixing required by earlier models (eddy diffusion coefficients of 10^8 cm^2s^{-1}) to explain the atmospheric composition observed by spacecraft is no longer necessary. Also, recent work has shown that heterogeneous chemistry could be quite important on Mars.

I will focus on the interactions between ozone and clouds and airborne dust. The ozone abundance on Mars is sensitive to the presence of clouds and airborne dust, in part due to the effects clouds and airborne dust have on photodissociative solar radiation. Also, the efficacy of the reflectance spectroscopy technique used in the past to infer ozone abundance on Mars is questioned due to masking by clouds and dust.

This work is being supported by a grant from the National Aeronautics and Space Administration. The views expressed herein are those of the author and do not necessarily reflect the views of NASA or any of its subagencies.

1994023387 N94- 27890

PROBING THE MARTIAN ATMOSPHERE IN THE ULTRAVIOLET

Bernhard Lee Lindner

44243-9

Atmospheric and Environmental Research, Inc.
840 Memorial Drive
Cambridge, Massachusetts 02139
(617)349-2280

Several fundamental differences in atmospheric chemistry exist between Mars and the Earth. The martian atmosphere is primarily CO_2 (95%), with strong vertical mixing, cold temperatures (typically 220K), low pressures (6 mb at the surface), high atmospheric dust and cloud particle content, and no man-made atmospheric constituents. Earlier difficulties in explaining why the atmosphere was not more decomposed into CO and O_2 have been placated with models using updated reaction rates, 'moderate' eddy mixing of order 10^7 cm^2 s^{-1}, and the odd hydrogen catalytic cycle (Shimazaki, 1989; Krasnopolsky, 1992). Odd nitrogen and sulfur catalytic cycles are of marginal importance, and other catalytic cycles shown to be important in the terrestrial atmosphere are unimportant on Mars (Yung et al., 1977; Krasnopolsky, 1992). Currently, much work is being undertaken to examine the importance of heterogeneous chemistry (e.g., Atreya and Blamont, 1990; Krasnopolsky, 1992), but uncertainties in particle properties make efficiencies difficult to evaluate. Also, atmospheric chemistry may significantly alter atmospheric composition on climatic timescales, particularly during periods of low obliquity (Lindner and Jakosky, 1985).

Ozone is a key to understanding atmospheric chemistry on Mars. The O_3 abundance has been inferred from UV spectra by several spacecraft, with the most complete coverage provided by Mariner 9 (Lane et al., 1973). The Mariner 9 UV spectrometer scanned from 2100 to 3500 Angstroms in one of its two spectral channels every 3 seconds with a spectral resolution of 15 Angstroms and an effective field-of-view of approximately 300 km^2. The only atmospheric absorption in the 2000 to 3000 Angstrom region was assumed to come from the Hartley band system of ozone, which has an opacity of order unity. Therefore the amount of ozone was inferred by fitting this absorption feature with laboratory data of ozone absorption, as shown in Fig. 1. Mars O_3 shows strong seasonal and latitudinal variation, with column abundances ranging from 0.2 µm-atm at equatorial latitudes to 60 µm-atm over the northern winter polar latitudes [Lane et al., 1973] (1 µm-atm is a column abundance of 2.689×10^{15} molecules cm^{-2}). However, the O_3 abundance is never great enough to significantly affect atmospheric temperatures (Lindner, 1991) or surface temperatures and frost budgets (Lindner, 1990). Figure 2 shows some of the inferred O_3 abundances.

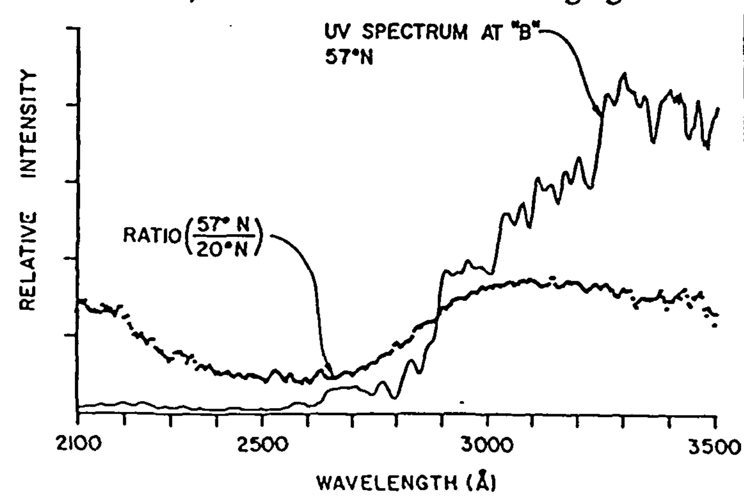

Figure 1. Ultraviolet spectrum measured by Mariner 9 at 57N latitude on orbit 144. To enhance the O_3 absorption feature, this spectrum was divided by one obtained at 20N latitude on orbit 144, where O_3 abundances are minimal (Lane et al., 1973).

I use a radiative transfer model based on the discrete ordinate method to calculate synthetic radiance spectra. Assuming a constant mixing ratio for ozone and no chemical or radiative interaction between O_3 and clouds/dust, Fig. 3

shows that when typical amounts of dust and cloud are present that significant underestimation of O_3 occurs. A factor of 3 times as much O_3 is needed to generate the same spectrum as for a clear atmosphere. If the scattering properties of martian clouds and dust were well known, then their appearance would not be a problem, as a model would be capable of retrieving the O_3 abundance. However, these properties are not well known, which raises doubts about the effectiveness of the current UV reflectance spectroscopy technique used to measure O_3.

Spatial and temporal variability in temperature and water vapor account have been claimed to account for the scatter of the data points in Fig. 2 (Barth and Dick, 1974). A decrease in temperature would result in a decrease in water vapor, if saturated as expected at prevalent temperatures. A decreased water vapor abundance decreases the availability of odd hydrogen, which converts CO and O into CO_2 catalytically, decreasing the abundance of O needed to form O_3. However, water vapor is a small source of odd hydrogen in the winter polar atmosphere compared to H_2, and may not account for most of the variability in Fig. 2 (Lindner, 1988). Masking by clouds and dust may also account for some of the observed O_3 variability, because the nature and opacity of the clouds and dust in the polar hood change dramatically in latitude and even on a day-to-day basis. As the maximum O_3 abundance resides near the surface (Lindner, 1988), spacecraft must be able to observe through the entire cloud and dust abundance in order to actually see the total O_3 column abundance. If reflectance spectroscopy is used, as on Mariner 9, then the cloud and the airborne dust must be traversed twice; first by the incoming solar flux down to the surface, and then once again upon reflection from the surface out to the spacecraft. In addition, the large solar zenith angles at winter polar latitudes mean several times the vertical opacity of cloud and dust must be traversed. Indeed, part of the observed latitudinal variation in O_3 in Fig. 2 may be due to the inability of the spacecraft to observe through the increasing effective optical depths as one goes poleward.

By using a photochemical model which included multiple scattering of solar radiation, Lindner (1988) showed that the absorption and scattering of solar radiation by clouds and dust actually increased O_3 abundances at winter polar latitudes. Hence, regions with high dust and cloud abundance could contain high O_3 abundances (heterogeneous chemistry effects have yet to be worked out). It is quite possible that the maximum O_3 column abundance observed by Mariner 9 of 60μm-atm is common. In fact, larger quantities may exist in some of the colder areas with optically thick clouds and dust. As the Viking period often had more atmospheric dust loading than did that of Mariner 9, the reflectance spectroscopy technique may even have been incapable of detecting the entire O_3 column abundance during much of the Mars year that Viking observed, particularly at high latitudes.

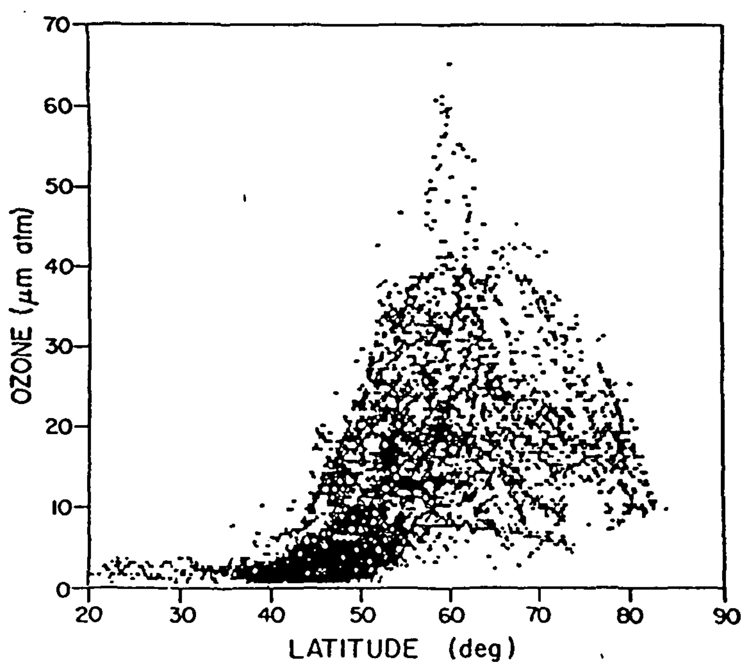

Figure 2. Measurements of the O_3 column abundance inferred from the Mariner 9 UV spectrometer data during the northern winter, L_S = 330-360, in the northern hemisphere (Barth, 1985).

However, observing the UV spectrum from the surface would greatly reduce the effects of clouds and dust, and hence significantly increase the accuracy of ozone abundance retrievals. A lander with a simple photometer having only 2 channels, one in the O_3 absorption band at 2500 Angstroms and one out of the band at 3500 Angstroms, would achieve this. Other possibilities for measuring ozone include solar occultation (Blamont et al., 1989), IR observations in the 9.6 μm O_3 band (e.g., Espenak et al., 1990), and observations of the O_2 dayglow at 1.27 μm, produced by photolysis of O_3 (Traub et al., 1979). However, further studies of these other techniques are required, especially as regards the effects of clouds and dust.

Atreya, S.K. and J.E. Blamont, 1990: Stability of the martian atmosphere: Possible role of heterogenous chemistry, *Geophys. Res. Lett.*, **17**, 287-290.

Barth, C.A., 1985: Photochemistry of the atmosphere of Mars, in *The Photochemistry of Atmo-spheres. Earth, other Planets, and Comets* (Ed. J. Levine). Academic Press, Orlando, Fla.

Barth, C.A. and M.L. Dick, 1974: Ozone and the polar hood of Mars, *Icarus*, **22**, 205-211.

Blamont, J.E., E. Chassefiere, J.P. Goutail, B. Mege, M. Nunes-Pinharanda, G. Souchon, V.A. Krasnopolsky, A.A. Krysko and V.I. Moroz, 1989: Vertical profiles of dust and ozone in the martian atmosphere deduced from solar occultation measurements, *Nature*, **341**, 600-603.

Espanek, F., M.J. Mumma, T. Kostiuk, and D. Zipoy, 1990: Ground based IR measurements of the global distribution of O3 in the atmosphere of Mars, *Bull. Amer. Astron. Soc.*, **22**, 1077.

Krasnopolsky, V.A., 1992: Photochemistry of the martian atmosphere (mean conditions), *J. Geophys. Res.*, in Press.

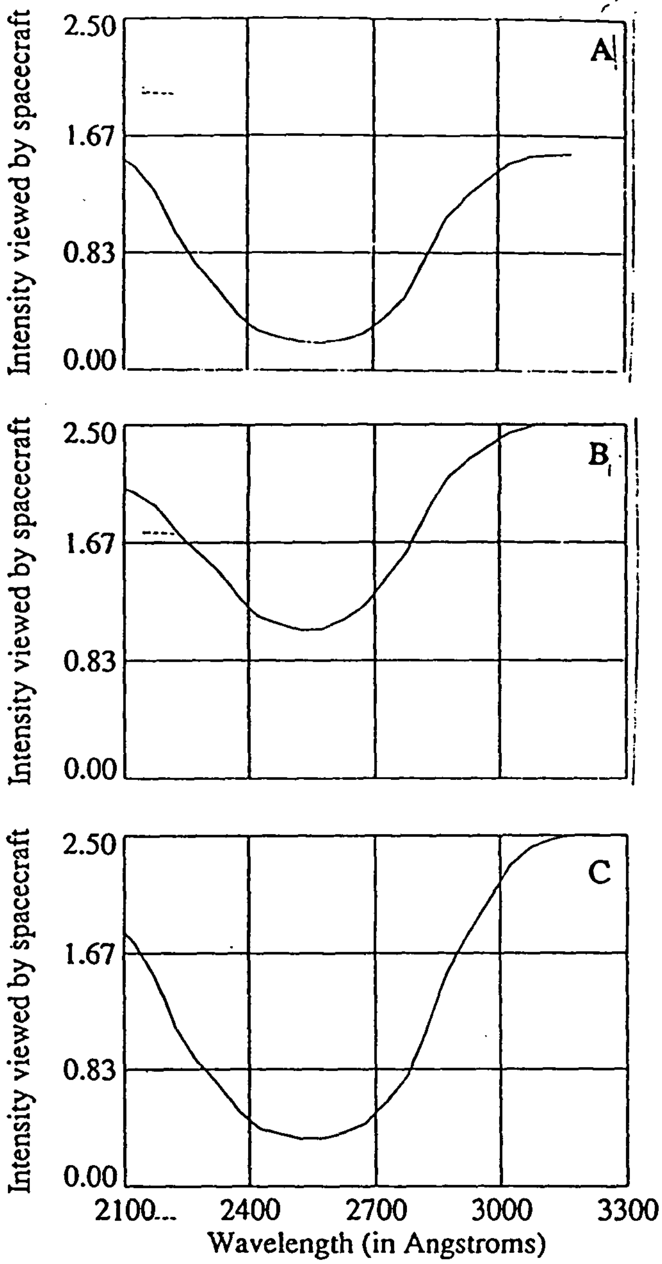

Figure 3. Synthetic spectra as would be observed by spacecraft for atmospheres with (A) no cloud or dust and 30 μm-atm O_3, (B) vertical opacities of dust and cloud of 0.3 and 1.0, respectively, and 30 μm-atm of O_3, and (C) vertical opacities of dust and cloud of 0.3 and 1.0, respectively, and 100 μm-atm of O_3. All cases assume a solar a zenith angle of 75 (typical for winter polar observations), and viewing angle of 60, with azimuth angle of 0 (typical for Mariner 9). Polar-cap albedo of 0.8 (new ice).

Lane, A.L., C. Barth, C. Hord, and A.I. Stewart, 1973: Mariner 9 UV spectro-meter experiment: Obser-va-tions of ozone on Mars, *Icarus*, **18**, 102-108.
Lindner, B.L., 1988: Ozone on Mars: The effects of clouds and airborne dust, *Planet. Space Sci.*, **36**, 125-144.
Lindner, B.L., 1990: The martian polar cap: Radiative effects of ozone, clouds, and airborne dust, *J. Geophys. Res.*, **95**, 1367-1379.
Lindner, B.L., 1991: Ozone heating in the martian atmosphere, *Icarus*, **93**, 354-361.
Lindner, B.L. and B.M. Jakosky, 1985: Martian atmospheric photochemistry and composition during periods of low obliquity, *J. Geophys. Res.*, **90**, 3435-3440.
Shimazaki, T., 1989: Photochemical stability of CO2 in the martian atmosphere: Reevaluation of the eddy diffusion coefficient and role of water vapor, *J. Geomag. Geoelectr.*, **41**, 273-301.
Traub, W.A., N.P. Carleton, P. Connes and J.F. Noxon, 1979: The latitudinal variation of O2 dayglow and O3 abundance on Mars, *Astrophys. J.*, **229**, 846-850.
Yung, Y.L., T.Y. Strobel, T.Y. Kong, and M.B. McElroy, 1977: Photochemistry of nitrogen in the martian atmosphere, *Icarus*, **30**, 26-41.

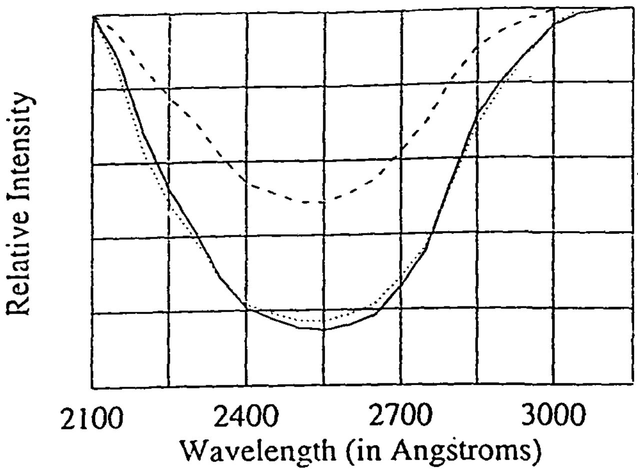

Fig. 3. Synthetic spectra as would be observed by spacecraft for atmospheres with no cloud or dust and 30 μm-atm O_3 (solid line), vertical opacities of dust and cloud of 0.3 and 1.0, respectively, and 30 μm-atm of O_3 (dashed line), and vertical opacities of dust and cloud of 0.3 and 1.0, respectively, and 100 μm-atm of O_3 (dotted line). All cases assume a solar zenith angle of 75° (typical for winter polar observations), and a polar cap albedo of 0.6.

to observe through the increasing effective optical depths as one goes poleward.

By using a photochemical model that included multiple scattering of solar radiation, Lindner [3] showed that the absorption and scattering of solar radiation by clouds and dust should actually increase O_3 abundances at winter polar latitudes. Hence, regions with high dust and cloud abundance could contain high O_3 abundances (heterogeneous chemistry effects have yet to be fully understood [2,9]). It is quite possible that the maximum O_3 column abundance observed by Mariner 9 of 60 μm-atm is common. In fact, larger quantities may exist in some of the colder areas with optically thick clouds and dust. As the Viking period often had more atmospheric dust loading than did that of Mariner 9, the reflectance spectroscopy technique may even have been incapable of detecting the entire O_3 column abundance during much of the Mars year that Viking observed, particularly at high latitudes. The behavior of O_3 is virtually unknown during global dust storms, in polar night, and within the polar hood, leaving large gaps in our understanding.

Acknowledgments: I thank K. Stamnes for providing the radiative transfer program, and NASA's MSATT Program for support.

References: [1] Shimazaki T. (1989) *J. Geomag. Geoelectr., 41*, 273–301. [2] Krasnopolsky V. A. (1993) *Icarus, 101*, 313–332. [3] Lindner B. L. (1988) *Planet. Space Sci., 36*, 125–144. [4] Barth C. A. et al. (1973) *Science, 179*, 795–796; Lane A. L. et al. (1973) *Icarus, 18*, 102–108. [5] Lindner B. L. (1991) *Icarus, 93*, 354–361; Lindner B. L. (1993) *Publ. Astron. Soc. Japan*, submitted. [6] Lindner B. L. (1990) *JGR, 95*, 1367–1379; Lindner B. L. (1992) *GRL, 19*, 1675–1678; Lindner B. L. (1993) *JGR, 98*, 3339–3344. [7] Barth C. A. (1985) in *The Photochemistry of Atmospheres. Earth, Other Planets, and Comets* (J. Levine, ed.), Academic, Florida. [8] Barth C. A. and Dick M. L. (1974) *Icarus, 22*, 205–211. [9] Atreya S. K. and Blamont J. E. (1990) *GRL, 17*, 287–290.

THE EFFECT OF POLAR CAPS ON OBLIQUITY.

B. L. Lindner, Atmospheric and Environmental Research, Inc., 840 Memorial Drive, Cambridge MA 02139, USA.

Rubincam [1] has shown that the martian obliquity is dependent on the seasonal polar caps. In particular, Rubincam analytically derived this dependence and showed that the change in obliquity is directly proportional to the seasonal polar cap mass. Specifically, Rubincam showed

$$d\psi/dt = 3 \times 10^{-10}\, M(t)/M(0) \quad \text{degrees/Earth year} \qquad (1)$$

where ψ is the obliquity and M is the mass of the seasonal polar caps, with time t of 0 being the present. This expression assumes uniformly thick spherical caps with identical angular radii of 45°. However, even if a very different polar cap mass distribution is used, Rubincam estimates the total uncertainty in the constant in equation (1) to be less than a factor of 2. Using the current mass of the seasonal polar cap as typical over geologic time, Rubincam calculates that the amount that the obliquity would secularly change is only 1.4°. Considering that the current obliquity of Mars is 25°, Rubincam concludes that seasonal friction does not appear to have changed Mars' climate significantly.

Using a computer model for the evolution of the martian atmosphere, Haberle et al. [2,3] have made a convincing case for the possibility of huge polar caps, about 10× the mass of the current polar caps, that exist for a significant fraction of the planet's history. Given the large uncertainties in input parameters and in the model itself, the results must be regarded as speculative. Also, the Haberle et al. results have been unable to favor or rule out a large polar cap scenario vs. a small polar cap scenario.

Nonetheless, since Rubincam showed that the effect of seasonal friction on obliquity is directly proportional to polar cap mass, a scenario with a ten-fold increase in polar cap mass over a significant fraction of the planet's history would result in a secular increase in Mars' obliquity of perhaps 10° (using equation (1)). Hence, the Rubincam conclusion of an insignificant contribution to Mars' climate by seasonal friction may be incorrect. Furthermore, if seasonal friction is an important consideration in the obliquity of Mars, this would significantly alter the predictions of past obliquity as presented by Ward [4–6], Murray et al. [7], Ward et al. [8], Rubincam [9], Chao and Rubincam [10], Bills [11], Ward and Ruby [12], Touma and Wisdom [13], and Laskar and Robutel [14]. That in turn would significantly alter the predictions of past climate, which are based on obliquity predictions [15–20]. The mechanics of the polar cap system also depend on obliquity [21–26]. If obliquities were often much smaller than at present, that could have implications for past atmospheric composition [27].

Given the enormity of the implications, the effect of the polar caps on the obliquity of Mars should be given more attention and study. Perhaps further modeling of obliquity could be used to rule out the possibility of large polar caps for extended times, which would assist modeling of atmospheric evolution. Similarly, modeling of atmospheric evolution should be given more attention and study because of the implications for obliquity history, and therefore climate history.

Acknowledgments: The author is indebted to the NASA MSATT program for support (Contract No. NASW-4614).

References: [1] Rubincam D. P. (1992) *JGR, 97*, 2629–2632. [2] Haberle R. M. et al. (1992a) *LPI Tech. Rpt. 92-08, Part 1*, 10–11. [3] Haberle R. M. et al. (1992b) *Bull. A.A.S., 24*; 1015–1016. [4] Ward W. R. (1973) *Science, 181*, 260–262. [5] Ward W. R. (1974) *JGR, 79*, 3375–3386. [6] Ward W. R. (1979) *JGR, 84*, 237–241. [7] Murray B. C. et al. (1973) *Science, 180*, 638–640. [8] Ward W. R. et al. (1979) *JGR, 84*, 243–259. [9] Rubincam D. P. (1990) *Science, 248*, 720–721. [10] Chao B. F. and Rubincam D. P. (1990) *JGR, 95*, 14755–14760. [11] Bills B. G. (1990) *JGR, 95*, 14137–14153. [12] Ward W. R. and Ruby D. J. (1991) *Icarus, 94*, 160–164. [13] Touma J. and Wisdom J. (1993) *Science, 259*, 1294–1297. [14] Laskar J. and Robutel P. (1993) *Nature, 361*, 608–612. [15] Sagan C. et al. (1973) *Science, 181*, 1045–1049. [16] Ward W. R. (1974) *JGR, 79*, 3387–3395. [17] Toon O. B. et al. (1980) *Icarus, 44*, 552–607. [18] Fanale F. P. et al. (1982) *Icarus, 50*, 381–407. [19] Pollack J. B. and Toon O. B. (1982) *Icarus, 50*, 259–287. [20] Francois L. M. et al. (1990) *JGR, 95*, 14761–14778. [21] Leighton R. B. and Murray B. C. (1966) *Science, 153*, 136–144. [22] James P. B. and North G. R. (1982) *JGR, 87*, 10271–10283. [23] Lindner B. L. (1990) *JGR, 95*, 1367–1379. [24] Lindner B. L. (1992) *GRL, 19*, 1675–1678. [25] Lindner B. L. (1993) *JGR, 98*, 3339–3344. [26] Wood S. E. and Paige D. A. (1992) *Icarus, 99*, 1–14. [27] Lindner B. L. and Jakosky B. M. (1985) *JGR, 90*, 3435–3440.

ESCAPE OF MARS ATMOSPHERIC CARBON THROUGH TIME BY PHOTOCHEMICAL MEANS.

J. G. Luhmann[1], J. Kim[2], and A. F. Nagy[3], [1]Institute of Geophysics and Planetary Physics, University of California, Los Angeles CA 90024-1567, USA, [2]KARI, Seoul, Korea, [3]Space Research Laboratory, University of Michigan, Ann Arbor MI 48109, USA.

Luhmann et al. [1] recently suggested that sputtering of the martian atmosphere by reentering O^+ pickup ions could have provided a significant route of escape for CO_2 and its products throughout Mars' history. They estimated that the equivalent of C in a ~140-mbar CO_2 atmosphere should have been lost this way if the Sun and solar wind evolved according to available models. Another source of escaping C (and O) that is potentially important is the dissociative recombination of ionospheric CO^+ near the exobase [2]. We have evaluated the loss rates due to this process for "ancient" solar EUV radiation fluxes of 1, 3, and 6× the present flux in order to calculate the possible cumulative loss over the last 3.5 Gyr. (Earlier estimates of loss by McElroy [2] used the present-day rates and thus represent underestimates.) The inputs and assumptions for this calculation are the same as used by Zhang et al. [3] for an evaluation of historical O escape by dissociative recombination of ionospheric O_2^+. We find loss rates of C that are at least comparable to the sputtering loss rates, thereby potentially accounting for another 100 mbar or more of Mars' original atmosphere.

References: [1] Luhmann J. G. et al. (1992) *GRL, 19*, 2151–2154. [2] McElroy M. B. (1972) *Science, 443*. [3] Zhang M. H. G. et al. (1993) *JGR, 98*, 10915–10923.

MIGHT IT BE POSSIBLE TO PREDICT THE ONSET OF MAJOR MARTIAN DUST STORMS?

L. J. Martin[1], P. B. James[2], and R. W. Zurek[3], [1]Lowell Observatory, Flagstaff AZ 86001, USA, [2]University of Toledo, Toledo OH 43606, USA, [3]Jet Propulsion Laboratory and California Institute of Technology, Pasadena CA 91109, USA.

This was done very successfully by the late "Chick" Capen in 1971, but we now believe that the chance of having a planet-encircling storm in any given Mars year is less than 50% [1]. Capen suggested that these storms begin around the time of perihelion. More recent storms have extended this season to nearly one-third of a martian year, during the same interval that the south polar cap is receding [2]. There is no observational evidence that storms of this size have occurred outside of that period, although smaller dust storms have been observed throughout most of the martian year. The circumstances that allow a limited storm to become a runaway or encircling storm are not well understood. Seasonal effects are apparently just one aspect of these circumstances, but apparently a critical one. Dust activity seen by Viking near the edges of the receding cap and data showing that the cap may be receding at a faster rate prior to these storms suggest that the seasonal south cap may be influencing dust activity.

We have also determined that the north polar hood recedes during major dust storms, but it is not clear whether impending storms might have an effect upon this atmospheric phenomenon. Viking images do show local storm clouds near the hood prior to the first 1977 planet-encircling dust storm, but the hood is such a dynamic feature that minor changes may not be meaningful. We are, however, continuing to analyze these data.

Several datasets indicate that Mars' atmosphere was less clear before the first 1977 encircling storm, although we cannot discount the possibility that this was merely a seasonal change. Data from other Mars years are less detailed and comprehensive, but the 1977 Viking data from both imaging [3] and infrared [4] suggest that dust in the atmosphere was increasing prior to the storm. Peter Boyce found that, prior to the 1971 planet-encircling storm, there was "violet haze" present on Mars. He attributed this to the impending storm, which may have been correct, but this condition, which could be due in part to atmospheric dust on Mars, is not uncommon at times when no storm is on the way. This may also be true for other indicators of increasing atmospheric dust mentioned above.

Capen also believed that smaller, precursor storms occurred before a planet-encircling storm. This generally seems to be the case, although the data are not conclusive. These earlier storms certainly provide a good vehicle for raising dust into the the atmosphere and regional dust storms may be a sign of an impending larger storm. However, many of these storms occur without any subsequent dust activity, even during the dust storm "season."

Investigations of dust-storm observations show that that the Hellas Basin is the most active area on Mars for all sizes of storms [2]. This area is probably their primary dust source.

Earth-based observations suggest that, during the expansion phase of planet-encircling storms, diurnal cycles often begin at Hellas, presumably with a new load of dust, as mountain climbers return to a base camp for more supplies to be cached along their route. Each day the storms carry an increasing supply of dust farther to the west, until Hellas is reached from the east, completing the

199402338 N94- 27891

HOW WELL WAS TOTAL OZONE ABUNDANCE INFERRED WITH MARINER 9? Bernhard Lee Lindner, AER, Inc., 840 Memorial Drive, Cambridge, Massachusetts 02139 USA 442652

Ozone is a key to understanding atmospheric chemistry on Mars. Over 20 photochemical models of the martian atmosphere have been published, and O_3 is often used as a benchmark for these models[1-3]. O_3 abundance has been inferred from instrumentation on several spacecraft, with the most complete coverage provided by Mariner 9[3,4]. The Mariner 9 UV spectrometer scanned from 2100 to 3500 Angstroms with a spectral resolution of 15 Angstroms and an effective field-of-view of approximately 300 km^2 [4]. The only atmospheric absorption in the 2000 to 3000 Å wavelength region was previously assumed to come from the Hartley band system of ozone[4], which has an opacity of order unity at winter polar latitudes[3]. Therefore the amount of ozone was inferred by fitting this absorption feature with laboratory data of ozone absorption, as shown in Fig. 1[4]. Mars O_3 shows strong seasonal and latitudinal variation, with column abundances ranging from 0.2 μm-atm at equatorial latitudes to 60 μm-atm over northern winter polar latitudes[4] (1 μm-atm is a column abundance of 2.689×10^{15} molecules cm^{-2}). However, the O_3 abundance is never great enough to significantly affect atmospheric temperatures[5] or surface temperatures and frost amounts[6]. Figure 2 shows some of the previously-inferred O_3 abundances[7].

A radiative transfer computer model is used to re-examine the Mariner 9 UV spectra. Assuming a constant mixing ratio for O_3 and no chemical or radiative interaction between O_3 and clouds/dust, Fig. 3 shows that when typical amounts of dust and cloud are present that significant underestimation of O_3 abundance occurs. A factor of 3 times as much O_3 is needed to generate the same spectrum the spacecraft would measure for a cloudy, dusty atmosphere as for a clear atmosphere. If the scattering properties of martian clouds and dust were well known, then their appearance would not be a problem, as a model would be capable of retrieving the O_3 abundance. However, these properties are not well known, which raises doubts about the effectiveness of the UV reflectance spectroscopy technique for measuring O_3 abundance on Mars. The simulations shown in Fig. 3 are repeated for a range in solar zenith angle (50°-90°), ground albedo (0.3-0.8), altitude distribution of O_3, satellite viewing geometries, and cloud, dust and O_3 abundances. A factor of 3 underestimation is typical, with greater underestimation for high ground albedo or high dust opacities. Even if scattering by clouds is properly accounted for (as previously done with Mariner 9 data reduction in [4]), masking by dust can easily result in factor of 2 underestimation. Results are not strongly dependent on solar zenith angle.

Spatial and temporal variability in temperature and water vapor have been claimed to account for the scatter of the data points in Fig. 2[8]. A decrease in temperature results in a decrease in water vapor, if saturated as expected at prevalent temperatures. A decreased water vapor abundance decreases the availability of odd hydrogen (H, OH, and HO_2), which converts CO and O into CO_2 catalytically, decreasing the abundance of O needed to form O_3. However, water vapor is a small source of odd hydrogen in the winter polar atmosphere compared to H_2, and may not account for most of the variability in Fig. 2[3]. Masking by clouds and dust may also account for some of the observed O_3 variability, because the nature and opacity of the clouds and dust at winter polar latitudes change significantly spatially and temporally. As the maximum O_3 abundance resides near the surface[3], spacecraft must be able to observe through the entire cloud and dust abundance in order to measure the total O_3 column abundance. If reflectance spectroscopy is used, as on Mariner 9, then the cloud and the airborne dust must be traversed twice; first by the incoming solar flux down to the surface, and then once again upon reflection from the surface out to the spacecraft. In addition, the large solar zenith angles at winter polar latitudes mean several times the vertical opacity of cloud and dust must be traversed. Indeed, part of the observed latitudinal variation in O_3 abundance in Fig. 2 may be due to the inability of the spacecraft to observe through the increasing effective optical depths as one goes poleward.

By using a photochemical model which included multiple scattering of solar radiation, Lindner[3] showed that the absorption and scattering of solar radiation by clouds and dust should actually increase O_3 abundances at winter polar latitudes. Hence, regions with high dust and cloud abundance could contain high O_3 abundances (heterogeneous chemistry effects have yet to be fully understood[2,9]). It is quite possible that the maximum O_3 column abundance observed by

Mariner 9 of 60μm-atm is common. In fact, larger quantities may exist in some of the colder areas with optically thick clouds and dust. As the Viking period often had more atmospheric dust loading than did that of Mariner 9, the reflectance spectroscopy technique may even have been incapable of detecting the entire O_3 column abundance during much of the Mars year that Viking observed, particularly at high latitudes. The behavior of O_3 is virtually unknown during global dust storms, in polar night, and within the polar hood, leaving large gaps in our understanding.

ACKNOWLEDGMENTS. I thank Knut Stamnes for providing the radiative transfer program, and NASA's MSATT Program for support.

REFERENCES

1. Shimazaki, T., *J. Geomag. Geoelectr.*, **41**, 273-301 (1989).
2. Krasnopolsky, V.A., *Icarus*, **101**, 313-332 (1993).
3. Lindner, B.L., *Planet. Space Sci.*, **36**, 125-144 (1988).
4. Barth, C.A. *et al.*, *Science*, **179**, 795-796 (1973); Lane, A.L., Barth, C., Hord,C. & Stewart, A.I., *Icarus*, **18**, 102-108 (1973).
5. Lindner, B.L., *Icarus*, **93**, 354-361 (1991); Lindner, B.L., submitted to *Publ. Astron. Soc. Japan* (1993).
6. Lindner, B.L., *J. Geophys. Res.*, **95**, 1367-1379 (1990); Lindner, B.L., *Geophys. Res. Lett.*, **19**, 1675-1678 (1992); Lindner, B.L., *J. Geophys. Res.*, **98**, 3339-3344 (1993).
7. Barth, C.A., in *The Photochemistry of Atmospheres. Earth, other Planets, and Comets* (ed. Levine, J.). (Academic Press, Orlando, Fla., 1985).
8. Barth, C.A. & Dick, M.L., *Icarus*, **22**, 205-211 (1974).
9. Atreya, S.K. & Blamont, J.E., *Geophys. Res. Lett.*, **17**, 287-290 (1990).

FIGURE CAPTIONS

Figure 1. Ultraviolet spectrum measured by Mariner 9 at 57°N latitude on orbit 144[7]. To enhance the O_3 absorption feature, this spectrum was divided by one obtained at 20°N latitude on orbit 144, where O_3 abundances are minimal[7].

Figure 2. Measurements of the O_3 column abundance previously inferred from the Mariner 9 UV spectrometer data during the northern winter, L_S = 330-360°, in the northern hemisphere[4].

Figure 3. Synthetic spectra as would be observed by spacecraft for atmospheres with no cloud or dust and 30 μm-atm O_3 (solid line), vertical opacities of dust and cloud of 0.3 and 1.0, respectively, and 30 μm-atm of O_3 (dashed line), and vertical opacities of dust and cloud of 0.3 and 1.0, respectively, and 100 μm-atm of O_3 (dotted line). All cases assume a solar a zenith angle of 75° (typical for winter polar observations), and a polar cap albedo of 0.6.

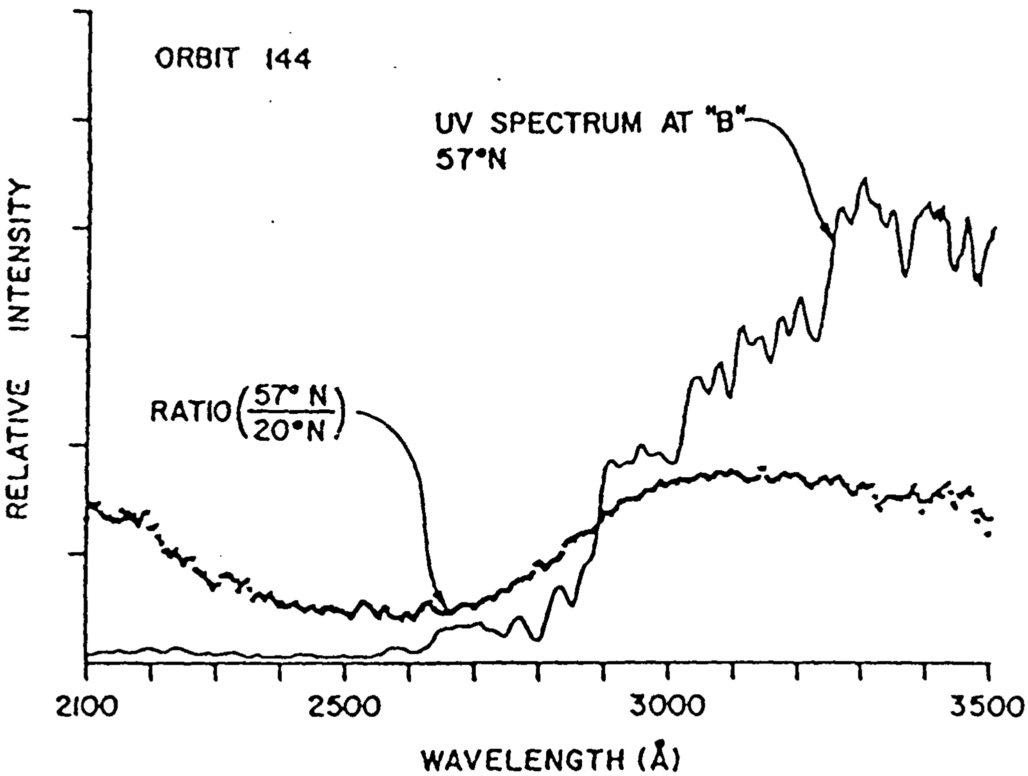
ORBIT 144
UV SPECTRUM AT "B" 57°N
RATIO (57° N / 20° N)
RELATIVE INTENSITY
2100
2500
3000
3500
WAVELENGTH (Å)

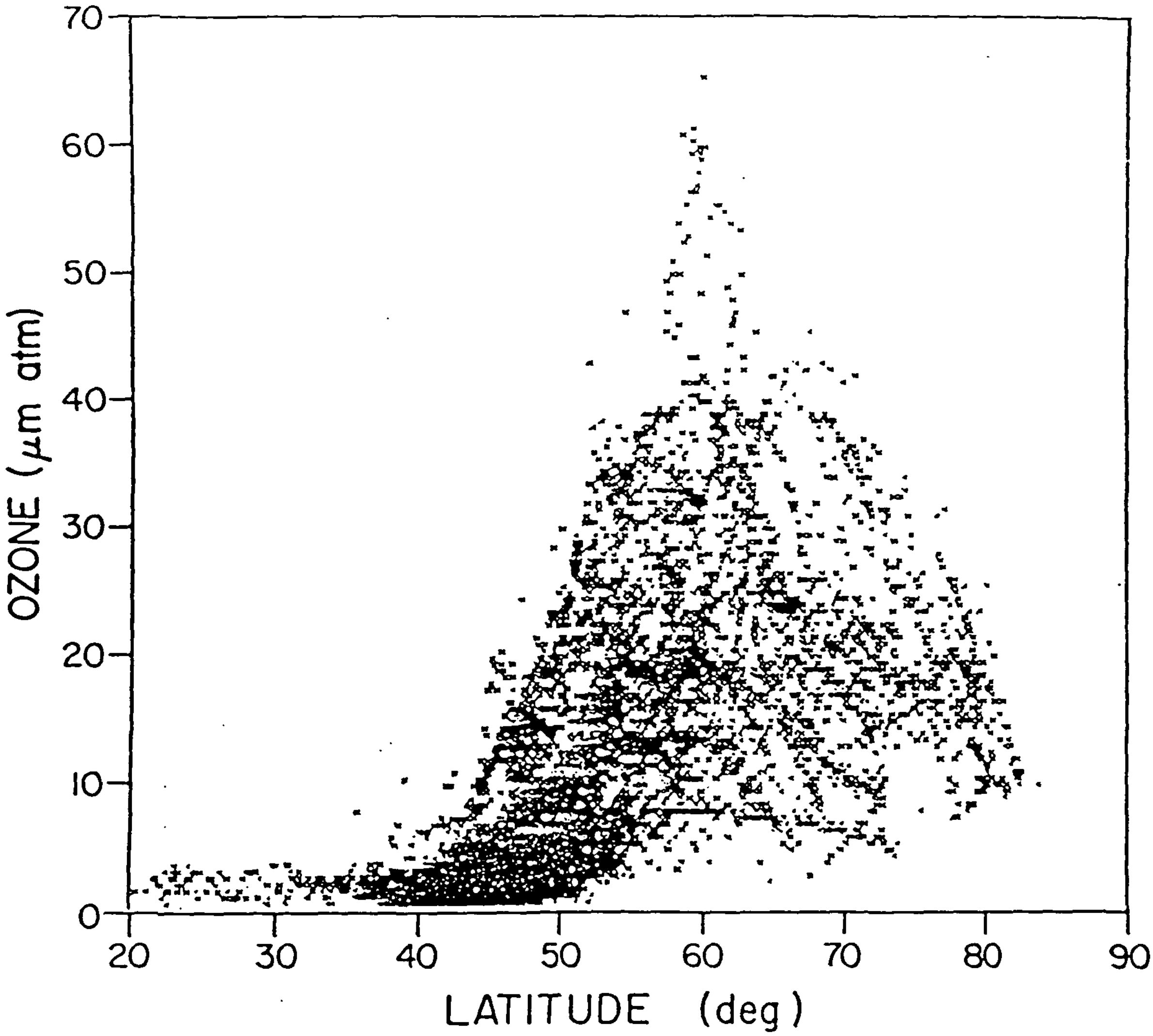

OZONE (μm atm)
0
10
20
30
40
50
60
70
LATITUDE (deg)
20
30
40
50
60
70
80
90

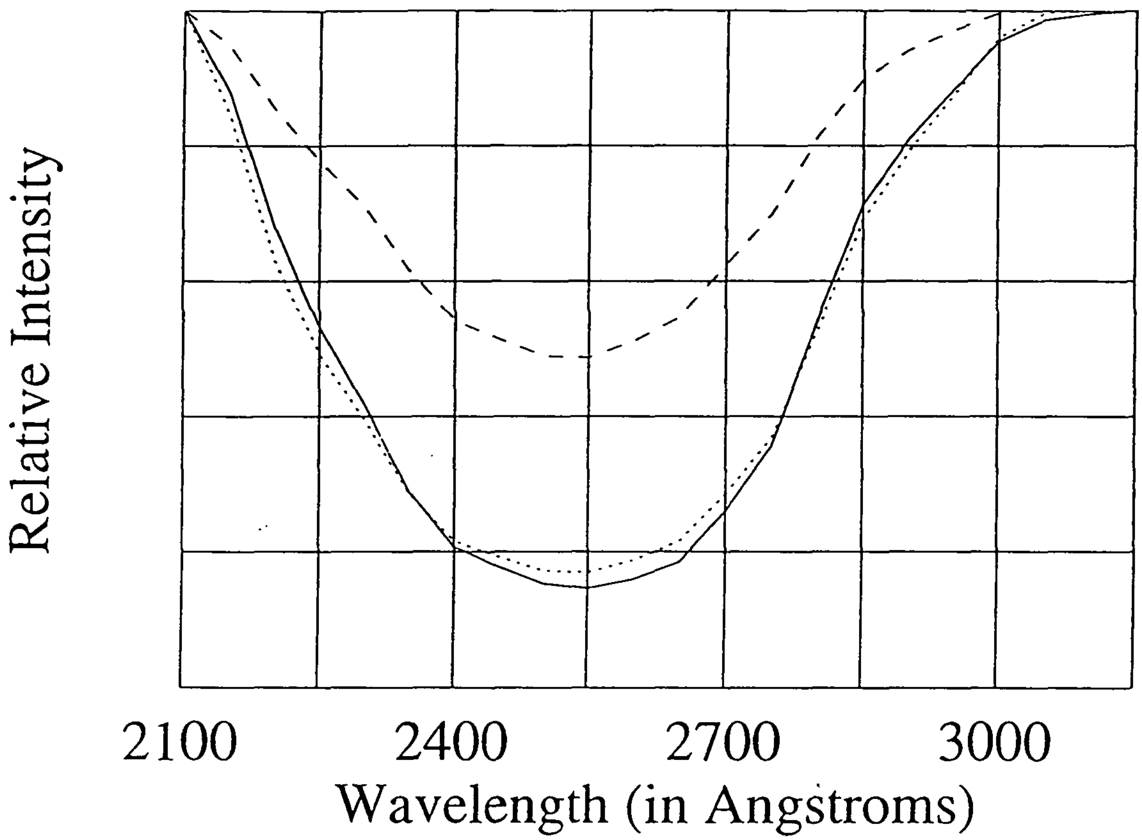

Relative Intensity
2100
2400
2700
3000
Wavelength (in Angstroms)

In Situ Mars Ozone Detector

Dr. B. Lee Lindner
Atmospheric and Environmental Research, Inc.
840 Memorial Drive, Cambridge, MA 02139
(617) 547-6207

Dr. Elliot M. Weinstock
Dept. of Chemistry and Center for Earth and Planetary Physics
Harvard University, Cambridge, MA 02139

We propose sending a balloon-borne UV photometer sensor package to measure atmospheric ozone on Mars, and this package could be a Discovery Program sensor candidate. Past measurements of ozone on Mars are highly uncertain, perhaps a factor of 3 or so uncertain (Lindner, 1993), due primarily to interference and masking by cloud and dust. In-situ balloon measurements would avoid these problems, and would provide 'ground truth' which remote sensing techniques cannot. We have explored this approach to measure ozone abundance in the terrestrial stratosphere with a balloon-borne UV absorption photometer (described in detail in Weinstock et al., 1986). Atmospheric pressures and temperatures and ozone concentrations near the surface of Mars are similar to those in the terrestrial stratosphere.

In brief, the instrument uses 245-nm radiation from a low-pressure mercury discharge lamp in a 40-pass white cell (1200-cm path length). The instrument has measured terrestrial stratospheric ozone with better than 3% precision and 5% accuracy. The instrument is small (approx. 30cm cubed), lightweight (approx. 20 kg), self-scrubbing (i.e., self-calibrating), and has in-flight diagnostics and a low data rate. This balloon-borne photometer is expected to be able to measure ozone throughout the polar winter region (poleward of 40° latitude) within the lower 20 km of the atmosphere but possibly not at equatorial latitudes where O_3 concentrations are extremely low (10^9 cm^{-3}), although slight improvements may allow for measurement of these low concentrations as well.

The objectives for this instrument are to observe O_3 variability with cloud and dust amount, to measure the altitude dependence of O_3, and to measure diurnal fluctuations in O_3. There are no measurements to date of any of these variations. The abundance of ozone during the great dust storms on Mars is totally unknown due to the inability to see through the dust. The possibility of heterogeneous chemistry of ozone with airborne dust and cloud on Mars is the most active topic in Mars aeronomy today, and the question can only be settled through an in situ study such as we propose. The dependence of ozone on altitude has never been measured, only the column abundance. An improved understanding of the altitude dependence of ozone would also determine the degree of vertical atmospheric transport. Because the instrument proposed here contains a lamp, ozone could be measured throughout the day/night cycle. Ozone in polar night has never been measured, and measurements here would greatly increase our understanding of heterogeneous chemistry and atmospheric transport.

Hence, in-situ ozone measurements would significantly improve our understanding of Mars atmospheric chemistry and composition and the interaction of atmospheric chemistry with atmospheric radiation and dynamics. Much interest has been generated over the past 5 years for a Mars Aeronomy Mission. This is a low cost alternative which in many respects will learn more information. This mission would complement a proposed Japanese mission to study the chemistry of the martian upper atmosphere (Tsuruda, 1991).

Lindner, B. L. (1993) Mars Ozone: Mariner 9 Revisited, submitted to *Geophys. Res. Lett.*
Tsuruda, K. (1991) In *Workshop on the Martian atmosphere through time*, LPI, Houston.
Weinstock, E.M., C.M. Schiller, and J.G. Anderson (1986) J. Geophys. Res. 91, 5237-5248.